Master's thesis

NTNU
Norwegian University of Science and Technology
Faculty of Natural Sciences
Department of Biotechnology and Food Science

Mina Gravdahl

Preparation, characterization, and solution properties of chitosan-*b*-dextran diblocks

Master's thesis in Biotechnology
Supervisor: Bjørn E. Christensen
Co-supervisor: Amalie Solberg
May 2021

NTNU
Kunnskap for en bedre verden

Mina Gravdahl

Preparation, characterization, and solution properties of chitosan-*b*-dextran diblocks

Master's thesis in Biotechnology
Supervisor: Bjørn E. Christensen
Co-supervisor: Amalie Solberg
May 2021

Norwegian University of Science and Technology
Faculty of Natural Sciences
Department of Biotechnology and Food Science

NTNU
Norwegian University of
Science and Technology

Preface

This master thesis was conducted at the Department of Biotechnology and Food Science (IBT) at the Norwegian University of Science and Technology (NTNU) between August 2020 and May 2021.

I would like to thank my supervisor Professor Bjørn E. Christensen for the opportunity to work with this project and for guidance and discussions throughout the work of the thesis.

Furthermore, I would like to thank PhD Candidate Amalie Solberg for being my co-supervisor and for all the help and advice during the laboratory work and the writing process of this master thesis.

Many thanks to my co-master students Hilde Kristoffersen, Trine Muren and Marianne Von Krogh, for good teamwork in the laboratory and for support throughout the last year at NTNU.

Thank you to Senior Engineer Wenche I. Strand and Senior Engineer Olav A. Aarstad for technical support in the laboratories and for creating a welcoming environment in the biopolymer lab. I would also like to thank Professor Christophe Schatz from Bordeaux, France, for letting me be a part of a research study.

It has been five great years at NTNU.

Trondheim, 15.05.21

Mina Gravdahl

Abstract

The overall aim of this master thesis was to prepare and characterize chitosan-*b*-dextran diblocks and to investigate their properties in solution. It is generally known that the solubility of chitosan oligomers with low F_A is strongly pH-dependent, leading to aggregation and precipitation when pH > pK_a. It was therefore of great interest to investigate how terminal conjugation of a water-soluble dextran block with chitosan affected the solution properties of the resulting diblock, compared to that of pure chitosan.

Size-exclusion chromatography (SEC) was used to obtain narrow fractions of chitosan oligomers (D_nM) and activated dextran oligomers ($Dext_m$-PDHA), for the preparation of chitosan-*b*-dextran diblocks. The decision to use the dextran oligomers as the first block in the preparation of chitosan-*b*-dextran diblocks, was due to the desire to utilize the high reactivity of the pending aldehyde of the M residue in the block conjugation. Fully de-*N*-acetylated oligomers with the highly reactive M residue (D_nM) was prepared by degradation of chitosan with low F_A using a sub-stoichiometric amount of nitrous acid (HNO_2). Purification of isolated D_nM oligomers can be troublesome due to reactions of the highly reactive M residues with the free amino groups of the D residues. This can lead to self-branching through Schiff base formation and subsequent degradation of the M residue (pH-dependent). Two possible methods to improve the preparation of purified and isolated chitosan oligomers (D_nM) were therefore explored. This led to the development of an optimized purification method, which resulted in higher preservation of the M residue at the reducing end, compared to previous methods.

The conjugation and reduction reaction of chitosan-*b*-dextran diblocks were studied by time course NMR to establish the course of the reactions as a tool to develop a preparative protocol. The conjugation of D_nM oligomers to $Dext_m$-PDHA using a 1:1 molar ratio was a rapid reaction and resulted in high yields of diblocks (≥ 85 %). In agreement with literature, only acyclic conjugates (E- and Z-oximes) were formed. The reduction kinetic study revealed that the reduction of the oximes, by the reducing agent α-Picoline borane (PB), was significantly slower compared to the conjugation reaction.

The solution properties of pure D_nM oligomers were studied by measuring the intensity of the scattered light as a function of pH by dynamic light scattering (DLS). Aggregation was observed at approximately pH 7, which was in good agreement with previous literature. Additional increase in pH resulted in precipitation. The solution properties of $D_{28}M$-PDHA-

$Dext_{52}$ diblocks were further investigated using the same approach. The study revealed that the chitosan-*b*-dextran diblocks remained soluble over a larger pH range compared to the pure D_nM, as no precipitation was observed at pH 10 for the diblocks. The size of the diblock particles formed at pH 6 and pH 10 suggested that there were no free chains in the solution. In addition, narrowing of the intensity distribution and slight increase in light scattering intensity from pH 6 to pH 10 may indicate structuring. A hypothesis is self-assembly of chitosan and the formation of a micellar structure with a dextran corona. However, further studies are needed to confirm this. Finally, a stability study of chitosan-*b*-dextran diblocks prepared without reduction indicated that the diblock structures are reversible at low pH values.

Sammendrag

Målet med denne masteroppgaven var å lage og karakterisere av kitosan-*b*-dekstran-diblokker og undersøke deres egenskaper i løsning. Det er kjent at løseligheten til kitosan-oligomerer med lav F_A er sterkt avhengig av pH i løsningen, noe som fører til aggregering og utfelling når pH > pK_a. Det var derfor av stor interesse å undersøke hvordan koblingen av en vannløselig dekstran-blokk med kitosan påvirker løseligheten til den resulterende diblokken, sammenlignet med ren kitosan.

Størrelseseksklusjons-kromatografi (SEC) ble brukt for å skaffe smale fraksjoner av kitosan-oligomerer (D_nM) og aktiverte dekstran-oligomerer ($Dext_m$-PDHA), for opplagingen av kitosan-*b*-dekstran-diblokker. Grunnen til at dextran-oligomerer ble brukt som den første blokken i opplagingen av kitosan-*b*-dekstran-diblokker var på grunn av ønsket om å utnytte den høyt reaktive M-enheten i koblingsreaksjonen. Fullstendig de-*N*-acetylerte oligomerer med den svært reaktive M-enheten som reduserende ende (D_nM) ble laget ved å bryte ned kitosan med lav F_A ved bruk av sub-støkiometrisk mengde salpetersyrling (HNO_2). Opprensing av isolerte D_nM-oligomerer kan være vanskelig på grunn av reaksjon mellom de høyt reaktive M-enhetene og aminogruppene på D-enhetene til kitosan. Dette kan føre til selv-forgreining gjennom en Schiff-basereaksjon og påfølgende nedbryting av M-enheten (pH-avhengig). To mulige måter å forbedre opplagingen av isolerte kitosan-oligomerer (D_nM) ble derfor utforsket. Dette førte til en ny rensemetode, noe som resulterte i økt bevaring av M-enheten på den reduserende enden, sammenlignet med tidligere metoder.

Koblingsreaksjonen og reduksjonsreaksjonen for kitosan-*b*-dekstran-diblokkene ble studert med time course NMR for å finne ut hvor lang tid reaksjonene tok slik at en preparativ protokoll kunne etableres. Koblingen av kitosan-oligomerer og dektran-PDHA ved bruk av molforholdet 1:1, var en rask reaksjon som resulterte i høyt utbytte av diblokker (≥ 85 %). I samsvar med litteraturen, ble det bare dannet asykliske konjugater (E- og Z-oksimer). Kinetikkforsøket for reduksjonen avslørte at reduksjonen av diblokkene, ved bruk av reduksjonsmiddelet α-Picoline boran (PB), var betydelig langsommere sammenlignet med koblingsreaksjonen.

Løseligheten av kitosan-oligomerer ble undersøkt ved å måle lysspredning som en funksjon av pH ved dynamisk lysspredning (DLS). Aggregering ble observert ved omtrent pH 7, som var i godt samsvar med tidligere litteratur. Ytterligere økning av pH resulterte i utfelling. Løseligheten til kitosan-*b*-dekstran-diblokker ble deretter undersøkt med samme metode, noe

som resulterte i at kitosan-*b*-dekstran-diblokkene viste seg å ha løselighet over et større pH-område sammenlignet med kitosan-oligomerer, da det ikke ble observert utfelling ved pH 10. Partikkelstørrelsen til diblokkene observert ved pH 6 og pH 10 antydet at det ikke kunne være frie kjeder i løsningen. I tillegg kan innsnevringen av intensitetsfordelingen og økningen i lysspredning fra pH 6 til pH 10 indikere strukturering av diblokkene. En hypotese er strukturering av kitosan og dannelsen av en micellar struktur med en dekstran-corona. Ytterligere studier bør gjøres for å bekrefte dette. En stabilitetsstudie av kitosan-*b*-dekstran-diblokker laget uten redusering indikerte at reversering av diblokkene forekommer ved lave pH-verdier.

ABBREVIATIONS

AcOH	acetic acid
AmAc	ammonium acetate
A_nM	chitin, comprised of n units of consecutive *N*-acetyl-D-glucosamines, with a 2,5-anhydro-D-mannose reducing end
A-unit	*N*-acetyl-D-glucosamine
BCP	block copolymer
CHOS	chitooligosaccharides
Dext	dextran
D_nM	chitosan, comprised of n units of consecutive D-glucosamines, with a 2,5-anhydro-D-mannose reducing end
DP_n	number average degree of polymerization
D-unit	D-glucosamine
F_A	fraction of *N*-acetyl-D-glucosamine units
GlcN	D-glucosamine
GlcNAc	*N*-acetyl-D-glucosamine
HMF	5-hydroxymethylfurfural
HMWC	high molecular weight chitosan
HNO_2	nitrous acid
LMWC	low molecular weight chitosan
M_n	number average molecular weight
M_w	weight average molecular weight
MP	mobile phase
M-unit	2,5-anhydro-D-mannose
PDHA	O,O'-1,3-propanediylbishydroxylamine
PECs	polyelectrolyte complexes
Pic-BH_3/PB	α-picoline borane
SEC	size-exclusion chromatography
MWCO	molecular weight cut-off

TABLE OF CONTENTS

1 INTRODUCTION

1.1 Background

Polysaccharides are natural polymers from renewable sources with remarkable structural diversity. They are an attractive alternative to synthetic polymers due to their biodegradability and biocompatibility [1]. Chemical modification of polysaccharides is usually performed to change their properties and allows for a large diversity of higher order structures [2]. Diblock polysaccharides are polysaccharides chemically linked at their reducing end. This design ensures retention of many of their intrinsic properties [1]. These diblock polysaccharides might represent a new class of biomaterials with potential applications in fields such as the plastic industry, the detergency and in pharmaceutics [3].

The exploration of polysaccharide-containing diblocks have attracted increased interest in the biopolymer field due to their new potential applications, as well as their ability to self-assemble into micellar structures, as seen for dextran-*b*-polystyrene in a study by Houga *et al.* [4]. These micellar structures may have potential new applications *e.g.*, as nanocarriers for drug delivery systems [3]. The first chitosan-based diblock was reported by Ganji and Abdekhodaie [5]. They synthesized and characterized a thermo responsive chitosan-*b*-PEG diblock. The diblock was soluble at low temperature but formed a gel at higher temperatures [5].

Chitin is a polysaccharide found in the exoskeleton of shrimp and crabs [1]. Chitosan is a polycationic polysaccharide produced by de-*N*-acetylation of chitin and has a wide range of applications in the biomedical field [6]. Nitrous acid depolymerization of chitosan is a method to prepare chitosan oligomers with a 2,5-anhydro-D-mannose (M) unit at the reducing end. The pending aldehyde of the M-unit makes such oligomers highly reactive and have been exploited to prepare chitosan-containing diblock polysaccharides [1].

Coupling of blocks can be performed by the use of a divalent chemical linker *e.g.*, adipic acid (ADH) or O,O′-1,3-propanediyl-bishydroxyl-amine (PDHA) [1]. The preparation of chitosan-*b*-dextran diblocks have been reported [7, 8]. The chitosan-*b*-dextran diblocks were in these cases prepared by conjugating D_nM-PDHA to $Dext_m$. However, the preparation of chitosan-*b*-dextran diblocks by conjugating D_nM to $Dext_m$-PDHA has not yet been explored. This preparation method is of great interest, as it exploits the highly reactive M-unit. Furthermore, potential new properties of such diblock polysaccharides have not yet been explored.

1.2 Aim

The aim of this master thesis was to prepare and characterize chitosan-*b*-dextran diblocks and to study the properties of the diblock in solution. The work was divided into four parts to achieve this goal:

1. Develop an improved method for preparation of purified and isolated chitosan oligomers with a high yield of 2,5-anhydro-D-mannose (M) units at the reducing end (D_nM-type oligomers).
2. Obtain kinetic data for the conjugation of D_nM to $Dext_m$-PDHA and the subsequent reduction of D_nM=PDHA-$Dext_m$ oximes.
3. Develop a preparative protocol for the preparation of D_nM-PDHA-$Dext_m$ diblocks.
4. Study solution properties of D_nM-PDHA-$Dext_m$ diblocks.

Nitrous acid depolymerization of chitosan is an established method to obtain chitosan oligomers with a 2,5-anhydro-D-mannose (M) unit at the reducing end (D_nM-type oligomers) [1]. This method was chosen to exploit the highly reactive M-unit for the preparation of chitosan-*b*-dextran diblocks. A protocol has not yet been reported for the subsequent preparation of isolated D_nM oligomers with high preservation of the M-unit. The previous method reported the preparation of isolated D_nM oligomers with 50 – 70 % having the M-unit at the reducing end [7, 8]. The conjugation of dioxyamines (*e.g.,* PDHA) to the reducing end of polysaccharides by reductive amination has previously been performed for a range of biopolymers *e.g.*, chitosan, chitin, alginate, and dextran. However, there exists no protocol for the preparation of D_nM-PDHA-$Dext_m$ diblock by conjugating D_nM oligomers to $Dext_m$-PDHA. Thus, it was of interest to develop this protocol and characterize the structure. The chemical structure of the desired diblock of the type D_nM-PDHA-$Dext_m$ is given in Figure 1.1.

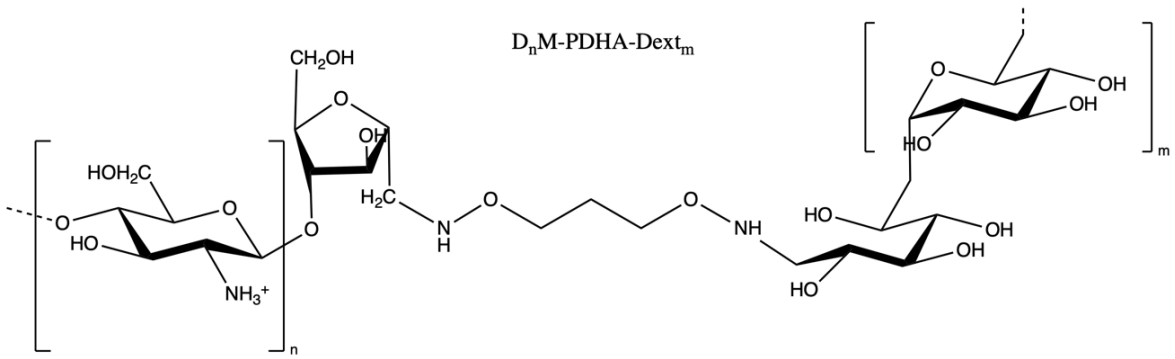

Figure 1.1 Chemical structure of the D_nM-PDHA-$Dext_m$ diblock.

Solution properties of chitosan-*b*-dextran diblocks have not yet been explored. It was therefore of great interest to explore the solution properties of chitosan-*b*-dextran diblocks and compare these with the solution properties of pure chitosan (D_nM) oligomers.

1.3 Contributions of this master thesis

The contributions to chitosan and chitosan-based diblock biopolymer science provided in this thesis includes:

- The development of an optimized method for the preparation of isolated D_nM-oligomers with high preservation of M-unit at the reducing end.
- The development of a new method for the preparation of D_nM-PDHA-$Dext_m$ diblocks by conjugating D_nM to $Dext_m$-PDHA.
- Obtained kinetic data for the conjugation of D_nM to $Dext_m$-PDHA.
- Obtained kinetic data for the reduction of D_nM oligomers.
- Obtained kinetic data for the reduction of D_nM=PDHA-$Dext_m$ diblocks.
- Discovered that unreduced D_nM=PDHA-$Dext_m$ diblocks are not stable at low pH.
- Discovered that chitosan-*b*-dextran diblocks remain soluble at pH > pK_a

2 THEORY

2.1 AB diblocks

Block copolymers (BCPs) are engineered polymers, which consist of two or more polymers linked by covalent bonds. BCPs may be conjugated in several different ways *e.g.*, linear block copolymers, graft copolymers, star-like polymers, cyclic polymers and dendritic polymers [9]. In graft copolymers, one or more homopolymer blocks are grafted as branches onto the backbone of the main chain [3]. Compared to graft copolymers, linear block copolymers, which are polymers conjugated at the reducing end [1], preserve the structure of the polymer *i.e.*, the lateral groups are not modified, and therefore will better preserve the chemical and biological properties of the polymers [10]. In addition, linear block copolymers allow much greater control over nanostructure properties [10].

Linear BCPs containing two types of blocks, A and B, may also have several different structures, see Figure 2.1a [11]. AB diblocks consists of two polymer blocks attached at the reducing end [1], and have been the focus in many studies [11]. The use of natural polymers in these AB diblocks provides a broad range of chemical, physical and biological properties that are very different from synthetic AB diblocks [1]. These properties include biodegradability and biocompatibility, which are important for biomedical applications [3]. The merging of blocks in AB diblocks may involve a non-repeating atom or groups of atoms, called a linker or a conjugating block, see Figure 2.1b [1].

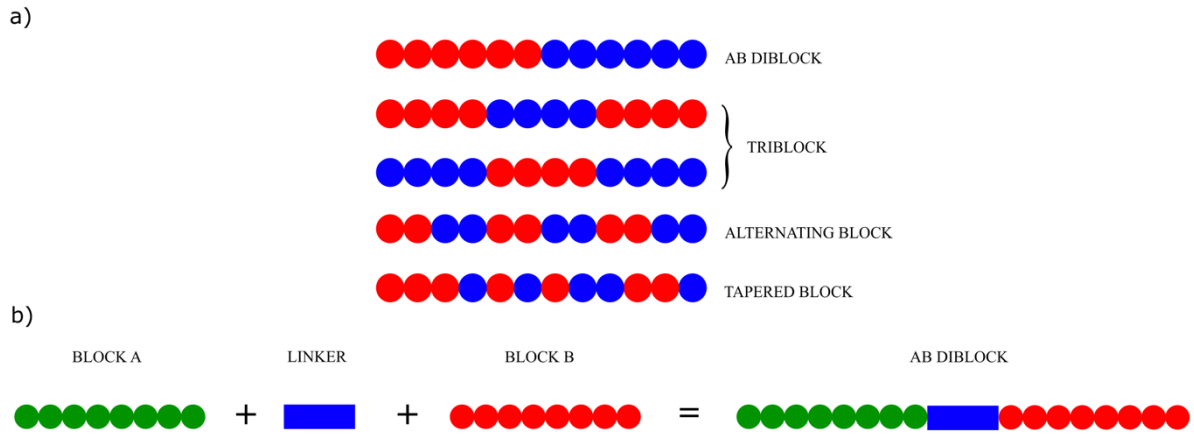

Figure 2.1 a) An illustration of typical structures of linear block copolymers containing two types of blocks (AB diblock, triblock, alternating block and tapered block). b) An illustration of an AB diblock conjugated by a linker molecule.

2.2 Chitin and chitosan

2.2.1 Chitin

Chitin is one of the most abundant naturally occurring biopolymers in nature [12] and is found in the exoskeleton of crustaceans and insects [1], as well as in the cell wall of fungi and some algae [13]. Chitin is therefore available in large quantities as a by-product in aquaculture [1]. Seafood processing industries produce large quantities of unwanted material. This can be exploited as a substrate for chitin and chitosan production, which further can be used in commercial applications, see Figure 2.2 [12].

Figure 2.2 A scheme showing how chitin and chitosan can be extracted from chitinous waste by chemical or biological extraction, which further can be used for commercial applications.

Pure chitin is exclusively composed of β-1,4-linked *N*-acetyl-D-glucosamine residues (A) [1]. However, this structure is rarely found in nature, as the more common form obtained upon extraction includes a limited amount of de-*N*-acetyl-D-glucosamine residues (D) [13]. In practice the fraction of *N*-acetyl-D-glucosamine (F_A) residues in chitin is usually between 0.9 and 1.0 [14, 15]. F_A is defined as

$$F_A = \frac{n_{GlcNAc}}{n_{GlcNAc}+n_{GlcN}} = \frac{n_A}{n_A+n_D} \qquad 2.1$$

where $n_{GlcNAc} = n_A$ is the number of A-units and $n_{GlcN} = n_D$ is the number of D-units in the chitin polymer. The degree of de-*N*-acetylation (DA) may be described by the equation [2]

$$DA = \text{degree of de-}N\text{-acetylation} = (1 - F_A) \times 100\%. \qquad 2.2$$

The residues of chitin have $^4C_1$ chair conformation, which makes the linkages (1,4) di-equatorial. Furthermore, the residues are rotated 180° relative to the neighboring residue [13]. Chitin with a degree of polymerization (DP) above 6 is insoluble in water and crystalline [1]. Due to its low water-solubility and crystallinity, one of the main applications of chitin is using it as raw material for the preparation of chitosan [7].

2.2.2 Chitosan: structure, chemical properties, and solubility

Partial de-*N*-acetylation of chitin provides chitosan [13], *i.e.*, chitin and chitosan have the same chemical structure and differ only by the fraction of A-units that are converted to D-units along the chain [16]. Chitosan based research have increased over the past decades due to chitosan's biodegradability, biocompatibility, non-toxicity, and other unique properties such as film forming ability, chelation and adsorption properties, and antimicrobial activity [15]. The chemical structure of chitosan is provided in Figure 2.3.

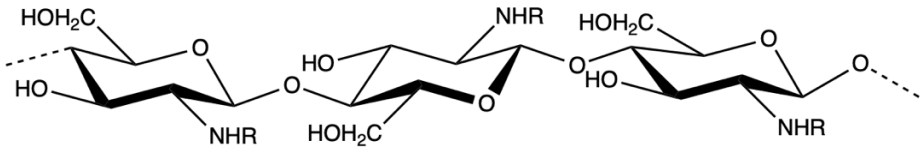

Figure 2.3 The chemical structure of chitosan. When R = H, the residue is D-glucosamine (D-unit); when R = Ac, the residue is N-acetyl-D-glucosamine (A-unit).

The fraction of A-units, as well as the distribution of A-units, has great impact on the solution properties of chitosan [17]. Homogenous deacetylation of chitin provides chitosan with a random distribution of A- and D-units [14]. Alternatively, heterogenous deacetylation provides chitin fractions with high F_A and chitosan fractions with low F_A [13]. Production of *N*-acetyl-D-glucosamine monomers can be obtained by chemical reacetylation of D-glucosamine. Other methods, such as enzymatic degradation of chitin, have also been reported for the production of *N*-acetyl-D-glucosamine monomers [14].

An increased number of charges on high molecular weight chitosan have also pronounced effects on solubility *i.e.*, it can cause insoluble chitosan to become water-soluble. The pK_a value of the amino group in chitosan has been determined to be 6.5. The solution properties of chitosan is responsive to the changes in pH [17]. Chitosans (F_A 0.1 – 0.2) are soluble at pH < pK_a, but precipitates at pH > pK_a [18]. In contrast, chitosan (F_A > 0.2) are soluble at much higher pH values [13]. Hence, the polyelectrolyte properties of chitosan are intimately related to acid-base properties, as charges can be turned on and off simply by varying the pH [19]. In chitosan, the -NH_2 groups are bases, which involves the equilibrium:

$$-\mathrm{NH_3}^+ \leftrightarrow -\mathrm{NH_2} + \mathrm{H}^+. \qquad 2.3$$

Polycationic chitosan with low F_A precipitates from aqueous solutions when the charged amino group ($-NH_3^+$) deprotonates into ($-NH_2$), resulting in a neutral polymer. Due to chitosans cationic properties, chitosans may interact with almost all kinds of surfaces, particles, cells, and macromolecules that are negatively charged, which is the basis for a wide variety of applications. Moreover, chitosans may be used in dietary supplements, water treatment, food preservation, agriculture, cosmetics, and medical applications [15].

2.2.3 Chitooligosaccharides

Chitooligosaccharides (CHOS) may be obtained by chemical or enzymatical degradation of chitin or chitosan [13]. CHOS are often defined as chitosans with a DP < 20, *i.e.*, with average molar masses lower than 4000 g/mol. The CHOS have some unique properties such as water solubility, cell membrane penetrability, easy absorption, and various biological activities. Lower molar masses also produces less viscos solutions, which makes it easier to work with higher concentrations [16]. The biological activities of CHOS include antimicrobial [20], anti-inflammatory [21] and antioxidant properties [22], which have been thoroughly studied over the last decades [23]. CHOS have also been reported to have neuroprotective effects for Alzheimer´s disease treatment [24], as well as being used in treatment for asthma, prevent tumor growth and controlling blood pressure [16].

The hydrochloride form of CHOS is completely soluble if dissolved in dilute conditions as it results in a solution pH of approximately 4. The solubility of CHOS as a function of pH can be determined by light scattering. Light scattering is a sensitive technique than can detect aggregation and precipitation phenomena, see Section 2.10.3. Figure 2.4 (left) shows how the onset of precipitation is observed within a narrow range of pH values. Furthermore, the corresponding critical pH values are lowered when the DP is increased and becomes constant from a DP of approximately 27, see Figure 2.4 (right). As seen in Figure 2.4 (right), the degree of protonation (γ) also increases with the DP and becomes constant from a DP of approximately 27 [25].

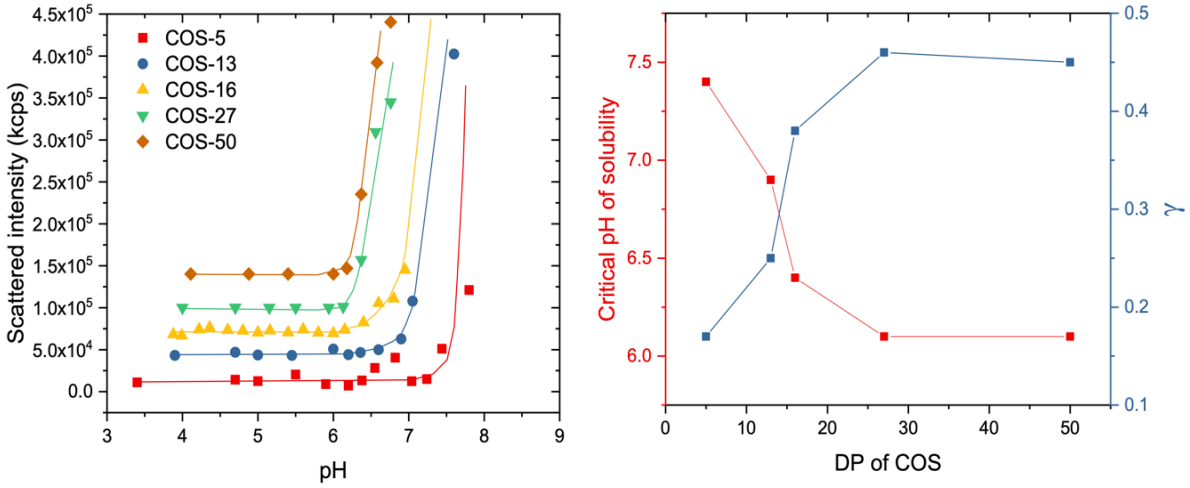

Figure 2.4 Left: The variation of scattering light intensity (in kcps, kilo counts-per-second) of CHOS/COS solution at 1mg/ml as a function of the pH. The plots are shifted along the y-axis for better visibility. **Right:** The variation of the pH at the onset of the CHOS precipitation as a function of the DP (in red). The corresponding values of degree of protonation (γ) at the critical pH are also plotted (in blue). The lines were added to guide the eye [25].

2.3 Nitrous acid depolymerization of chitosan

2.3.1 The mechanism of nitrous acid depolymerization of chitosan

Many different degradation methods of chitosan have been described in the literature, including chemical methods, enzymatic methods, mechanical methods and the use of high energy radiation [26]. Although being very precise, enzymatic methods are expensive and difficult to apply on a large scale. Physical methods are mostly used to reduce molar masses and viscosities of chitosan solutions, as they do not lead to the formation of oligomers. Furthermore, physical methods are often combined with chemical methods, but are hard to control and reproduce [16].

Nitrous acid (HNO_2) depolymerization of chitosan, which is a type of acid hydrolysis, produces oligomers with a 2,5-anhydro-D-mannose (M) unit at the reducing end [16, 27]. The mechanism involves a deamination of D-glucosamine (D-units) forming M-units at the reducing end of the newly formed oligomers [17], see Figure 2.5. Nitrous acid depolymerization of chitosan can produce chitin oligomers (A_nM), chitosan oligomers (D_nM) or oligomers with a mixture of A- and D-units with the M-unit at the reducing end [1]. In D_nM- and A_nM-oligomers n refers to the number of D or A residues. The degree of polymerization for such oligomers is therefore, DP = n + 1 [1].

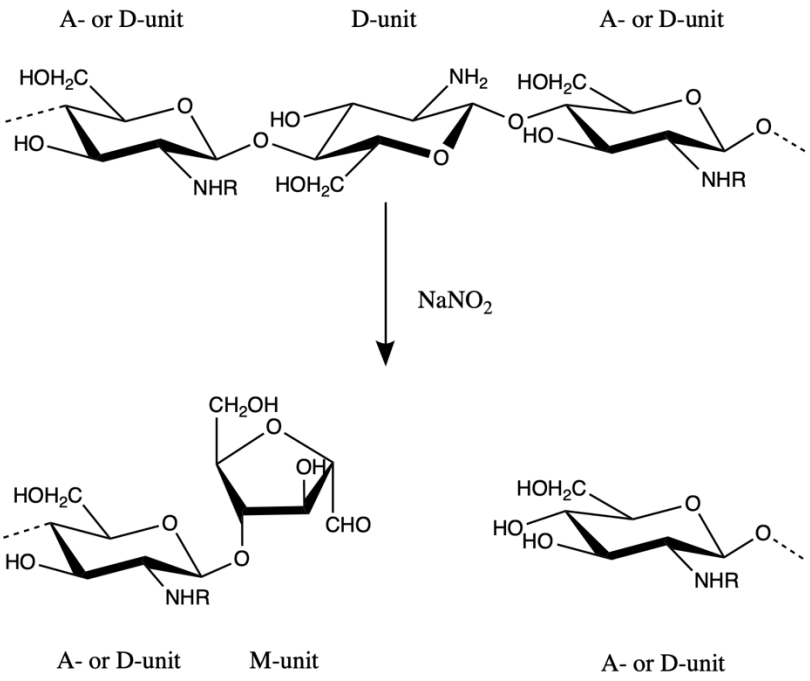

Figure 2.5 The mechanism by which the nitrous acid reaction leads to chain cleavage of a chitosan, resulting in oligomers with 2,5-anhydro-D-mannose at the reducing end. When R = H, the residue is D-glucosamine (D-unit); when R = Ac, the residue is N-acetyl-D-glucosamine (A-unit).

The nitrous acid only affects the D-units of chitosan, as the A-units are acetylated and therefore protected from chemical attack [28]. The homogenous deamination reaction is expected to occur randomly [28]. A_nM-oligomers can be obtained by using an excess of nitrous acid, while D_nM-oligomers are obtained by using restrained amounts, since the number of cleaved linkages corresponds roughly stoichiometrically to the amount of added nitrous acid [17]. The molecular size distribution of D_nM-oligomers can therefore be precisely modified by depolymerization with nitrous acid [28].

2.3.2 2,5-anhydro-D-mannose (M-unit)

Oligomers with an M-unit at the reducing end are particularly reactive due to the pending aldehyde of the M-unit, which has been exploited to prepare self-branched chitosans [17], see Section 2.3.3, as well as a range of end-activated chitosan oligomers for the preparation of chitosan-containing diblocks [1]. The M-unit is a furanose, see Figure 2.6, and is found to be quite unstable as a reducing end. The standard procedure to prevent M-unit degradation has therefore been to use sodium borohydride ($NaBH_4$) to reduce the 2,5-anhydro-D-mannose residue to a 2,5-anhydro-D-mannitol residue [7, 17].

The aldehyde of the M-unit exists in both the hydrated form (gem diol) (-$CH(OH)_2$)) and the free aldehyde form (-CHO). The gem diol is found to be the most abundant [17]. An advantage the M-unit has over a normal reducing end is that the M-unit does not mutarotate in solution, meaning it does not participate in the hemiacetal-aldehyde equilibrium and is more available for chemical reactions. This makes D_nM oligomers an interesting precursor in chitosan-containing diblocks [17].

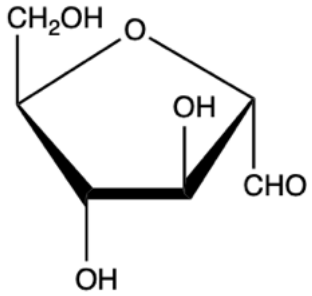

Figure 2.6 Chemical structure of the 2,5-anhydro-D-mannose (M) unit.

2.3.3 Side reactions of the M-unit in D_nM-oligomers

D_nM-oligomers may react intermolecularly if the pH > 4.5, see Figure 2.7. Self-branching by Schiff base reaction occurs between the amino group of the D-unit and the aldehyde of the M-unit. The reaction results in a reversible imino bond with the release of a water molecule. Reduction of the Schiff base results in a secondary amine. Acidification of the Schiff base facilitates cleavage of the glycosidic bonds next to the M-unit and the formation of 5-hydroxymethylfurfural (HMF). This reaction is known as Maillard browning, and HMF is produced by two eliminations of water followed by chain cleavage [17]. The formation of Schiff bases and the following side reactions are not ideal when preparing D_nM-oligomers as precursors for chitosan-*b*-dextran diblocks, due to loss of the highly reactive M-unit. However, the formation of HMF (loss of M-unit) can be avoided by maintaining a low pH, which prevents self-branching by Schiff base reaction [17].

Tømmeraas *et al.* [17] discovered that the M-unit in D_nM oligomers was unstable because of the preparation procedure. The oligomers were first separated by size-exclusion chromatography (SEC), using a buffer containing ammonium acetate and acetic acid, to obtain narrow fractions of D_nM oligomers. During the freeze-drying process of the isolated D_nM oligomers from the buffer, the pH value changed from 4.5 to 8 as water and acetic acid

evaporated first, leaving ammonia. The D_nM oligomers were therefore deprotonated during freeze-drying to give a strong nucleophile, which reacted with the aldehyde of the M-unit.

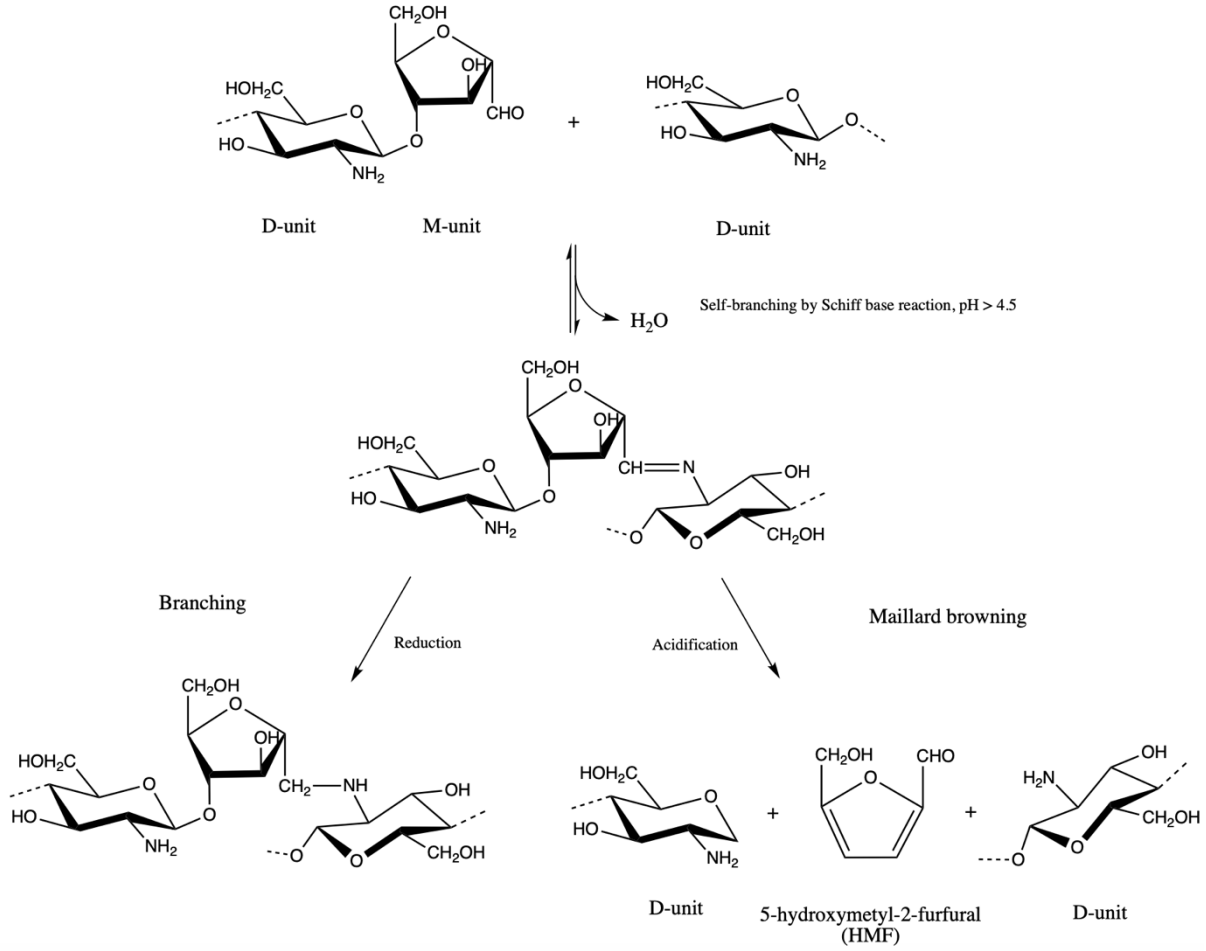

Figure 2.7 Side reactions of the M-unit in D_nM oligomers. Self-branching by Schiff base reaction when pH > 4.5. Reduction resulting in branching and acidification resulting in Maillard browning and loss of M-unit.

2.4 Dextran

Dextran is a highly flexible branched polysaccharide comprised of α-1,6-linked D-glucose residues as the main chain, see Figure 2.8, with short branches consisting of α-1,6 glucans attached by α-1,2, α-1,3 or α-1,4 linkages. Dextran is produced by bacteria and the degree and nature of branching depends on the bacterial strain. Dextran may be used for both medical and industrial applications [29]. The natural polysaccharide has been suggested as a natural analogue to the synthetic polymer polyethylene glycol (PEG) as it is biocompatible, biodegradable and has low immunogenicity [30]. Dextran is also highly water-soluble and the α-1,6-linkages gives the polysaccharide considerable conformation flexibility due to free rotation at three single bonds [29].

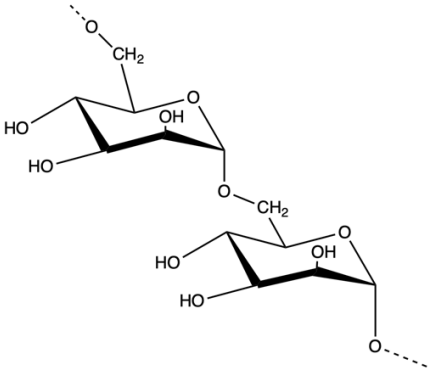

Figure 2.8 The structure of the main chain of dextran.

2.5 Reductive amination

Reductive amination is a chemical reaction in two steps, where carbonyls react with amines to form imines (Schiff bases) followed by an irreversible reduction resulting in stable secondary amines [13], see Figure 2.9. The reaction rate of the amination reaction depends on the pH and is catalyzed by acid. This is due to the protonation of the carbonyl oxygen which makes it susceptible to nucleophilic attack by the amine, which must have an unshared electron pair to be reactive [13]. Thus, the pH of the reductive amination reaction should be optimized for the product formation, which is estimated to be the pH close to, but not below, the pK_a value of the amine used in the reductive amination reaction. Furthermore, Borch *et al.* [31] discovered that the selectivity of the reducing agent may also depend on the pH of the reaction mixture. Reductive amination is commonly used in polymer chemistry [32], and has been used for the preparation of AB diblocks or conjugating a polysaccharide to a dihydrazide (*e.g.* ADH) or a dioxyamine (*e.g.* PDHA), as demonstrated for A_nM-*b*-MA_n diblocks and A_nM-ADH/PDHA conjugates performed by Mo *et al.* [1].

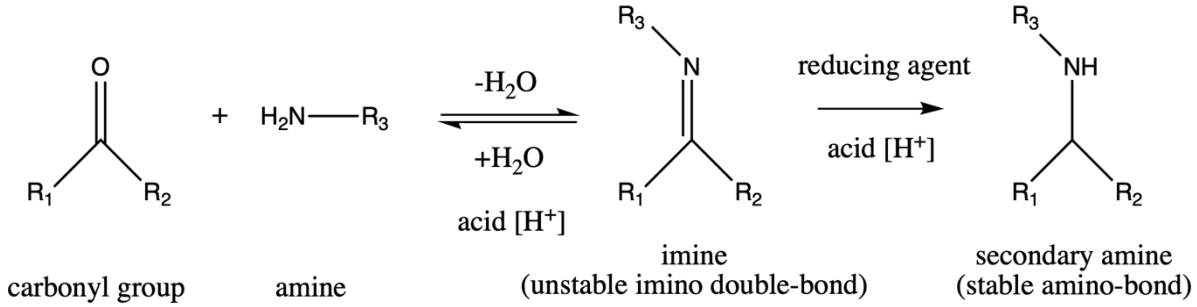

Figure 2.9 Reaction mechanism for reductive amination. A carbonyl group and an amine condense to form an imine with an unstable imino double bond. Reduction of the imine by a reducing agent results in a secondary amine with a stable amino bond.

2.6 α-picoline borane (PB) as a reducing agent for reductive amination

Reductive amination requires a reducing agent that selectively reduces the imine intermediates over the aldehydes and ketones [13], to irreversibly transform the unstable imine intermediate to a stable secondary amine [33]. A commonly used reducing agent for reductive amination is sodium cyanoborohydride ($NaBH_3CN$), which is selective towards reduction of imines under certain conditions. The selectivity of the cyanohydridoborate anion (BH_3CN^-) was observed to be strictly pH dependent, with an optimal pH in the range of 6 – 8 [31], whereas aldehyde reduction was favored in the pH range 3 – 4 [13]. Hence, the reduction of the aldehydes could be prevented by controlling the pH of the reaction [31]. A major disadvantage of the use of sodium cyanoborohydride as a reducing agent is the formation of the toxic and volatile compound hydrogen cyanide (HCN) upon hydrolysis. This resulted in a search for an alternative reducing agent for reductive amination [34].

α-picoline borane (PB), see Figure 2.10, is a relatively new reducing agent, which has been applied for end labeling of polysaccharides and glycans by reductive amination [2]. The reducing agent is non-toxic and a commercially available alternative to $NaBH_3CN$. The use of PB over $NaBH_3CN$ has been found to be an advantage, as the health risk is reduced and it has a lower environmental toxicity [34]. PB is a stable solid and can be stored for long periods of time without detectable decomposition [35]. Successfully reductive amination reactions of a variety of aldehydes and ketones with primary and secondary amines using PB have been confirmed [35]. PB have shown to be equally efficient as $NABH_3CN$ for reductive amination reactions and can be used under both aqueous and non-aqueous conditions [34, 35].

Since local flexibility, as well as charge and pK_a are generally different for the reduced and unreduced forms, reduction may also be used to tailor the properties of polysaccharides [2]. Finally, the rate of the reduction using PB depends significantly on the nature of the reducing end residue. This finding was established when the reduction of dextran oligomers was compared the reduction of chitin oligomers (A_nM) [2].

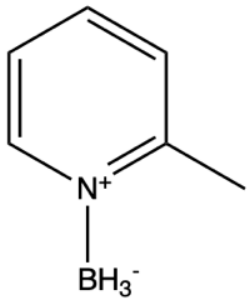

Figure 2.10 The chemical structure of α-picoline borane (PB).

2.7 O,O'-1,3-propanediylbishydroxylamine as a chemical linker

O,O'-1,3-propanediylbishydroxylamine (PDHA) is a dioxyamine and has been exploited in conjugation reactions with the reducing end of polysaccharides via the reductive amination pathway [2]. Oxyamines have also been applied for several other applications *e.g.*, to introduce fluorescent tags [36]. PDHA is a symmetrical molecule with amino groups as reactive ends, see Figure 2.11, and can therefore be used as a chemical linker to obtain AB diblocks. The conjugation of polysaccharides with oxyamines are reversible, and the stability of the conjugates may vary considerably [2]. Oxyamines form acyclic oximes (Schiff bases) with polysaccharides, both in the (E)- and (Z)-configuration, in equilibrium with cyclic N-glycosides [2], but the relative distribution of conjugates depends on the chemistry of the reducing end residue [37]. When oxyamines are conjugated with chitooligosaccharides with an M-unit at the reducing end (D_nM-type oligomers), only E- and Z-oximes are formed [1].

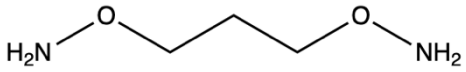

Figure 2.11 The chemical structure of O,O'-1,3-propanediylbishydroxyl-amine (PDHA).

2.8 Properties and applications of polysaccharide block copolymers

Conjugating a second block to the reducing end of a polysaccharide may alter the solution properties of that polysaccharide *e.g.*, the solubility. Recently, Delas [25] conjugated chitosan oligomers to mPEG hydrazides and performed a study on the solubility of the diblocks compared to that of chitosan oligomers alone as a function of the pH. Turbidimetry was used to assess the solubility, since the optical density (OD) increases when the solubility of the polymer decreases. As seen in Chapter 2.2.3, the solubility of a chitosan oligomer will strongly depend on the pH of the solution, leading to aggregates when the critical pH of solubility is reached. Figure 2.12 illustrates that the chitosan-containing diblock are soluble over a larger pH range due to the introduction of a long hydrophilic PEG block [25].

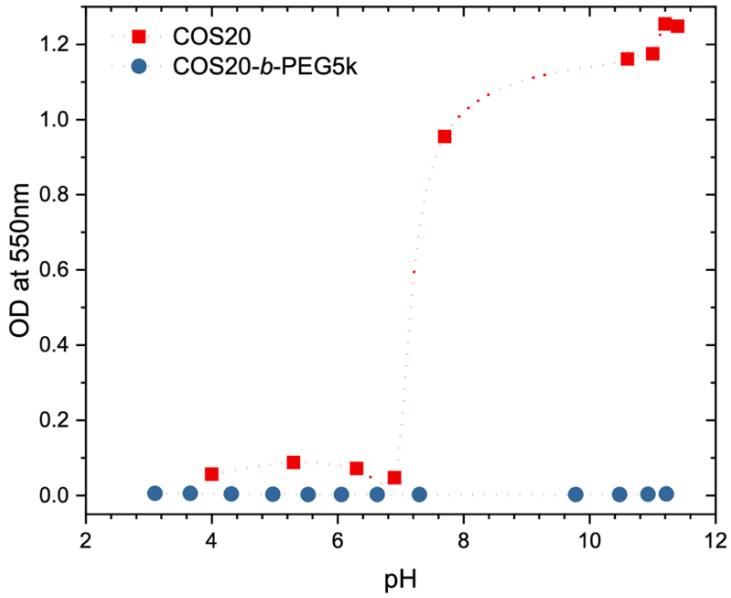

Figure 2.12 Turbidimetry of solution of COS20 (CHOS, DP = 20) and COS20-b-PEG5k at 2 g/L as a function of pH. The optical density of the solution is measured at λ = 500 nm [25].

Self-assembly properties of block copolymers (BCPs) in solution have attracted considerable attention in nanotechnology and biopolymer science for several decades, due to their potential applications in many fields, such as biomedicine, biomaterials, microelectronics and photoelectric materials [9, 11]. BCPs have shown to yield ordered structures in a wide range of morphologies, including spherical and cylindrical micelles, bicontinuous structures, lamellae, and vesicles, among others. In addition, polymer aggregates exhibit higher stability and durability, compared to small-molecule aggregates [11]. Li and Zhang [38] synthesized a maltoheptaose-*b*-PCL diblock and discovered that it could self-assemble into nanosized spherical micelles in aqueous solution. The self-assembly was induced by dissolving the

diblock in a common solvent followed by the addition of a selective solvent for one of the blocks resulting in the formation of the micellar core [38]. Drug nanocarriers assembled from polypeptides-based block polymers have been reported [39].

Polysaccharides have great potential for biological applications *e.g.*, in therapy or medical diagnosis, due the their biocompatibility and their capacity to develop specific interactions towards biological substrates [3]. Polysaccharide-containing BCPs present a new class of biomaterials, in addition to their self-assembly properties [1], with potential applications in many different fields, such as the plastic industry, the detergency, cosmetics and the pharmaceutics. For instance, some studies show that polysaccharide-containing block copolymers may be used as surfactants in aqueous solutions [3], and Kallin *et al.* [40] researched the use of polysaccharide BCPs for immunizing antigens.

The use of polysaccharides in AB diblocks provides biodegradability properties and makes them very attractive for environmentally sensitive applications. The presence of a synthetic block in polysaccharide-containing diblocks have been suggested to slow down the degradation of the polysaccharide chain [3]. Kim *et al.* [41] prepared cellulose-*b*-polyether block copolymers and reported a slightly decrease in the enzymatic degradation rate of these polysaccharide-containing diblocks compared to that of pure cellulose. The slight decrease was assumed to be due to the restricted accessibility of the cellulose in the polysaccharide-containing copolymer chain.

2.9 Analysis methods and techniques

2.9.1 Size exclusion chromatography (SEC)

Chromatography is the collective term for several separation methods where molecules are separated based on differences in hydrodynamic volume, charge, solubility, volatility etc., and have become a valuable analytical tool in many areas of analytical chemistry. The main types of chromatography include gas chromatography (GC) and liquid chromatography (LC), where the separation technique employs two phases: one stationary phase and one mobile phase. The designations GC and LC indicate the physical state of the mobile phase, a gas or a fluid, respectively [42]. The mobile phase transports the sample components into contact with the stationary phase throughout a column or another carrier of the stationary phase. Due to different interactions between the sample components and the stationary phase, the sample components migrate through the system at different speeds and elute from the column with different retention times. The retention time is defined as the time between the sample introduction and the elution from the column, where a detector provides a signal for eluting components. The signals from the detector are usually visualized as a function of time, a chromatogram [43].

Most biopolymers, particularly polysaccharides, are disperse, which means that a description of the molecular weight distribution requires fractionation and quantification of the relative amount of the different molecular weight classes in the sample [19]. This can be achieved experimentally using size-exclusion chromatography (SEC), which separates the polymers based on differences in hydrodynamic volume [43]. The SEC system is comprised of a pump, an injector, one or multiple SEC columns, one or multiple on-line or off-line detectors, a sample collector and a computer analysis system as illustrated in Figure 2.13.

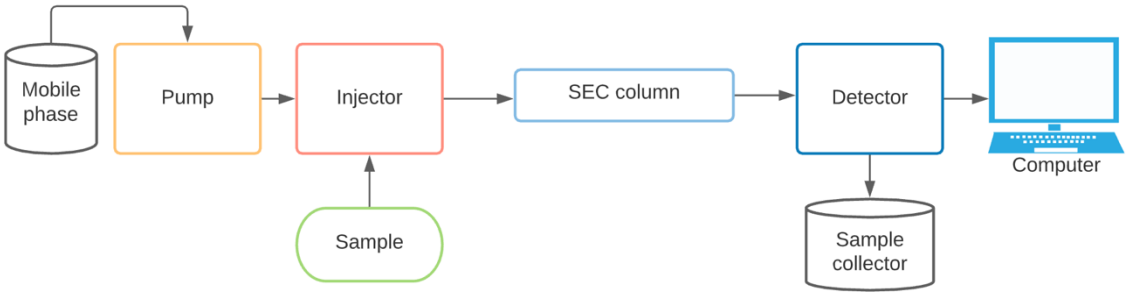

Figure 2.13 Schematic overview of a standard size exclusion chromatography setup. A SEC system is comprised of a pump, an injector, one or several SEC columns, a detector, a sample collector, and a computer system. A mobile phase is continuously eluting through the system and the sample can be injected into the injector.

The disperse sample is dissolved in the mobile phase and injected into the SEC-system. The sample will then elute through the SEC column containing porous particles *i.e.*, the stationary phase. The smaller oligomers will to a larger extent, compared to larger oligomers, penetrate the pores and will therefore be more retained compared to the larger ones. The oligomers small enough to penetrate all the pores, and smaller, will eluate together. Moreover, the oligomers that are too large to penetrate into the pores are excluded and will not be retained inside to SEC-column [19, 43]. Separation of biopolymers by SEC may also be called gel filtration chromatography (GFC).

The distribution of pore sizes should match those of the molecules to be separated. The columns used to separate oligomers may be solids ranging from synthetic polymers to glasses [19]. When choosing the mobile phase, there are some requirements that need to be meet. Firstly, it should be a good solvent for the sample. It should also have low viscosity, not interact with the stationary phase and be compatible with the detector being used. There are several types of detectors, *e.g.* ultraviolet (UV) detector or refractive index (RI) detector, which depends on what compound that are separated [43].

At any given time during the migration through the system, there is a distribution of molecules of each component between the two phases: $k = n_s/n_m$, were n_s and n_m are the number of molecules in the stationary and mobile phase, respectively, at a given time, and *k* is the retention factor. If one component migrates through the column in the mobile phase only, with no interactions with the stationary phase, the migration time is called t_M. An analyte with interactions with the stationary phase will be retained and will elute at t_R [42]:

$$\mathrm{t_R = t_M + t_M k = t_M(1 + k)} \qquad 2.4$$

2.9.2 SEC combined with a multi-angle light scattering (MALS) detector

Size-exclusion chromatography combined with a multi-angle light scattering detector (SEC-MALS) is one of the most common methods to determine molecular weight distribution. The method is based on the use of two on-line detectors in the chromatography system: a concentration sensitive detector and a light scattering detector [19]. The Debye equation is the basis of the calculations performed in SEC-MALS:

$$\frac{\mathrm{R_{\theta,i}}}{\mathrm{Kc_i}} = \mathrm{M_i P_i(\theta) - 2A_{2,i} c_i {M_i}^2 {P_i}^2(\theta)} \qquad 2.5$$

where $R_{\theta,i}$ is the Rayleigh factor, c_i is the concentration, M_i is the molar mass, $A_{2,i}$ is the second virial coefficient, $P_i(\theta)$ is the particle scattering function and K is an optical constant [44].

The data processing software records raw data from the detectors at regular intervals. A single experiment can be divided into 1000-5000 elution slices, which are stored in the computer memory and processed separately. The software calculates $\frac{R_{\theta,i}}{Kc_i}$, M_i and $R_{G,i}$ (only for molecules with an R_G > 10 nm) for each elution slice. R_G is the radius of gyration and may indicate whether the polymer is very expanded or very contracted. A_2 is not determined in SEC-MALS and needs to be known from separate experiments or literature [19, 44].

2.9.3 Dynamic light scattering

Dynamic light scattering (DLS) is a widely known characterization technique to obtain information about the size of molecules and particles in dilute solutions [44]. Light scattering occurs when light interacts with matter. The intensity of light scattered by a dilute polymer solution consists of the intensity scattered by macromolecules, as well as the intensity scattered by the solvent itself. The difference between the two scattered intensities contains information about the polymers hydrodynamic radius and their state of motion [45]. There are several types of light scattering techniques *e.g.*, static light scattering and dynamic light scattering. In dynamic light scattering, the wavelength measured is the same wavelength as that of the incident light and the fluctuations of the scattered light intensity over time are measured [44].

The intensity of scattered light fluctuates, due to Brownian motion of the scattering particles, which is random movement of particles as a result of collisions with surrounding particles. Hence, the fluctuation of intensity reflects the motion of the scattering particles. Large particles move more slowly compared to smaller particles; thus, the light scattering intensity of larger particles fluctuates more slowly compared to smaller particles. The intensity fluctuation is analyzed by transformation into an intensity autocorrelation function using correlator hardware. The autocorrelation function expresses the probability that after time delay τ the intensity of the scattered light will be identical to that in the initial time [44], and is defined as

$$g(\tau) = \frac{I(t)I(t+\tau)}{I(t)^2}, \qquad 2.6$$

where $I(t)$ is the detected intensity as a function of time (t), $I(t)^2$ is the average scattered intensity squared and τ is a delay time. The correlation is high at short delay times, due to the particles not having enough time to change their position to great extent compared to the original position. In this case, the two signals are almost identical. However, with increasing time delay, the correlation will begin to exponentially decrease, due to no correlation between the scattering intensity at the initial time (t) and the final time $(t + \tau)$. A slow decay indicates large molecules, while faster decay indicates smaller molecules [44].

The translation diffusion coefficient (D) of the particles can be determined by the autocorrelation analysis. Assuming the shape of the particles are spherical, the diffusion coefficient may be used to calculate the hydrodynamic radius (R_H) of the particles by the Stokes-Einstein relation:

$$R_H = \frac{kT}{6\pi\eta D} \qquad 2.7$$

here (k) is the Boltzmann´s constant, T is the absolute temperature and η is the viscosity. The hydrodynamic radius (R_H) is the radius of the hydrodynamically equivalent sphere with the same diffusion coefficient as the particles being analyzed. The diffusion coefficient and the hydrodynamic radius can only be accurately measured for dilute solutions [44].

The autocorrelation function may present two decays for a mixture of small and large particles. A fast decay for the smaller particles and a slow decay for the larger particles. The autocorrelation function of light scattered from a polydisperse solution is described by the sum of the autocorrelation functions of all particles, weighed by their normalized intensities. The size distribution is obtained by analysis of the autocorrelation function. Different types of distributions *e.g.*, intensity %, mass % or number %, are measured by different analytical methods. The two latter distributions are shifted towards lower hydrodynamic radii compared to the intensity distributions [44].

2.9.4 Proton nuclear magnetic resonance (^{1}H-NMR) spectroscopy

Nuclear magnetic resonance spectroscopy (NMR) is an important analytical tool in biochemistry and polymer chemistry. The method is used for structural characterization of organic molecules and is based on the quantum mechanical properties of the atomic nuclei [46].

The intrinsic angular momentum associated with the magnetic nucleus may be described by the concept of *nuclear spin* [46]. The nuclear spin angular momentum is described in terms of its nuclear spin quantum number *I*. The nuclear spin quantum number depends on nuclear mass and atomic number, and have values of 0, ½, 1, 3/2, etc., with $I = 0$ meaning no spin. The intrinsic magnitude of the magnetic dipole is expressed in terms of the nuclear magnetic moment, μ. The nuclear spin quantum number *I* for ^{1}H is ½. The spin number *I* determines the number of quantum mechanical states (m) in accordance with the formula $2I+1$ [46].

For nuclei with spin of ½, there are two energy states, one upper energy state and one lower energy state ($N_\alpha > N_\beta$) [46]. The energy difference between the two states, ΔE, is given by

$$\Delta E = \left(\frac{h\gamma}{2\pi}\right) B_0 = h\nu \qquad 2.8$$

where γ and π are constants, v is the frequency of radiation in megahertz (MHz) and h is Planck´s constant. B_0 corresponds to the magnetic field strength [46].

The NMR instrument provides electromagnetic pulses of high-power radiofrequency energy, which excites all the ^{1}H nuclei in the sample. When the nuclei are excited to a higher energy state, the radiation is absorbed. The radiation released when the excited nuclei return to equilibrium is recorded and digitized by a computer as resonance signals. Due to the nuclear shielding effect electrons have on protons, different protons in a molecule will absorb energy at different radiofrequencies [46]. The degree of shielding depends on the density of circulating electrons.

Characterization of a molecule by ^{1}H-NMR provides a spectrum of chemical shifts given in ppm for the protons in the molecule. Protons in different chemical environments in the molecule give rise to various chemical shifts. Characterization by ^{1}H-NMR is a non-destructive analysis method.

^{1}H-NMR analysis of chitosan oligomers

Chitosan oligomers have previously been characterized by ^{1}H-NMR. A ^{1}H-NMR spectrum of a chitosan oligomer standard (DP = 4) is presented in Figure 2.14, with the chemical shifts (ppm) for the protons assigned by Domard *et al.* [47]. The chemical shifts of a chitosan oligomer (DP = 3) in D_2O at 30 ℃ (pH* ≈ 4.25) are given in Table 2.1. Domard *et al.* [47] discovered that the chemical shifts of the various protons of chitosan oligomers are sensitive to variations in pH. A ^{1}H-NMR study of the pH dependence on the behavior of the chitosan oligomers revealed that the chemical shifts decrease with increasing pH. Moreover, the α/β ratio also varied with the pH. Furthermore, a second experiment revealed that the chemical shifts of a chitosan oligomer (DP = 3) also depend on temperature. The ppm increases with increasing temperature [47].

Table 2.1 ^{1}H-NMR chemical shifts for a chitosan oligomer (DP = 3) in D_2O at 30 ℃ (pH* 4.25) [47].

	Chemical shifts (ppm)						
	H-1	H-2	H-3	H-4	H-5	H-6a	H-6b
1α	5.23	3.13	3.83	3.67	3.85	3.65	3.56
1β	4.75	2.83	3.67	[a]	[a]	[a]	[a]
2	4.66	2.96	3.67	[a]	[a]	[a]	[a]
3	4.63	2.92	3.48	3.28	3.33	3.77	3.57

[a]Assignment of these protons – which resonate in the 3.5-3.9 ppm region – were not possible, due to signal overlapping.

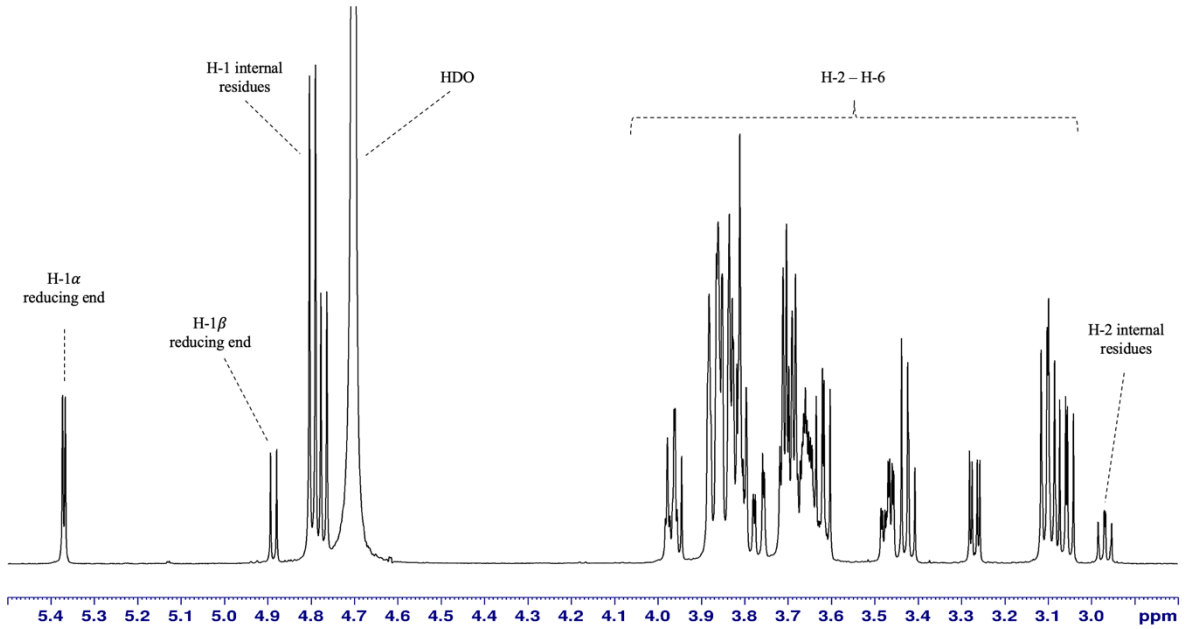

Figure 2.14 ^{1}H-NMR spectrum of a chitosan oligomer standard (DP = 4), 25 ℃, 600 MHz, pH* 6.0.

^{1}H-NMR spectrum of D_nM-oligomers produced by nitrous acid degradation of chitosan

Chitosan oligomers produced by nitrous acid degradation of chitosan have previously been characterized by ^{1}H-NMR. The chemical shifts (ppm) for the protons in the M-unit and the D-units of chitosan oligomers produced by nitrous acid degradation of chitosan have been assigned by Tømmeraas *et al.* [17], and are listed in Table 2.2. A ^{1}H-NMR spectrum of a D_nM-oligomers after self-branching by Schiff base reaction, pH > 4.5 and a ^{1}H-NMR spectrum after Maillard browning, is presented in Figure 2.15.

Table 2.2 ^{1}H-NMR (400.13 MHz) chemical shifts (ppm) for the reducing end (M-unit) on a N-deacetylated trimer (D-D-M) in D_2O at 43℃ and pH* 5.7 [17].

	Chemical shifts (ppm)								
M-unit	H-1, free aldehyde	H-1, gem diol	H-1, Schiff base	H-2	H-3	H-4	H-5	H-6a	H-6b
	9.49	5.09	7.93-7.97	3.84	4.44	4.22	4.13	a	a
D-units	H-1 α	H-1β							
	5.44	4.92							

[a]Assignment of these protons – which resonate in the 3.5-3.9 ppm region – was not possible, due to signal overlapping.

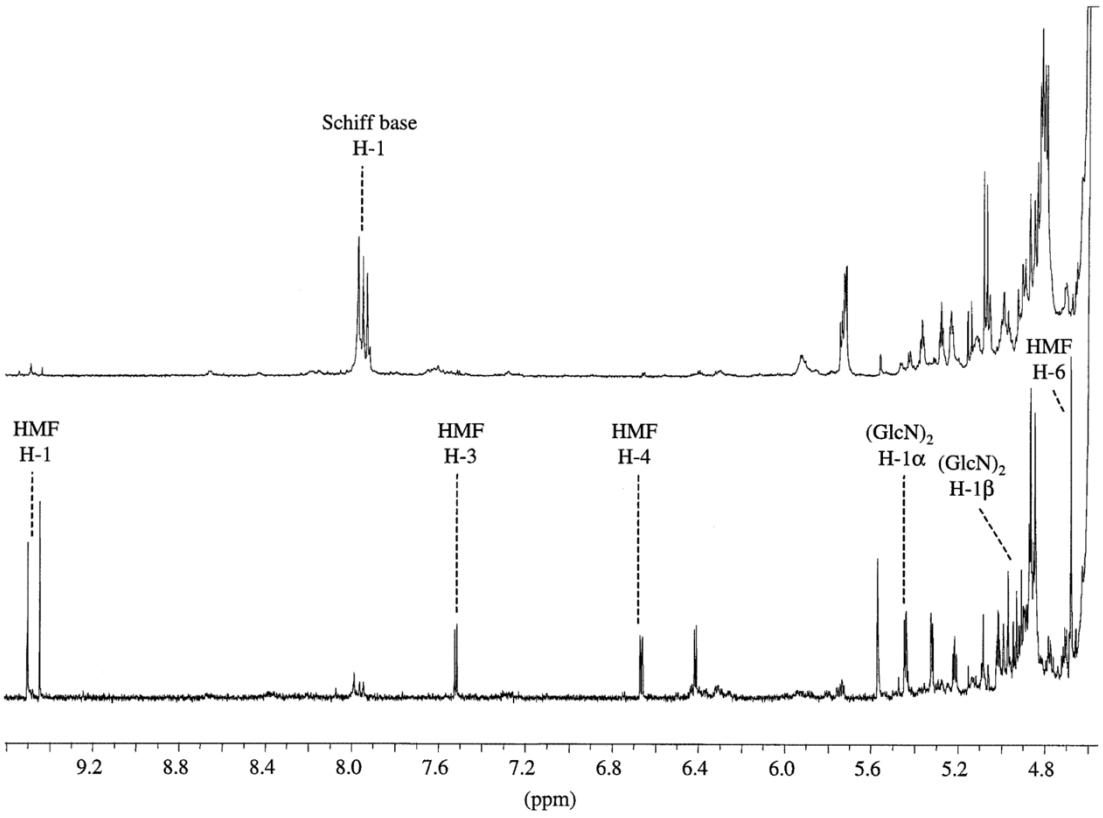

Figure 2.15 ^{1}H-NMR spectrum (400.13 MHz, 43 ℃ in D_2O) of a N-deacetylated trimer (D-D-M) after lyophilization: Top: pH* 5.7. The intensities of the imino protons (Schiff base) are indicated in the spectrum (8.1 ppm). Bottom: pH* 4.0 (adjusted with 0.1 M DCl). The resonances of HMF and the reducing end of the GlcN-dimer (D-D) are indicated [17].

^{1}H-NMR spectrum of dextran oligomers

Dextran has previously been characterized by ^{1}H-NMR [48, 49], and the chemical shifts are listed in Table 2.3.

Table 2.3 ^{1}H-NMR chemical shifts (ppm) of dextran according to Paulo *et al.* [48] and Cheetham *et al.* [49].

Proton	Chemical shift (ppm)
H-1 α	5.22
H-1 β	4.63
H-1 non-reducing end	4.95
H-1 branches	5.28
H-2	3.58
H-3	3.74
H-4	3.53
H-5	3.92
H-6	3.99

By comparing the intensities of the H-1 non-reducing end with H-1 α and H-1 β, the DP of the sample can be found by the equation

$$\mathrm{DP_n} = \frac{\mathrm{H{-}1\ non\ reducing\ end}}{\mathrm{H{-}1\alpha + H{-}1\beta}}, \tag{2.9}$$

and the degree of branching (DB) can be found by

$$\mathrm{DB} = \frac{\mathrm{H{-}1\ branches}}{\mathrm{H{-}1\ branches + H{-}1\alpha + H{-}1\beta + H{-}1\ non{-}reducing\ end}}. \tag{2.10}$$

2.9.5 Dialysis

Dialysis is a method to remove *e.g.*, salts and other unwanted small contaminants or products from an aqueous solution. In polymer science, a dialysis bag, with varying sized pores, made from cellulose or cellulose derivatives is often used to purify a polysaccharide sample. The dialysis bag behaves as a semi permeable membrane, containing the biopolymer inside the bag during the purification process. The pore diameter determines the molecular weight cut off (MWCO), which is chosen depending on the purpose of the dialysis. The solution containing the biopolymer is contained in the dialysis bag closed off from the solution it is submerged in. Depending on the dialysis, the solution may be either pure water, water containing salts or other molecules. Moreover, small molecules, ions and other small products can diffuse through the pores in the membrane, purifying the biopolymer solution. In theory, a dialysis bag with a molecular weight cut-off point at 100 Da will contain all molecules above this size inside the bag, while smaller molecules may diffuse through the membrane. Although, polysaccharides with the shape of *e.g.*, a random coil, which might be elongated in solution, may be retained inside the dialysis bag even at lower molecular weight than the cut-off point, due to their increased diameter in solution.

3 MATERIALS AND METHODS

3.1 Materials and chemicals

High molecular weight chitosan (M_w = 153 kDa, F_A = 0.002) was an in-house sample. Low molecular weight chitosan (D_nM-type oligomers, M_w = 4.9 kDa) was kindly provided by Professor Christophe Schatz, Laboratorie de Chimie des Polyméres Organiques, Université de Bordeaux. High molecular weight dextran T-2000 (M_w = 2000 kDa) was obtained from Pharmacia Fine Chemicals. O,O'-1,3-propanediylbishydroxylamine (98%) (PDHA) and α-picoline borane (Pic-BH_3/PB) were purchased from Sigma-Aldrich. Ultrapure water was provided by an OmniPure water system (Stakpure). Dialysis was performed using Spectrum Spectra/Por Dialysis Membrane Standard PC Tubing with varying MWCO and diameter. All other chemicals were obtained from commercial sources and were of analytical grade.

3.2 Size-exclusion chromatography (SEC)

Three different SEC set-ups were used for the preparation of narrow fractions of chitosan oligomers and $Dext_m$-PDHA, see Table 3.1. Separation was monitored by an on-line RI detector (SHODEX R1 – 101). The pump was a LC-10AD vp SHIMADZU. Fractions were collected using an LKB 2111 MultiRac collector. All material was filtered through a 0.45 μm nylon filter (Acrodisc 13 mm, Pall Corporation) prior to injection. All experiments were carried out in 22 ℃ (RT).

Table 3.1 SEC set-ups (system 1 – 3), including column type, number of columns, packing material, mobile phase, and flow rate.

System	Column type	Number of columns	Packing material	Mobile phase	Flow rate
1	HiLoadTM 26/60 (26 mm x 60 cm)	3 (connecter in a series)	Superdex 30	0.15 M AmAc, pH 4.5 0.15 M AmAc, pH 6.9	0.8 ml/min
2	HiLoadTM 26/60 (26 mm x 60 cm)	1	Superdex 30	0.15 M AmAc, pH 4.5 0.1 M AcOH, pH 2.9 0.015 M AmAc, pH 4.5 0.03 M AmAc, pH 4.5	0.8 ml/min
3	HiLoadTM 26/60 (26 mm x 60 cm)	1	Superdex 75	0.15 M AmAc, pH 4.5	2.0 – 2.6 ml/min

3.3 Preparation and characterization of chitosan oligomers

3.3.1 Characterization of in-house chitosan sample by SEC-MALS

Sample and standards (pullulan, dextran and PEO) were dissolved (2 mg/ml) in the mobile phase (0.2 M AmAc, pH 4.5) and left on a shaker device (200 rpm) for 24 hours in 22 ℃ (RT). The material was filtered through a 0.45 μm nylon filter (Acrodisc 13 mm, Pall Corporation) and injected on an HPLC system consisting of a mobile phase reservoir, an on-line degasser, a pump, an autoinjector, a precolumn, and two serially columns (TKSgel G 5000 PWXL and TKSgel G 6000 PWXL, 7.8 cm x 30 cm). The column outlet was connected to two serially connected detectors, a multiangle light scattering photometer (Wyatt, USA) followed by an RI detector (Wyatt, USA). The analysis was carried out in 22 ℃ (RT) with a flow rate of 0.5 ml/min, using a refractive index increment $(dn/dc)_{\mu}$ of 0.142 ml/g and a A_2 of 5.0 x 10^{-3} for chitosan. Injections were performed twice (100 μL per injection). Astra software (Wyatt technology) was used to collect and process the data.

3.3.2 Exploring potential new SEC mobile phases for chitosan separation

Chitosan (2 mg/ml) was dissolved in SEC buffer, filtered through a 0.45 μm nylon filter (Acrodisc 13 mm, Pall Corporation) and injected into the SEC system (system 1 (using 0.15 M AmAc, pH 4.5) and system 2), see Table 3.1. The areas under the chromatograms using the different mobile phases were calculated using trapezoidal numerical integration, by the trapz-function in MATLAB.

3.3.3 Nitrous acid degradation of chitosan

Chitosan (M_w = 153 kDa, F_A = 0.002, 20 mg/ml) was dissolved in MQ water containing 2.5 % v/v acetic acid (AcOH) and placed on stirring overnight at 22 ℃ (RT). The solution was degassed using N_2 (g) for 20 min followed by cooling to 4 °C. A freshly prepared $NaNO_2$ (l) solution was degassed and cooled (4 °C) before added to the chitosan solution (0.06 and 0.25 molar ratio to the number of D-units). The degradation mixture was left on stirring at 4°C overnight in the dark.

3.3.4 Separation of chitosan oligomers by SEC

The nitrous acid degraded chitosan (D_nM) was separated by SEC (0.15 M AmAc, pH 4.5), see Section 3.1, by directly injection of the degradation mixture (20 mg/ml) into the SEC-system (system 1), see Table 3.1.

3.3.5 Purification and characterization of chitosan oligomers

Following SEC, pooled fractions were dialyzed against MQ water adjusted to pH 4.5 using diluted HCl for 2 days. Subsequently, the sample was dialyzed against MQ water for 6 hours to remove excess salts, (12-14 or 3.5 MWCO) and freeze-dried. Purified chitosan oligomers were dissolved in D_2O (600 μl, 3 mg/ml) and transferred to 5 mm NMR tubes. ^{1}H-NMR spectra were recorded at 25 ℃ on a BRUKER Advance 600 MHz spectrometer. Spectra processing was performed with TopSpin 4.0.9. Purified chitosan oligomers were analyzed by SEC-MALS (TKSgel G 3000 PWXL and TKSgel G 4000 PWXL, 7.8 cm x 30 cm) using the same method as described in Section 3.3.1.

3.4 Preparation of chitosan from LCPO

Chitosan (D_nM oligomers, M_w = 4.9 kDa) was characterized by SEC-MALS (TKSgel G 3000 PWXL and TKSgel G 4000 PWXL, 7.8 cm x 30 cm) using the same method as described in Section 3.3.1. Chitosan (40 mg/ml) was separated by SEC (system 3), see Table 3.1. Pooled fractions purified by dialysis using the same method as described in Section 3.3.5. Purified chitosan was characterized by ^{1}H-NMR spectroscopy using the same method as described in Section 3.3.5. Purified chitosan was characterized by SEC-MALS (TKSgel G 3000 PWXL and TKSgel G 4000 PWXL, 7.8 cm x 30 cm) using the same method as described in Section 3.3.1.

3.5 Preparation of activated dextran oligomers

3.5.1 Acid degradation of dextran

Dextran T-2000 (M_w = 2000000, 50mg/ml) was dissolved (25 mg/ml dextran) in MQ water and HCl was added to give a final concentration of 0.05 M HCl. The degradation was performed at 95 °C for 190 minutes. The degradation mixture was purified by dialyzed against MQ water until the conductance was below 3 μS/cm and freeze-dried. The dextran oligomers were characterized by ^{1}H NMR using the same method as described in Section 3.3.5.

3.5.2 Activation and reduction

The degraded dextran oligomers (20.1 mM) were dissolved in acetate buffer (500 mM). O,O´-1,3-propanediylbishydroxyl-amine (PDHA) (10x mol) were added to the solution and the mixture was left on a shaker device (200 rpm) for 24 hours at 22 ℃ (RT). α- picoline borane (Pic-BH_3) (20x mol) was further added to the reaction mixture for 69 hours at 40 ℃. The degradation mixture was purified by dialysis, first against NaCl (50 mM) to remove excess Pic-

BH_3, followed by dialysis against MQ water to remove excess salt until the conductance was below 2 μS/cm and freeze-dried. The $Dext_m$-PDHA sample were characterized by ^{1}H NMR using the same method as described in Section 3.3.5.

3.5.3 Separation of dextran oligomers by SEC and characterization

The $Dext_m$-PDHA sample were fractionated by SEC (0.15 M AmAc, pH 6.9), see Section 3.2, (system 1), see Table 3.1. The pooled fractions were then freeze-dried five times to remove ammonium acetate from the samples. The dextran fractions were analyzed by ^{1}H-NMR using the same method as described in Section 3.3.5, and by SEC-MALS (TKSgel G 3000 PWXL and TKSgel G 4000 PWXL, 7.8 cm x 30 cm), using a refractive index increment $(dn/dc)_\mu$ of 0.148 ml/g and A_2 of 2.0 x 10^{-4} for dextran, see Section 3.3.1.

3.6 Conjugation kinetics studies of D_nM to $Dext_m$-PDHA by time-course NMR

The deuterated sodium acetate (NaAc) buffer (500 mM, pH 4.0) was prepared by mixing 3 ml D_2O, 0.5 ml 1 % sodium 3-(trimethylsilyl)-propionate-d_4 (TSP) and 143.2 μl deuterated acetic acid, with a pH* of 2.50 and a volume of 3.6 ml. NaOD and D_2O was added to a total volume of 5 ml and pH* = 4.0. D_nM oligomers (7.0 mM and 3.5 mM) was dissolved in deuterated NaAc buffer (500 mM), pH 4.0 and put on a shaker device (200 rpm) for 1 hour at 22 ℃ (RT). $Dext_{24}$-PDHA (1:1 molar ratio) was added to the solution and put on a shaker device (200 rpm) for 1 min at 22 ℃ (RT). The reaction mixture was transferred to NMR tubes and the conjugation reaction was monitored by obtaining ^{1}H-NMR spectra at various times for approximately 24 hours. The NMR instrument was the same as described in Section 3.3.5.

3.7 Reduction kinetics studies by time-course NMR

D_4M oligomers (7 mM) was dissolved in deuterated NaAc buffer (500 mM), pH 4.0, put on a shaker device (200 rpm) for 1 hour at 22 ℃ (RT) and transferred to an NMR tube. Three equivalence of PB (21 mM) was added to the solution and the reduction reaction was monitored by time course ^{1}H-NMR for 48 hours at 25 ℃. The reduction of D_4M=PDHA-$Dext_{24}$ oximes (7 mM) was studied using the same approach. After 5 days 7 additional equivalents of PB (to a total of 70 mM) were added to the reaction mixture. 11 days after reaction start, the reaction mixture was heated to 40 ℃. ^{1}H-NMR spectra were obtained at specific time points until the reduction reaction was complete. The NMR instrument was the same as described in Section 3.3.5.

3.8 Preparation of D_nM=PDHA-$Dext_m$ diblocks

Purified D_nM oligomers (3.5 mM) were dissolved in NaAc buffer (500 mM), pH 4.0 and put on a shaker device (200 rpm) for 1 hour at 22 ℃ (RT). $Dext_m$-PDHA (1:1 molar ratio) was added to the solution and the reaction mixture was put on a shaker device (200 rpm) for 1 hour at 22 ℃ (RT). The reaction mixture was dialyzed against MQ water for 6 hours to remove salt introduced by the buffer and freeze-dried. The diblocks equilibrium mixture were characterized by SEC-MALS using a refractive index increment $(dn/dc)_\mu$ of 0.142 ml/g and A_2 of 2.0 x 10^{-4}, using the method described in Section 3.3.1.

3.9 Solubility behavior analysis of chitosan and chitosan conjugates by dynamic light scattering (DLS)

The dynamic light scattering (DLS) instrument was a Malvern analytical, Zetasizer Nano ZS, with a back scattering angle detection at 173°. The Zetasizer Nano software determined the scattering intensity in kcps (kilo counts per second) at 25 °C. All analyses were set to 5 measurements per sample, with 8 runs at 30 seconds each measurement. All samples were filtered through a 0.45 μm nylon filter (Acrodisc 13 mm, Pall Corporation) before transferring to micro cuvettes.

3.9.1 Solubility of D_nM as function of pH

$D_{19}M$ oligomers were dissolved (1 mg/ml) in MQ water, left on a shaker device (200 rpm) for 24 hours at 22 ℃ (RT), and filtered. The solution was transferred to a micro cuvette. The pH of the D_nM solution was increased by adding NaOH (0.1 M), and measurements were taken at various pHs. The measurements were performed directly after adding NaOH to the desired pH value.

3.9.2 Solubility behavior of D_nM=PDHA-$Dext_m$ as function of pH

D_nM=PDHA-$Dext_m$ was dissolved (1 mg/ml) in 10 mM NaCl, left on a shaker device (200 rpm) for 24 hours at 22 ℃ (RT), and filtered. The solution was transferred to a micro cuvette. The pH of the solution increased by adding NaOH (0.1 M). Measurements were obtained at pH 6.3 and pH 10.4. The solution was put on a shaker device (200 rpm) for 10 min after adding NaOH to the desired pH value before the measurements were performed.

3.9.3 Stability of D_nM=PDHA-$Dext_m$ as function of pH

D_nM=PDHA-$Dext_m$ was dissolved (1 mg/ml) in 10 mM NaCl, left on a shaker device (200 rpm) for 24 hours at 22 ℃ (RT), and filtered. The solution was transferred to a micro cuvette. The pH of the solution was decreased by adding HCl (0.1 M) to a pH value of 3.1. The solution pH was further increased by adding NaOH (0.1 M). Measurements were taken at various pHs from 3.1 to 10. The solutions were put on a shaker device (200 rpm) for 10 min at 22 ℃ (RT) after adding NaOH to the desired pH values before the measurements were performed.

4 RESULTS

The aim of this master thesis was to prepare and characterize chitosan-*b*-dextran diblocks and to study the properties of the diblock in solution. The results from this master thesis are presented in six sections. Preparation of D_nM oligomers with high preservation of M-unit at the reducing end and the results from a collaboration with Laboratoire de Chimie des Polyméres Organiques (LCPO) will be presented in Section 4.1. The preparation of $Dext_m$-PDHA will be presented in Section 4.2. The following two sections, Section 4.3, and Section 4.4, include kinetic studies for the conjugation of D_nM to $Dext_m$-PDHA and the reduction of D_nM oligomers and D_nM=PDHA-$Dext_m$ oximes. A preparative protocol for D_nM=PDHA-$Dext_m$ diblocks without reduction is presented in Section 4.5. Finally, Section 4.6 includes a solubility behavior study of D_nM oligomers and chitosan-*b*-dextran diblocks and a final study focusing on the pH dependent stability of the D_nM=PDHA-$Dext_m$ oximes.

4.1 Preparation and characterization of chitosan oligomers

The first step towards preparation of chitosan-*b*-dextran diblocks was to investigate an improved method for the preparation of isolated D_nM oligomers with high preservation of M-unit at the reducing end. In previous work [7, 8], 50 – 70 % of the D_nM oligomers prepared had the M-unit at the reducing end. It would be beneficial to achieve an even higher percentage. However, high preservation of M-units is difficult to achieve due to the formation of Schiff bases during freeze-drying after separation by SEC. Self-branching by Schiff base reaction occurs when the pH rises above 4.5, which occur as water and acetic acid evaporates first during freeze-drying, leaving ammonia [17], see Section 2.3.3. This reaction is unfortunate because it results in loss of M-unit upon subsequent acidification. Hence, the M-unit cannot be utilized in the conjugation with $Dext_m$-PDHA. To avoid the loss of the M-unit, two possible routes for reducing the amount of ammonia in the sample before freeze-drying were investigated:

1. Using a SEC buffer without or with less ammonium acetate
2. Optimizing the purification process after SEC separation

Section 4.1.1 includes a collection of SEC experiments using different mobile phases. The second possible method will be presented in Section 4.1.2 and includes preparation and characterization of D_nM oligomers using an optimized purification method. Finally, Section 4.1.3 includes the results from a collaboration with LCPO involving preparation of narrow fractions of chitosan oligomers for the preparation of chitosan-*b*-PEG diblocks.

4.1.1 Exploring potential new SEC mobile phases for chitosan separation

As preparation for exploring new mobile phases, a method for speeding up these experiments was tested. The use of three consecutive columns for SEC separation is time-consuming (~ 20 hours). Hence, an alternative would be to switch to one single column when performing these experiments. A nitrous acid degraded chitosan sample was separated by SEC using a set of three consecutive columns and compared with the use of one single column using 0.15 M AmAc, pH 4.5 as the mobile phase. The chromatograms obtained from the two set-ups were compared to verify that one single column provides acceptable separation, see Figure 4.1.

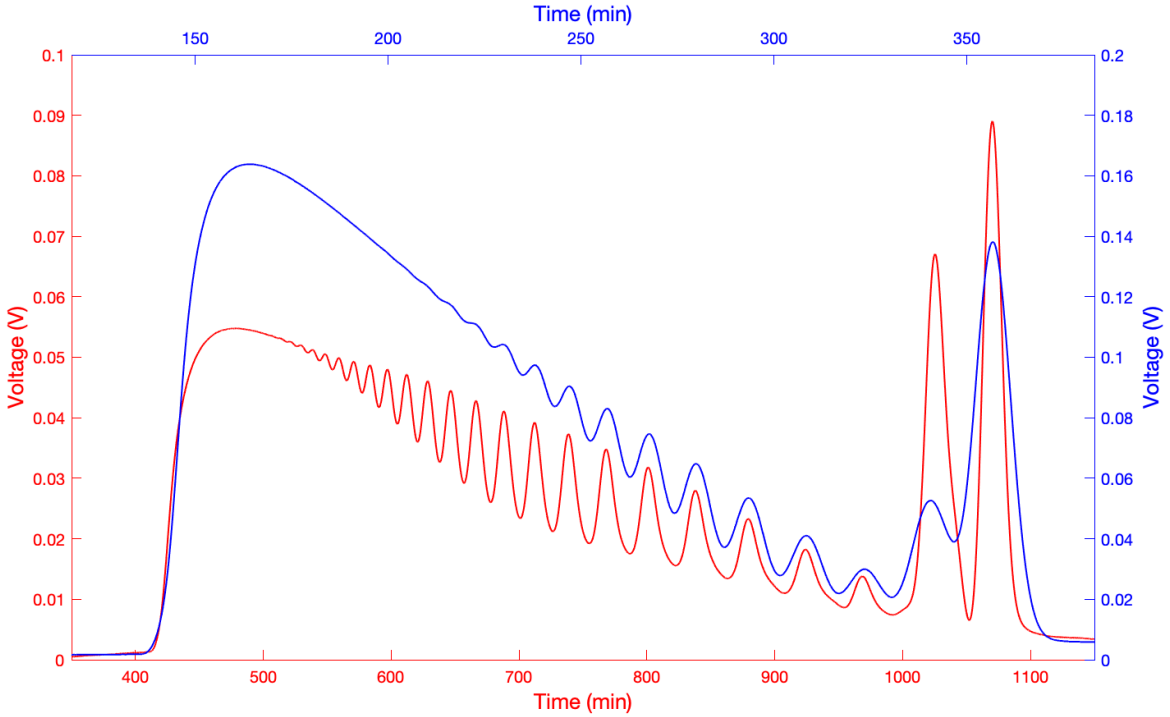

Figure 4.1 Separation of chitosan by SEC (3 mg/ml per injection) using three consecutive columns (red) compared to one single column (blue), with 0.15 M AmAc, pH 4.5 as mobile phase.

The peaks representing eluted oligomers are clearly visible in both chromatograms, see Figure 4.1, but a decrease in separation, particularly at low elution times, is observed when switching to one single column, as expected. However, the separation using a single column is adequate as the peaks are clearly distinguishable. Thus, one single column was used to save time when exploring new SEC mobile phases for D_nM separation by SEC.

Three potential mobile phases were explored and compared to the standard mobile phase. The SEC chromatograms obtained when separating chitosan using 0.15 M AmAc, pH 4.5; 0.1 M AcOH, pH 2.9; 0.015 M AmAc, pH 4.5, and 0.03 M AmAc, pH 4.5 as the mobile phase are presented in Figure 4.2.

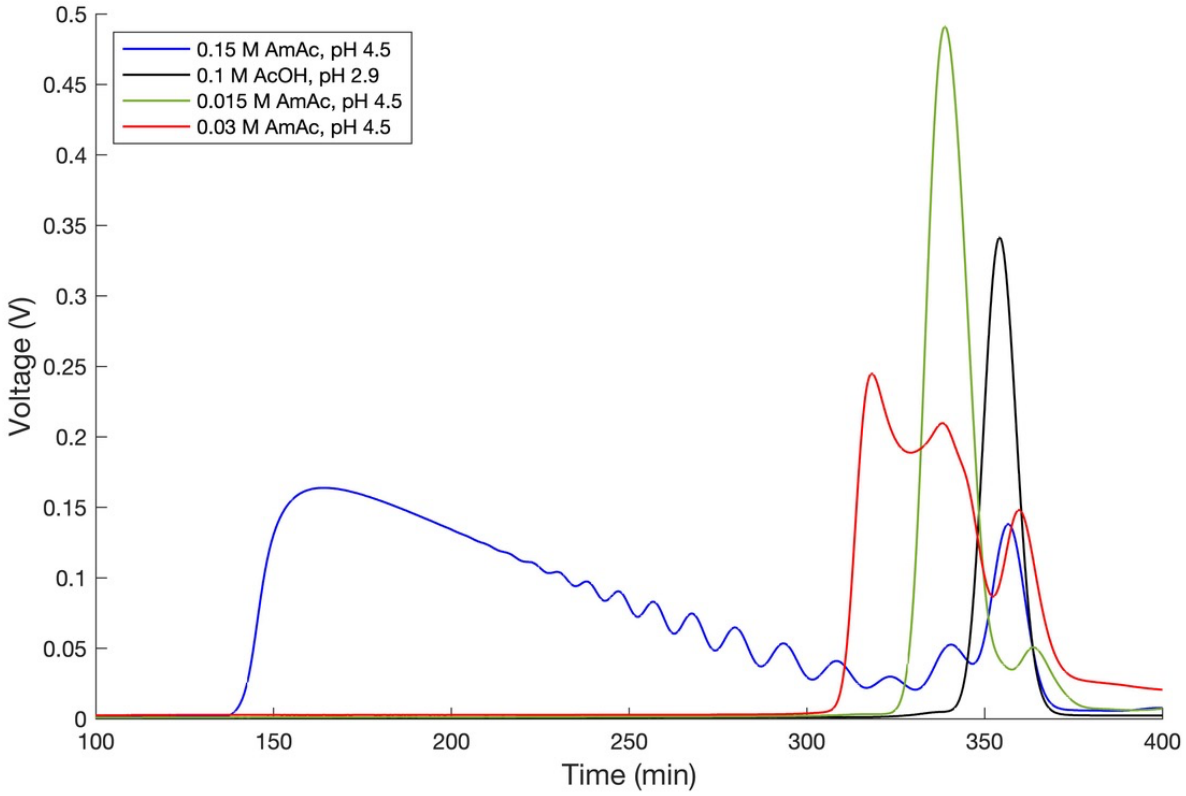

Figure 4.2 Separation of chitosan by SEC (3 mg/ml per injection): 0.15 M AmAc, pH 4.5 (blue), 0.1 M AcOH, pH 2.9 (black), 0.015 M AmAc, pH 4.5 (green) and 0.03 M AmAc, pH 4.5 (red).

The chromatogram obtained using the standard 0.15 M AmAc, pH 4.5 (blue) mobile phase was included for comparison. Figure 4.2 demonstrates that chitosan eluted simultaneously with the salt peak using 0.1 M AcOH, pH 2.9 (black) as the mobile phase. The peak area does not correspond to the volume of the whole chitosan sample, indicating that some of the sample may remain bound to the column. Sample recovery corresponds to approximately 20 % of the injected mass. When using 0.015 M AmAc, pH 4.5 (green) as the mobile phase, the chitosan eluted just before the salt peak. However, the sample was not well separated, but eluted as a single narrow peak. Sample recovery was found to be approximately 40 %. Finally, the sample separated with 0.03 M AmAc, pH 4.5 (red) as the mobile phase eluted as two partially resolved peaks appearing just before the salt peak, with a sample recovery of approximately 60 %. Both sample recovery (%) and separation improved for 0.03 M AmAc, pH 4.5 (red) compared to the use of 0.015 M AmAc, pH 4.5 (green) as the mobile phase. However, a sample recovery of 60 %, as well as a two peak separation is still far from satisfactory. A further increase in ionic strength would likely be necessary to obtain sufficient sample recovery and separation. However, this would not be in line with the purpose of the experiment, which was to minimize the use of AmAc. Further experiments were therefore discontinued.

4.1.2 Preparation of chitosan oligomers using an improved purification method

The second possible method to obtain isolated D_nM oligomers with high preservation of M-unit at the reducing end was to optimize the purification method after SEC separation prior to freeze-drying. High molecular weight chitosan (M_w = 153 kDa, F_A = 0.002) was degraded by nitrous acid to obtain D_nM oligomers. The D_nM oligomers were further separated by SEC and the obtained chromatogram is presented in Figure 4.3, confirming the degradation. The DP of the oligomers was determined after the DP of the oligomers assumed to be the pentamers was confirmed by ^{1}H-NMR.

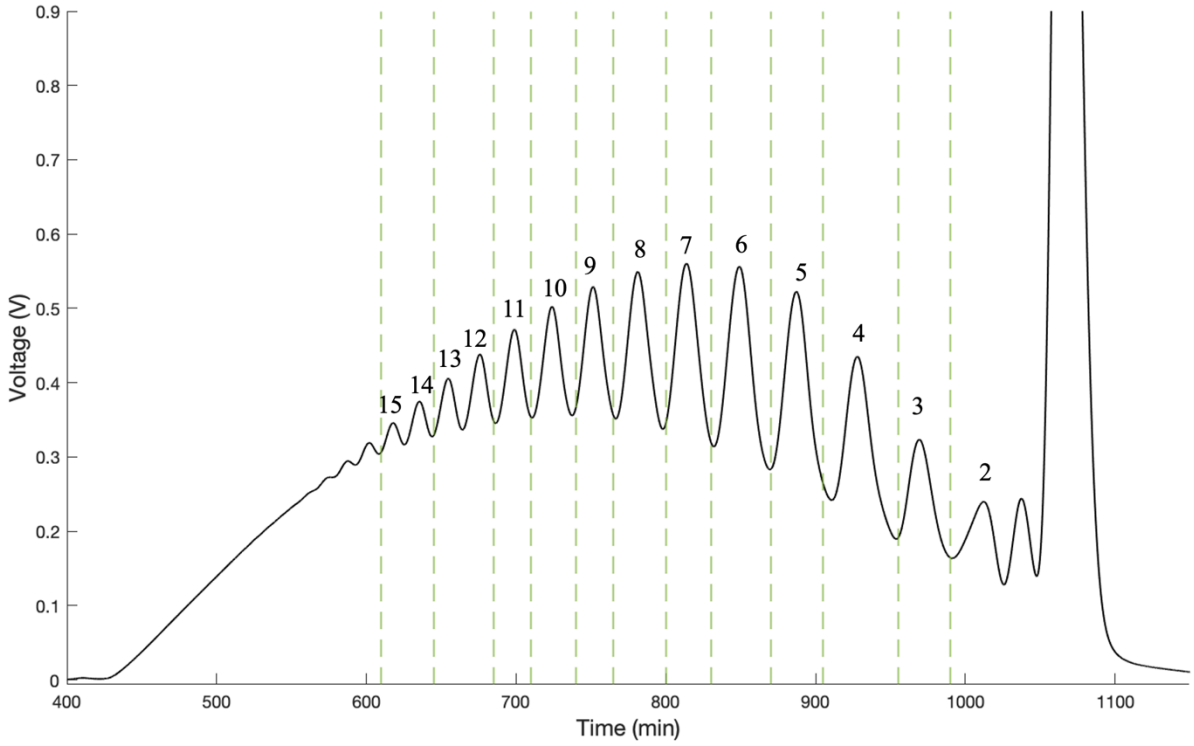

Figure 4.3 Size-exclusion chromatogram of a nitrous acid depolymerized chitosan sample (2 mg/ml). The SEC-system was comprised of three HiLoad 26/60 columns connected in series packed with Superdex 30, using 0.15 M AmAc, pH 4.5 as the mobile phase, flow rate 0.8 ml/min.

The fractions collected after SEC separation are illustrated as dotted lines in Figure 4.3. The fractions containing the pentamers (D_4M) and the decamers (D_9M) were purified using the new method described in Section 3.3.5. The D_nM oligomers were dialyzed against MQ water adjusted to pH 4.5 using dilute HCl for approximately 2 days to remove AmAc introduced by the SEC buffer and followed by dialysis against MQ water for 6 hours to remove excess HCl from the sample. The purified fractions were then freeze-dried and characterized by ^{1}H-NMR. The results from the ^{1}H-NMR analysis are presented in Table 4.1.

Table 4.1 Yield of chitosan oligomers with M-unit at the reducing end (%) (major and minor resonances), chitosan oligomers with D-unit at the reducing end (%) and Schiff bases (%) obtained by integration of ^{1}H-NMR spectra of D_4M and D_9M.

	M-unit at the reducing end (%)			D-unit at the reducing end (%)	Schiff base (%)
	Major	Minor	Sum		
D_4M	82	3	85	5	10
D_9M	83	4	87	4	9

As seen in Table 4.1, the optimized purification method resulted in 85 % of the D_4M oligomers and 87 % of the D_9M oligomers having M-unit at the reducing end. Hence, the above presented protocol is an excellent alternative to those presented in literature. The integrated ^{1}H-NMR spectra of D_4M and D_9M are included in Appendix B. The percentage of the D_nM oligomers with the M-unit at the reducing end was approximately the same for the pentamer (85 %) and the decamer (87 %). It is therefore reasonable to assume that similar percentages may be obtained for oligomers of similar DP using this purification method. This purification method provides the opportunity to use D_nM oligomers as the second block in the preparation of chitosan-*b*-dextran diblocks. The annotated ^{1}H-NMR spectrum of D_4M is presented in Figure 4.4. The D_4M oligomers and the D_9M oligomers prepared using this method will be used for the preparation of chitosan-*b*-dextran diblocks.

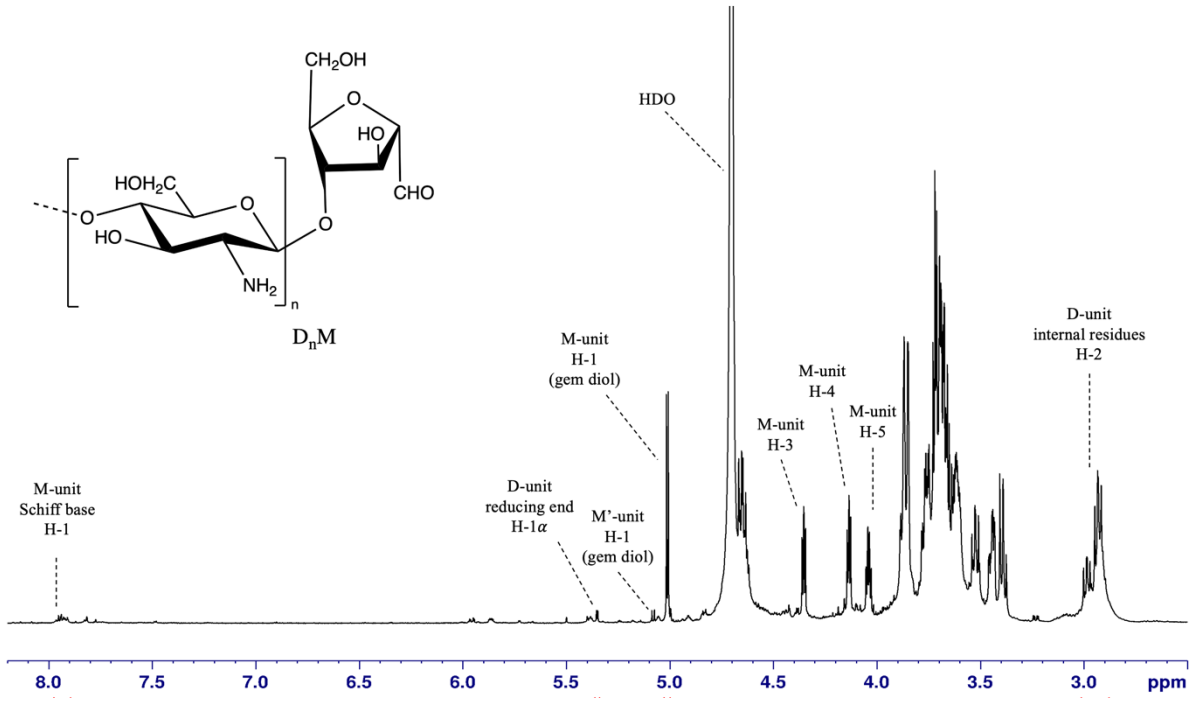

Figure 4.4 A ^{1}H-NMR spectrum of D_4M oligomers in D_2O. The spectrum was recorded at 600 MHz, 25 °C and pH* 6.0. The spectrum is annotated according to Tømmeraas *et al.* [17] and Domard *et al.* [47].

The chemical shift of H-1 M-unit (gem diol) is observed at 5.0 ppm in the ^{1}H-NMR spectrum, see Figure 4.4. This signal arises from H-1 in the M-unit in the hydrated aldehyde form where a water molecule has been added to the carbonyl group (gem diol). The minor resonance appearing at 5.1 ppm is assigned to the alternative form of the M-unit (marked as M' in Figure 4.4). The chemical shift of H-1 M-unit (free-aldehyde) is not observed in the spectrum (should be at approximately 9.5 ppm). The chemical shift of H-1 M-unit (Schiff base) is observed at 7.9 ppm, indicating that self-branching by Schiff base reaction has occurred during the freeze-drying process. The chemical shift of H-1α D-unit reducing end is observed at 5.4 ppm, indicating loss of M-unit. The chemical shift of the H-2 D-unit internal residues is observed at 2.9 ppm. The H-3, H-4 and H-5 of the M-unit is observed at 4.4, 4.1 and 4.0 ppm, respectively. These results are in good accordance with a previously performed ^{1}H-NMR-analysis of D_nM oligomers produced by nitrous acid depolymerization of chitosan [17].

It was of interest to obtain chitosan oligomers of higher DP for the preparation of longer chitosan-*b*-dextran diblocks. A new degradation of chitosan by nitrous acid was therefore performed. The D_nM oligomers were separated by SEC, further purified, and freeze-dried. The chromatogram is presented in Figure 4.5. The dotted lines indicate the collected fractions.

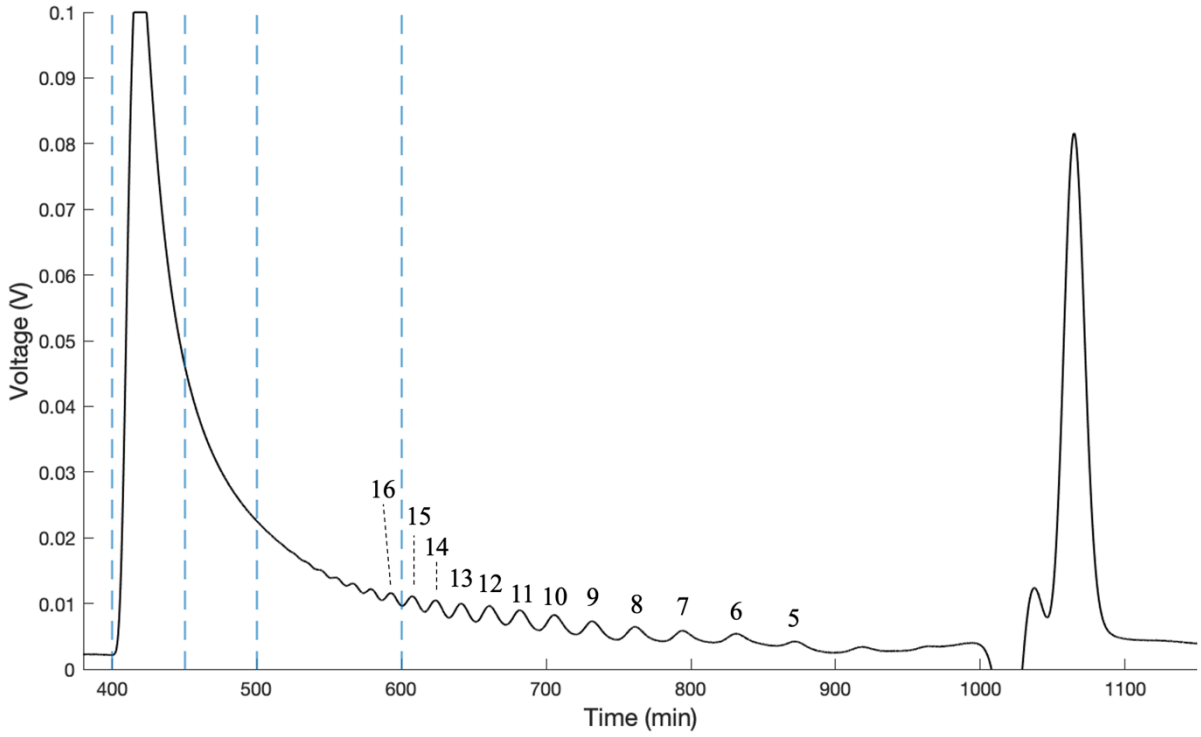

Figure 4.5 Size-exclusion chromatogram of a nitrous acid depolymerized chitosan sample (2 mg/ml). The SEC-system was comprised of three HiLoad 26/60 columns connected in series packed with Superdex 30, using 0.15 M AmAc, pH 4.5 as the mobile phase, flow rate 0.8 ml/min. Fraction 1: 400 – 450 min, fraction 2: 450 – 500 min and fraction 3: 500 – 600 min.

Using ^{1}H-NMR spectroscopy for characterizing longer oligomers is not ideal due to a high signal to noise ratio. The collected fractions from the second degradation were therefore characterized by SEC-MALS. The SEC-MALS chromatograms, and the molecular masses (M_n and M_w) and polydispersity (M_n/M_w) obtained from the SEC-MALS analysis, are shown in Figure 4.6 and Table 4.2, respectively. The calculated DP_n, see Table 4.2, indicate that the fractions were successfully separated with increasing DP_n by SEC. The $D_{28}M$ oligomers (DP = 29, sample 3) were further used for the preparation of longer chitosan-*b*-dextran diblocks. The polydispersity (M_n/M_w) for all fractions are between 1.0 – 1.1, indicating narrow fractions.

Table 4.2 Molecular masses (M_n and M_w) and polydispersity (M_n/M_w) obtained from the SEC-MALS analysis, and calculated DP_n (M_n/M_0). M_0 (HCl form) = 197,5 g/mol. Chitosan fraction 1 – 3 (Figure 4.6).

Sample	M_n (kDa)	M_w (kDa)	Polydispersity (M_n/M_w)	DP_n (M_n/M_0)
1	16.2	18.0	1.1	90
2	9.0	9.5	1.1	50
3	5.2	5.4	1.0	29

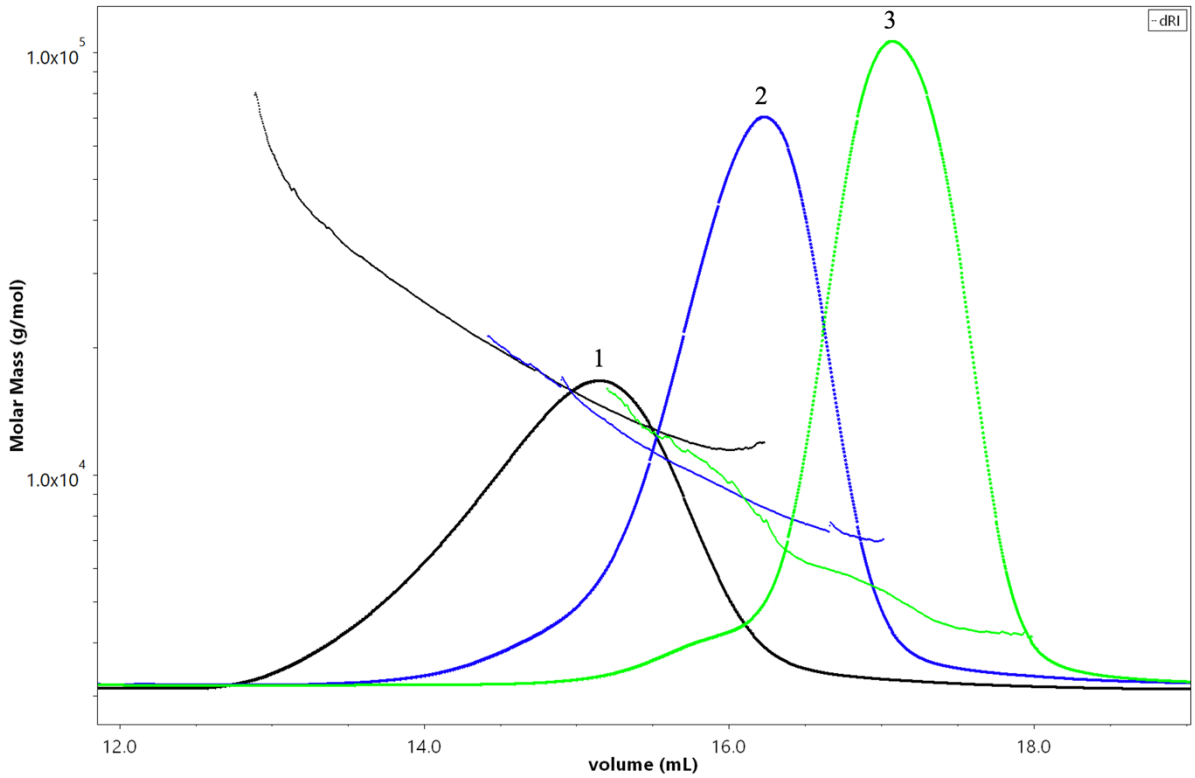

Figure 4.6 Chromatograms obtained from SEC-MALS analysis of chitosan fraction 1 – 3.

4.1.3 Preparation of D_nM fractions for conjugation with PEG at LCPO

A part of this master thesis included a collaboration with Laboratorie de Chimie des Polyméres Organiques (LCPO). Chitosan (D_nM) sent from LCPO, see Appendix C, was separated by SEC, purified using the same method as in Section 4.1.2, and characterized by SEC-MALS and ^{1}H-NMR. An analytical chromatogram is presented in Figure 4.7, where the dotted lines indicate the fractions collected. The SEC-MALS chromatograms, and the molecular masses (M_n and M_w) and polydispersity (M_n/M_w) obtained from the SEC-MALS analysis are shown in Figure 4.8 and Table 4.3, respectively.

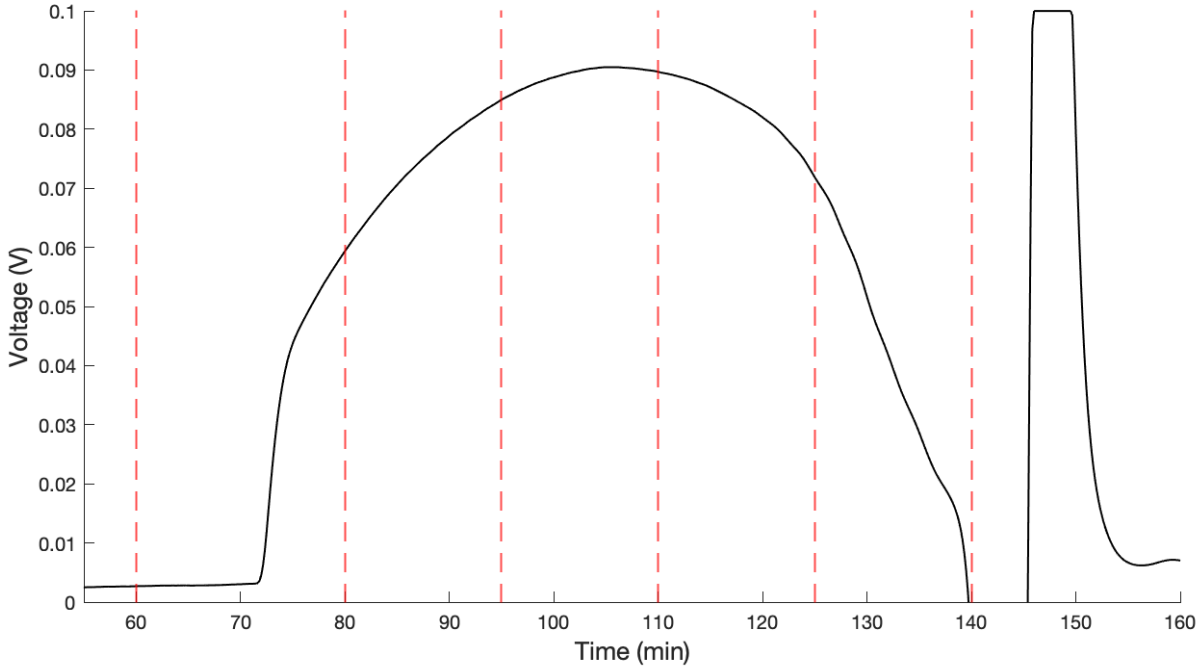

Figure 4.7 Analytical chromatogram of the chitosan sample separated with a Superdex G75pg column (2 mg/ml injection), using 0.15 M AmAc, pH 4.5 as the mobile phase with a flow rate of 2.6 ml/min. F1: 60 – 80 min, F2: 80 – 95 min, F3: 95 – 110 min, F4: 110 – 125 min and F5: 110 – 140 min.

Table 4.3 Molecular masses (M_n and M_w) and polydispersity (M_n/M_w) obtained from the SEC-MALS analysis, and calculated DP_n (M_n/M_0) M_0 (HCl form) = 197,5 g/mol. Chitosan fraction F1 – F5 (Figure 4.8).

Sample	M_n (kDa)	M_w (kDa)	Polydispersity (M_n/M_w)	DP_n (M_n/M_0)
F1	13.0	13.9	1.1	73
F2	8.5	8.8	1.0	47
F3	6.1	6.3	1.0	34
F4	4.4	4.6	1.0	25
F5	3.5	3.7	1.0	20

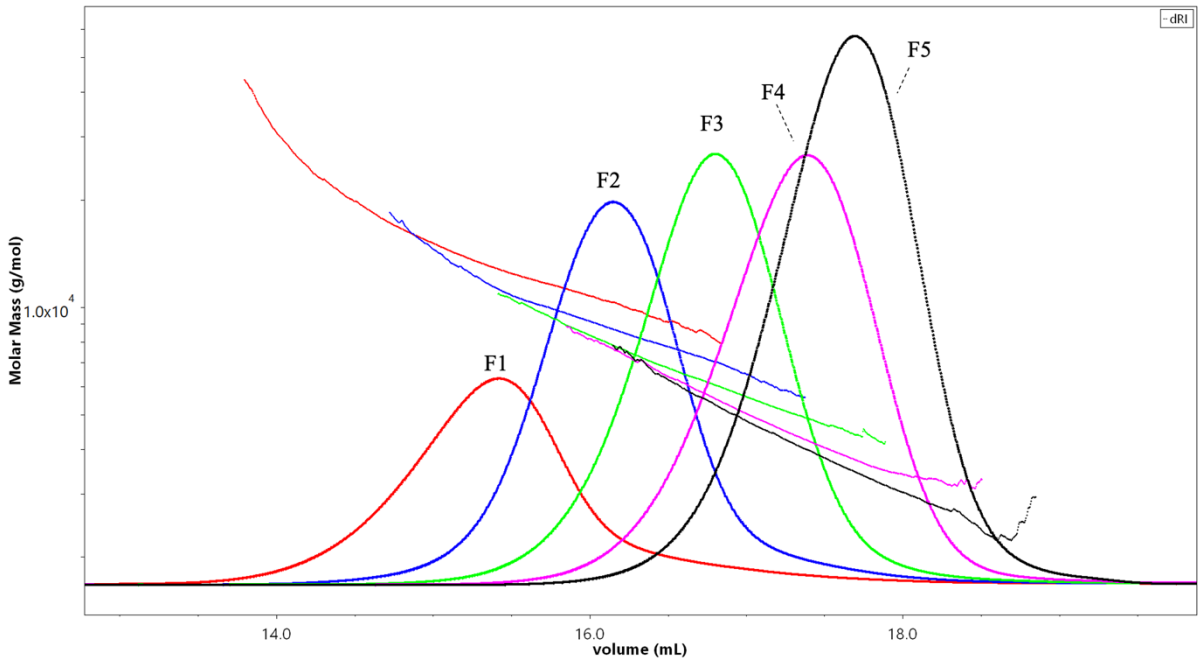

Figure 4.8 SEC-MALS chromatogram of the five chitosan fractions from LCPO.

The molar mass distribution from SEC-MALS were in excellent agreement with the decreasing DP_n for fractions prepared using SEC. Some overlap between neighboring peaks can be observed, suggesting that oligomers with the same hydrodynamic volume is present in several fractions. The polydispersity (M_n/M_w) for all fractions are between 1.0 – 1.1, indicating narrow fractions.

^{1}H-NMR spectroscopy was performed to confirm the chemical structure of the separated chitosan oligomers. The ^{1}H-NMR spectrum obtained for the oligomers in fraction 5 (F5) is presented in Figure 4.9. Peak assignment was based on data published by Tømmeraas *et al.* [17] and Domard *et al.* [47].

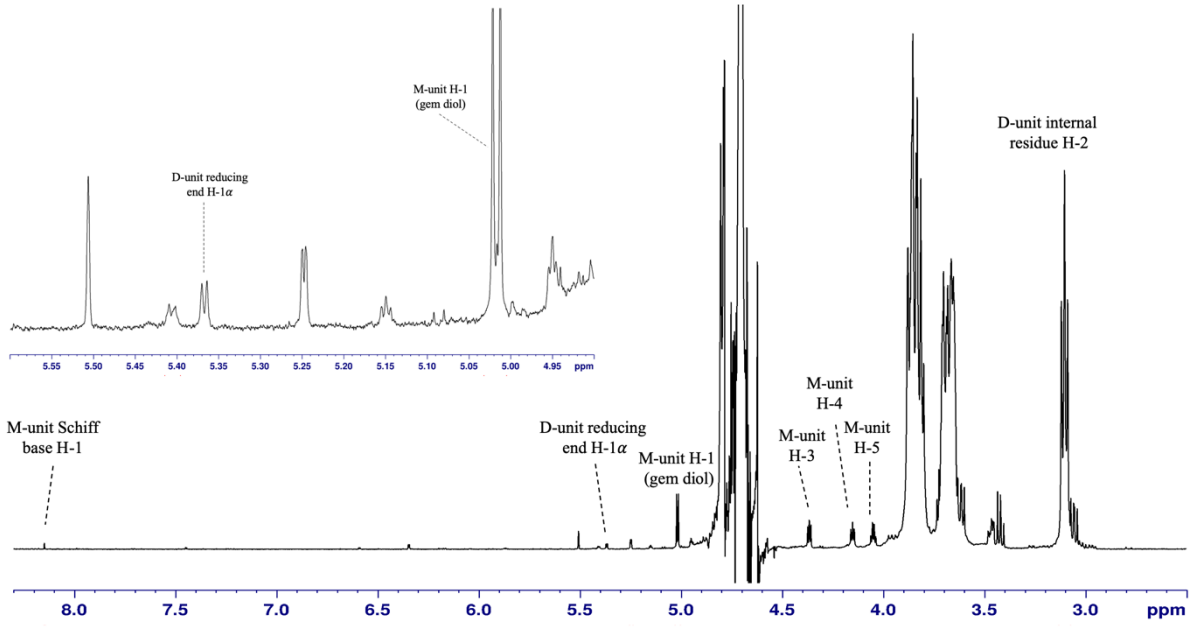

Figure 4.9 ^{1}H-NMR spectrum of the chitosan oligomers from fraction 5 (F5) in D_2O. Some additional 0.1 M DCl was added for total dissolution. The spectrum was recorded at 600 MHz, 25 °C and pH* 2.0.

The chemical shift of H-1 M-unit (gem diol) is observed at 5.0 ppm in the ^{1}H-NMR spectrum, see Figure 4.9. The chemical shift of H-1 M-unit Schiff base is observed at 8.2 ppm. The chemical shift of H-1α D-unit reducing end is observed at 5.4 ppm and H-2 of the D-unit internal residues is observed at 3.1 ppm. The chemical shifts appearing at 4.1, 4.2 and 4.4 ppm are H-5, H-4, and H-3 M-unit, respectively. There was no visible peak corresponding to H-1β of the D-unit reducing end. However, this is unsurprising considering that it is less abundant compared to H-1α of the D-unit reducing end, which is this case corresponded to a very small peak in the ^{1}H-NMR spectrum.

The DP_n of fraction 5 (F5) obtained by integration of the ^{1}H-NMR spectrum, was found to be 20, which corresponds well with the DP_n found in the SEC-MALS analysis. The intensity of the chemical shifts corresponding to the H-1 M-unit (gem diol), the H-1 M-unit Schiff base, and the H-1α D-unit reducing end were compared to determine the percentage of oligomers with the M-unit at the reducing end. It was found that 91 % of the D_nM oligomers had the M-unit at the reducing end. Furthermore, 3 % had formed Schiff bases and 6 % had a D-unit at the reducing end. The D_nM fractions were further used for the preparation of chitosan-*b*-PEG (experiments performed by Schatz at LCPO).

4.2 Preparation of activated dextran oligomers

The aim of this master thesis was to prepare chitosan-*b*-dextran diblocks by conjugating D_nM oligomers to $Dext_m$-PDHA. The new purification method provided the opportunity of using the D_nM oligomers as the second block in the preparation of chitosan-*b*-dextran diblocks. Hence, narrow fractions of $Dext_m$-PDHA had to be prepared prior to conjugation. This section includes preparation and characterization $Dext_m$-PDHA and was executed in collaboration with other master students at The Norwegian Biopolymer Laboratory (NOBIPOL).

High molecular weight dextran (T-2000, M_w = 2000 kDa) was degraded by acid degradation, conjugated with PDHA, reduced by PB, separated by SEC and freeze-dried. ^{1}H-NMR spectra of dextran before and after conjugation to PDHA (prior to separation by SEC) are shown in Figure 4.10. The DP_n of the degraded dextran sample was calculated to be 28 prior conjugation with PDHA using Equation 2.9, and the degree of branching (DB) was calculated using Equation 2.10 and was found to be approximately 3.0 %.

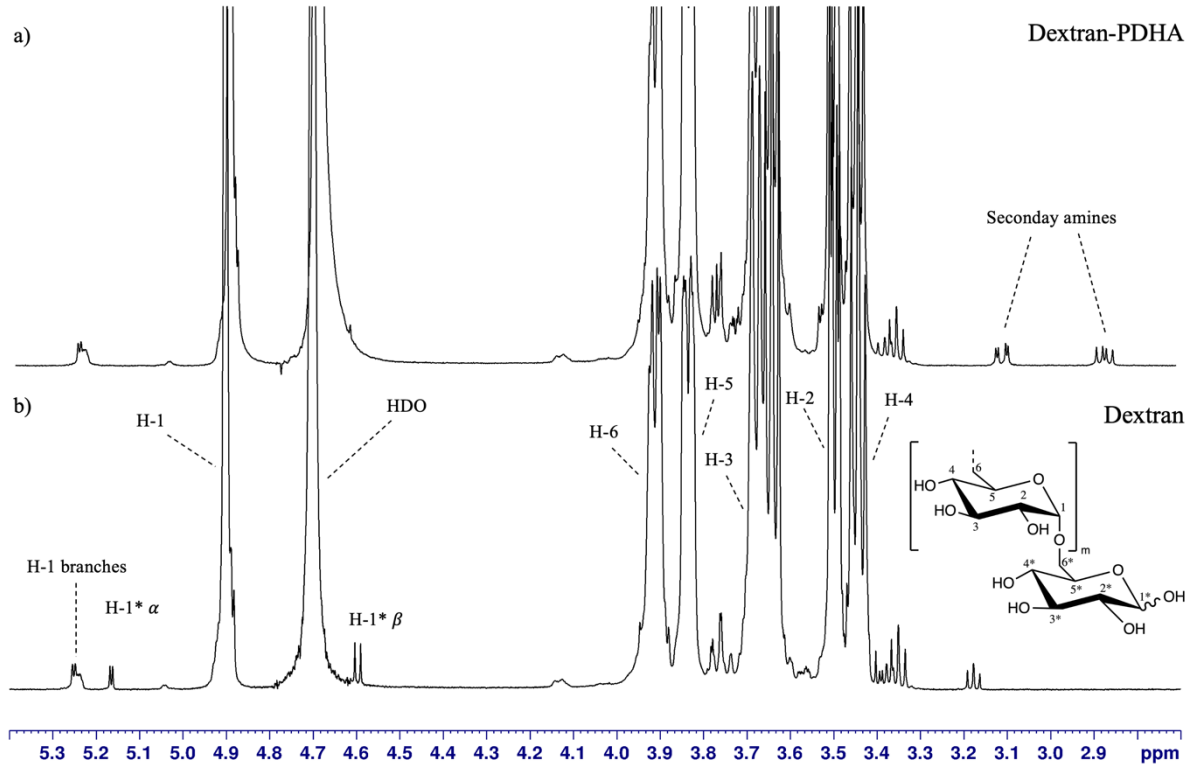

Figure 4.10 ^{1}H-NMR spectrum of a) dextran conjugated with PDHA and b) unreacted dextran oligomers. The spectra were recorded at 600 MHz, 25℃ with D_2O as the solvent. The ^{1}H-NMR spectrum of dextran was annotated according to Paulo *et al.* [48] and Cheetham *et al.* [49].

The chemical shifts corresponding to the H-1α and the H-1β of dextran are observed at 5.2 ppm and 4.6 ppm, respectively, see Figure 4.10b. After conjugation to PDHA, the chemical shift of H-1α and H-1β are no longer visible in the spectrum, indicating that dextran was successfully conjugated to PDHA. In addition, the ^{1}H-NMR spectrum of Dext$_m$-PDHA, Figure 4.10a, shows signals from secondary amines at 2.8 ppm and 3.1 ppm. Dext$_m$-PDHA were further separated by SEC, and the chromatogram is presented in Figure 4.11.

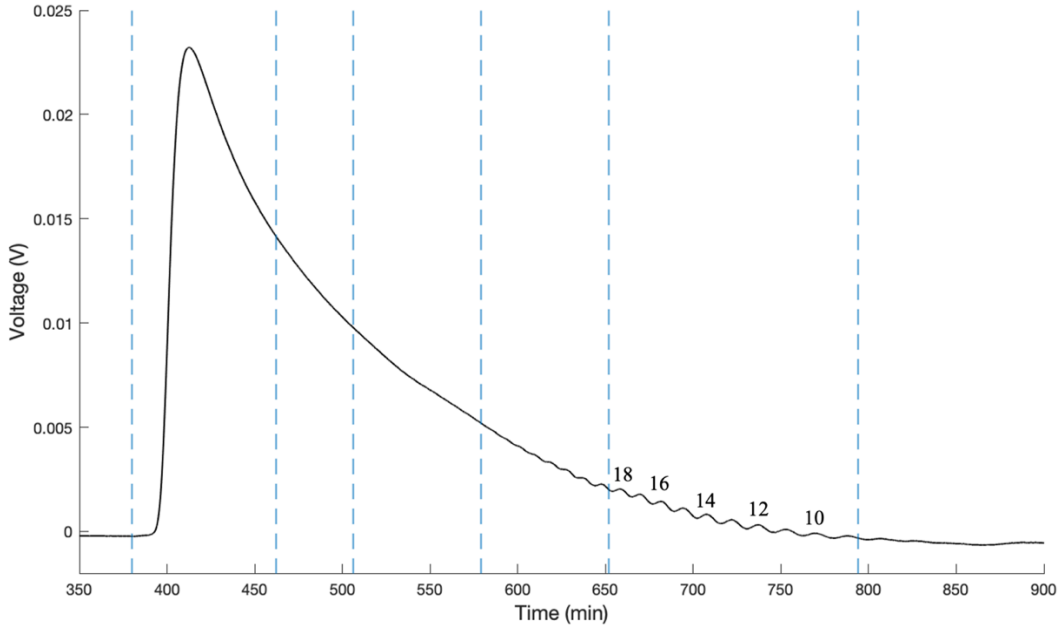

Figure 4.11 Chromatogram of activated dextran oligomers (2 mg/ml upon injection). The SEC-system was comprised of three HiLoad 26/60 columns connected in series packed with Superdex 30 at gain 500, using ammonium acetate (AmAc) buffer (0.15 M, pH = 4.5) as the mobile phase. F1: 380 – 462 min, F2: 462 – 506 min, F3: 506 – 579 min, F4: 579 – 652 min and F5: 652 – 794 min.

The dotted lines in Figure 4.11 indicate the collected fractions. The narrow fractions of Dext$_m$-PDHA were further analyzed by SEC-MALS, and the obtained data can be found in Table 4.4. The polydispersity (M_n/M_w) of all fractions of Dext$_m$-PDHA were between 1.0 – 1.1, indicating that narrow fractions were successfully obtained by SEC. The calculated DP_n (M_n/M_0) indicate that the fractions eluted the SEC column according to decreasing hydrodynamic volume.

Table 4.4 Molecular masses (M_n and M_w) and polydispersity (M_n/M_w) obtained from the SEC-MALS analysis, and calculated DP_n (M_n/M_0). M_0 = 162 g/mol. Dextran fraction F1 – F5 (Figure 4.11).

Fraction	M_n (kDa)	M_w (kDa)	Polydispersity (M_n/M_w)	DP_n (M_n/M_0)
F1	15.6	17.5	1.1	96
F2	8.4	8.5	1.0	52
F3	5.9	6.3	1.1	36
F4	3.9	3.9	1.0	24
F5	2.6	2.6	1.0	15

4.3 Conjugation of D_4M to $Dext_{24}$-PDHA studied by time course NMR

The second step towards the aim of this master thesis included obtaining kinetic data for the conjugation of D_nM oligomers to $Dext_m$-PDHA. Chitosan oligomers (D_4M) prepared in Section 4.1.2 and $Dext_{24}$-PDHA prepared in Section 4.2 were initially chosen as a model system, since short oligosaccharides give relatively simple NMR spectra [2]. The conjugation of D_4M to $Dext_{24}$-PDHA (1:1) was studied in detail by time course NMR in deuterated sodium acetate (NaAc) buffer (500 mM) at pH 4.0 (RT). The conjugation was studied twice using 7.0 mM and 3.5 mM. ^{1}H-NMR spectra of unreacted D_4M oligomer and of the equilibrium mixtures for the conjugation with $Dext_{24}$-PDHA (7.0 mM and 3.0 mM, 1:1) are given in Figure 4.13 and Figure 4.14, respectively. In agreement with the literature [50], only E- and Z-oximes were formed, see Figure 4.12. Kinetics plots for the oxime formation is given in Figure 4.15. The combined yield is the sum of the yields for E- and Z-oximes for the M residue (gem diol).

Reaction modeling was used to obtain rate constants for the formation and dissociation of E- and Z-oximes. A detailed description of the model used, have been published by Mo *et al.* [1]. Rate constants for best fits are given in Table 4.5. The times to reach 50 % and 90 % of the combined equilibrium yields ($t_{0.5}$ and $t_{0.9}$ (h)) are also included in Table 4.5.

Table 4.5 The kinetics parameter obtained from the modeling of the conjugation of A (D_4M) to B ($Dext_{24}$-PDHA) for 7.0 mM and 3.5 mM at pH 4.0 (1:1).

					A + B ↔ E		A + B ↔ Z				
A	B	mM	A:B	pH	k_1 (h^{-1})	k_{-1} (h^{-1})	k_2 (h^{-1})	k_{-2} (h^{-1})	$t_{0.5}$ (h)	$t_{0.9}$ (h)	equilibrium yield (%)
D_4M	$Dext_{24}$-PDHA	7.0	1:1	4.0	1.7	4.0×10^{-1}	6.0×10^{-1}	4.0×10^{-1}	0.04	0.22	85
D_4M	$Dext_{24}$-PDHA	3.5	1:1	4.0	2.4	3.3×10^{-1}	8.0×10^{-1}	3.3×10^{-1}	0.06	0.31	87

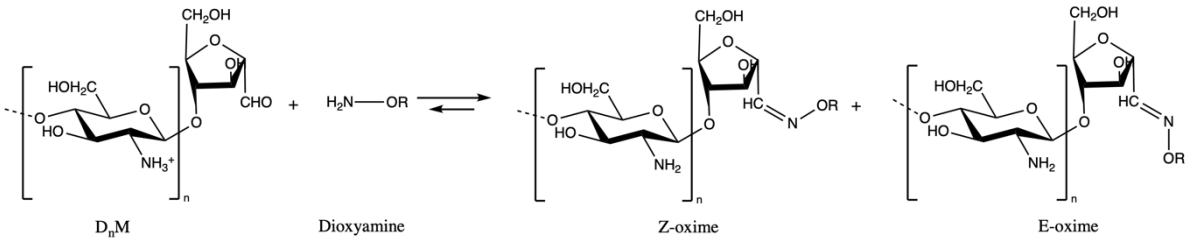

Figure 4.12 The formation of Z- and E-oximes when D_nM oligomers are conjugated to dioxyamine (PDHA).

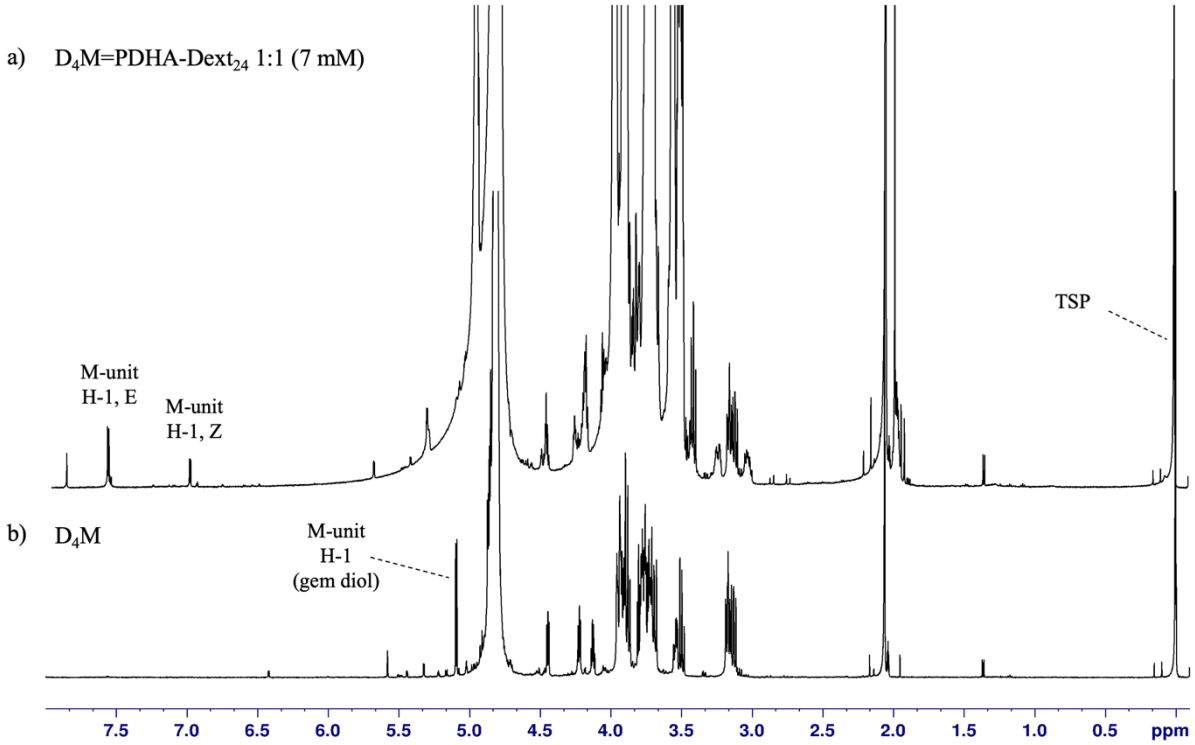

Figure 4.13 ^{1}H-NMR spectra of the a) D_4M-PDHA-$Dext_{24}$ diblocks at equilibrium (1:1, 7.0 mM) and b) D_4M in deuterated sodium acetate (NaAc) buffer (500 mM) at pH 4.0 The combined yield of the reaction was approximately 85 %. The ^{1}H-NMR spectra were recorded at 600 MHz at 25 ℃.

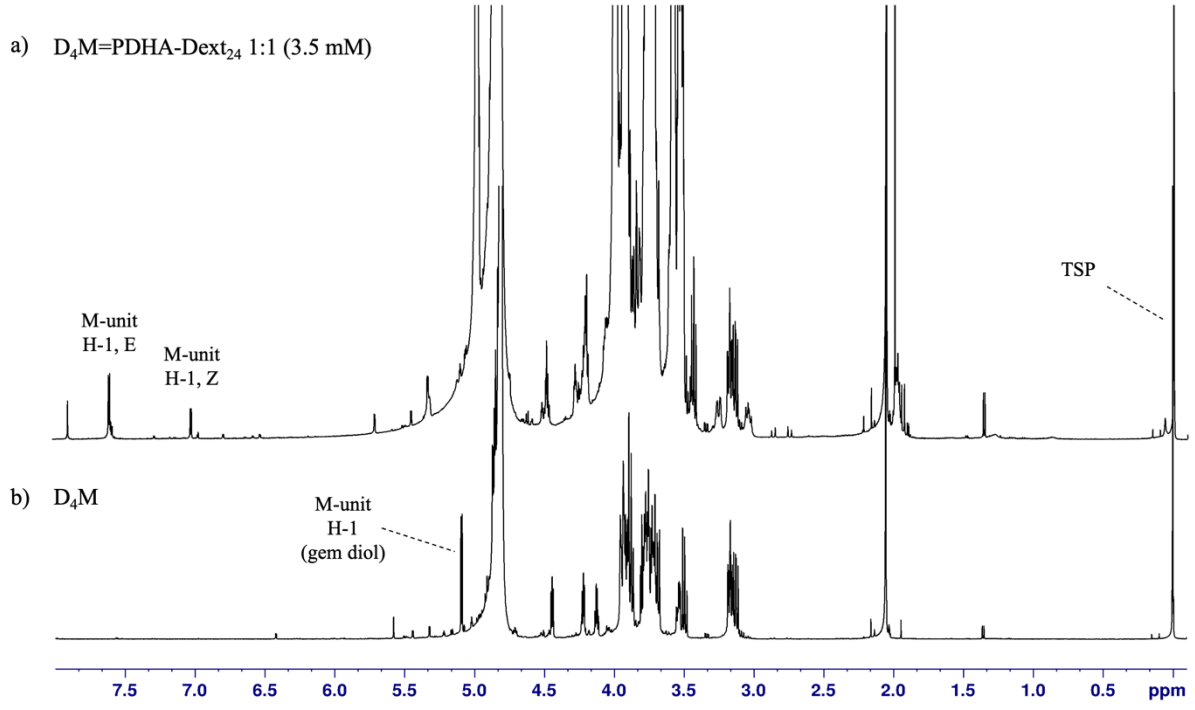

Figure 4.14 ^{1}H-NMR spectra of the a) D_4M-PDHA-$Dext_{24}$ diblocks at equilibrium (1:1, 3.5 mM) and b) D_4M in deuterated sodium acetate (NaAc) buffer (500 mM) at pH 4.0 The combined yield of the reaction was approximately 87 %. The ^{1}H-NMR spectra were recorded at 600 MHz at 25 ℃.

a)

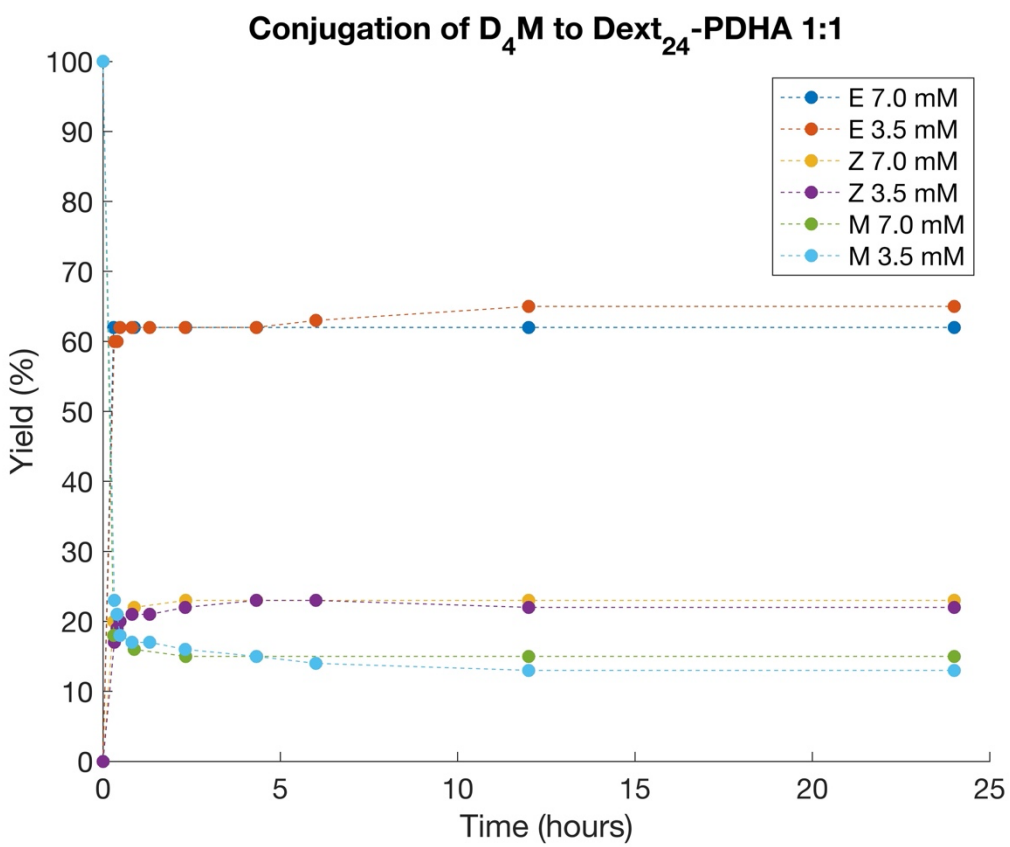

b)

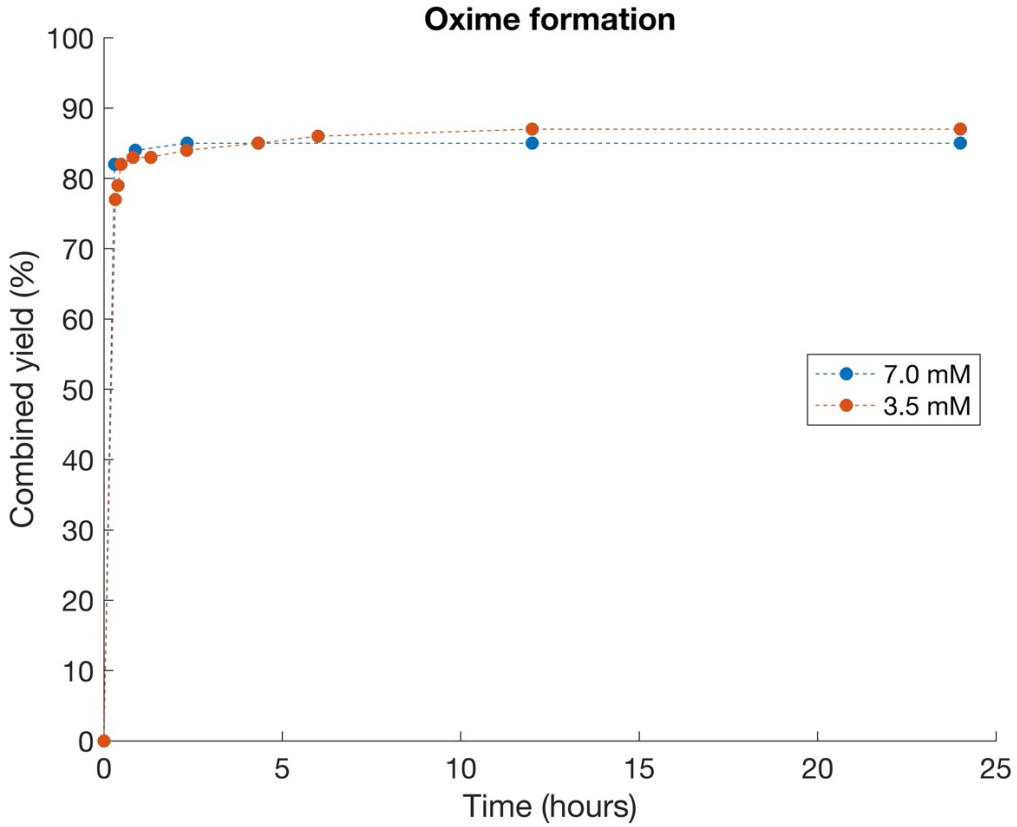

Figure 4.15 Reaction kinetics for the conjugation of D_4M oligomers to $Dext_{36}$-PDHA 1:1 at pH 4.0. a) The yield of the formation of E- and Z-oximes and the decrease in yield for D_4M, b) the combined yield for the oxime formation. Lines were added to better illustrate the experimental data.

The ^{1}H-NMR spectra of D_4M, see Figure 4.13b and 4.14b, were obtained prior to conjugation with $Dext_{24}$-PDHA. The chemical shift of H-1 M-unit (gem diol) is observed at 5.0 ppm in the ^{1}H-NMR spectra of D_4M. The chemical shifts of the E- and Z-oxime are observed at 7.5 ppm and 7.0 ppm, respectively, in the ^{1}H-NMR spectra of the equilibrium mixture containing D_4M-PDHA-$Dext_m$ oximes, indicating that conjugation have occurred, see Figure 4.13a and Figure 4.14b. At equilibrium, the chemical shift of H-1 M-unit (gem diol) is present as a small peak, indicating that some unreacted D_4M oligomers are still present in the sample. The ratio between the E- and Z-oxime (3:1) was the same for both experiments.

Figure 4.15a illustrates the increase in yield of the E- and Z-oximes, and the decrease in yield of the unreacted D_nM oligomers, plotted as a function of time (hours). The combined yield, the sum of E-oximes and Z-oximes, was 85 % and 87 % for the reaction with 7.0 mM and 3.5 mM, respectively, differing by only 2 %, see Figure 4.15b. The combined yield (%) is plotted as a function of time (hours) and illustrates that both reactions were close to equilibrium after approximately 0.5 hour.

4.4 Reduction kinetics studies of D_nM and D_nM=PDHA-$Dext_m$ oximes by time course NMR

The second step towards the aim of this master thesis also involved obtaining kinetic data for the reduction of the chitosan-*b*-dextran oximes, as most AB polysaccharide diblocks are combined with an irreversible reduction step to obtain stable secondary amine conjugates [1]. Kinetic data for the reduction of pure D_nM and D_nM=PDHA-$Dext_m$ oximes by PB are presented in Section 4.4.1 and Section 4.4.2, respectively. In addition, the equilibrium mixture containing reduced D_nM-PDHA-$Dext_m$ diblocks were characterized by SEC-MALS and the results are presented in Section 4.4.3.

Based on literature [1], PB was expected to be a good alternative to $NaCNBH_3$ for the reduction of D_nM=PDHA-$Dext_m$ oximes. The reduction of D_4M and D_4M-PDHA-$Dext_{24}$ diblocks by PB was studied by time course NMR at pH 4.0. Reaction modeling was used to obtain rate constants for both reduction reactions. A detailed description of the model used have been published by Mo *et al.* [1]. The obtained rate constants are summarized in Table 4.6.

Table 4.6 The obtained rate constants for the reduction of the unreacted chitosan oligomers (D_4M) and chitosan-*b*-dextran oximes (D_4M-PDHA-$Dext_{24}$) by PB (3x) at pH 4.0. The rate for reductant decomposition was set to 2.00 x 10^{-3} to best fit the model to the experimental data.

	Equivalents of PB	pH	Rate constants (h^{-1})
D_4M (unreacted oligomer)	3	4.0	4.5 x 10^{-2}
D_4M=PDHA-$Dext_{24}$ (oxime)	3	4.0	3.0 x 10^{-4}

4.4.1 Reduction kinetics of chitosan oligomers

The possible reduction of D_nM oligomers was investigated prior to the reduction of the D_nM=PDHA-$Dext_m$ oximes. It was of great interest to obtain kinetic data for the reduction of unreacted chitosan oligomers due to the high reactivity of the pending aldehyde (gem diol) of the M residue. Additionally, differences in rate constants for the reduction of D_nM oligomers and D_nM=PDHA-$Dext_m$ oximes are important to know when exploring an optimized protocol for chitosan-*b*-dextran diblocks. The reduction of D_4M oligomers by PB was assayed by time course NMR at pH 4.0, and the resulting kinetic data is plotted as yield of reduced oligomer (%) as a function of time (hours), see Figure 4.16. The obtained rate constant for the reduction of D_4M by 3 equivalents of PB at pH 4.0 is listed in Table 4.6. ^{1}H-NMR spectra of the reduction of D_4M by PB after 0, 3 and 48 hours are given in Figure 4.17.

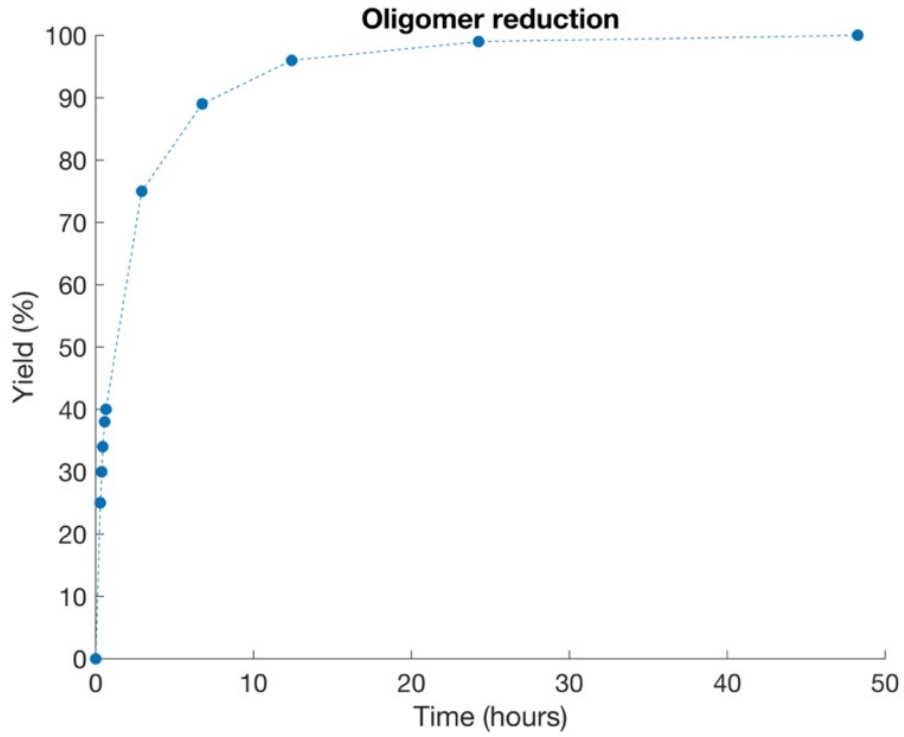

Figure 4.16 Yield of reduced oligomer (%) as a function of time (hours) for D_4M oligomers at pH 4.0 using 3 equivalents PB (RT). Lines were added to better illustrate the experimental data.

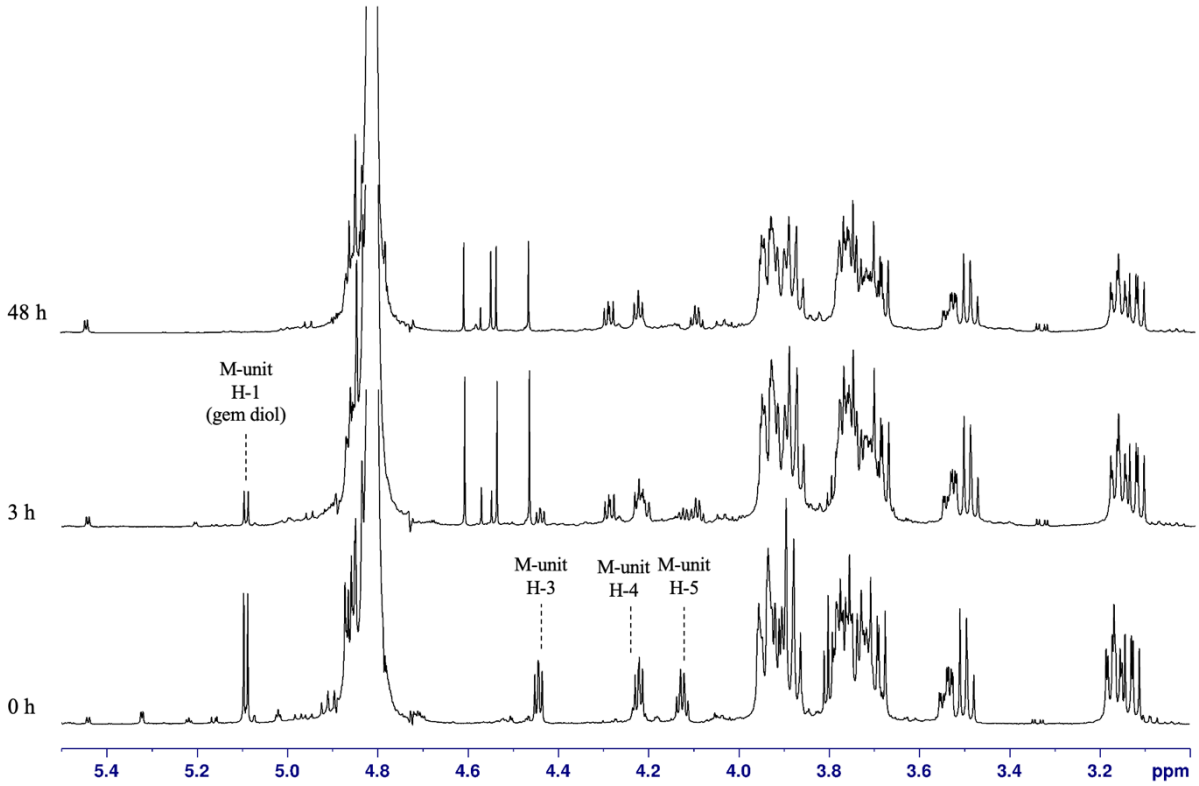

Figure 4.17 ^{1}H-NMR spectra obtained at defined points for the reduction of D_4M oligomers (7 mM) in deuterated acetate buffer, pH 4.0, RT using 3 equivalents of PB (21 mM).

Figure 4.16 illustrates that the reduction reaction by PB was 99 % complete after 24 hours, and fully completed after approximately 48 hours at pH 4.0. The course of the reduction reaction was studied by monitoring the disappearance of the H-1 M-unit (gem diol) resonance. The chemical shift of H-1 M-unit (gem diol) is observed at 5.1 ppm in the ^{1}H-NMR spectrum. After 3 hours, the intensity of the M-unit H-1 resonances were significantly decreased, indicating reduction of D_4M oligomers. The chemical shift of H-1 M-unit (gem diol) was no longer visible in the ^{1}H-NMR spectrum obtained after 48 hours of reduction by PB, indicating that the reduction has reached completion.

4.4.2 Reduction kinetics of D_4M-PDHA-$Dext_{24}$ oximes

The reduction of D_4M=PDHA-$Dext_{24}$ oximes by PB at pH 4.0 (RT) was monitored by time course NMR. The course of the reduction reaction was studied by monitoring the disappearance of E- and Z-oxime proton resonances and the disappearance of the remaining H-1 M-unit (gem diol) resonance. The obtained rate constant for the reduction by 3 equivalents of PB is listed in Table 4.6.

It was necessary to obtain information about the course of the reaction to complete reduction to provide a preparative protocol. Due to a slow reduction using 3 equivalents of PB, some additional methods were explored to speed up the reaction. After 5 days additional PB was added to the reaction mixture. Furthermore, the reaction mixture was heated to approximately 40 °C after an additional 6 days. Reduction was complete after 16 days. The different stages of the experiment are presented in Table 4.7. ^{1}H-NMR spectra of the equilibrium mixture containing D_4M-PDHA-$Dext_{24}$ oximes before reduction, after 5 days (3 x PB), after 11 days (10 x PB) and after 16 days (10 x PB, 40 °C) can be found in Figure 4.18.

Table 4.7 Reduction of D_4M=PDHA-$Dext_{24}$ diblocks

Equivalents of PB	Temperature (°C)	Days	Reduction (%)
0	25	0	0
3	25	5	37
10	25	11	81
10	40	16	100

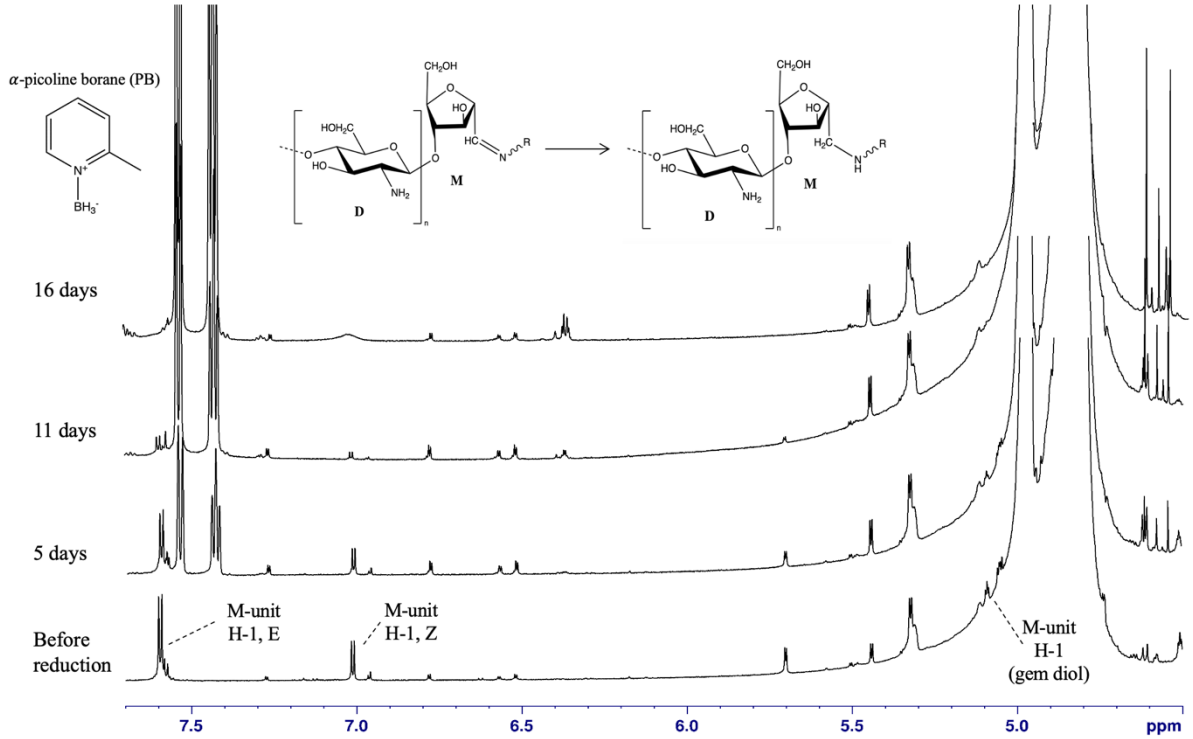

Figure 4.18 ^{1}H-NMR spectra of the D_4M-PDHA-Dext$_{24}$ diblocks before reduction, after 5 days with 3 equivalents of PB, after 11 days with 10 equivalents of PB and after 16 days being heated to approximately 40 ℃.

The chemical shifts of E- and Z-oximes are observed at 7.6 ppm and 7.0 ppm, respectively, while the chemical shift of the H-1 M-unit (gem diol) is observed at 5.1 ppm, see Figure 4.18. A slight decrease in intensity can be observed for all three resonances after 5 days of reduction. After 11 days, the intensities of the E- and Z-oxime had decreased significantly, while the resonance for the H-1 M-unit (gem diol) is completely gone. The reaction mixture was then heated to 40 ℃, which resulted in complete reduction after 16 days. The reduction yield (%) is plotted as a function of time (hours), see Figure 4.19.

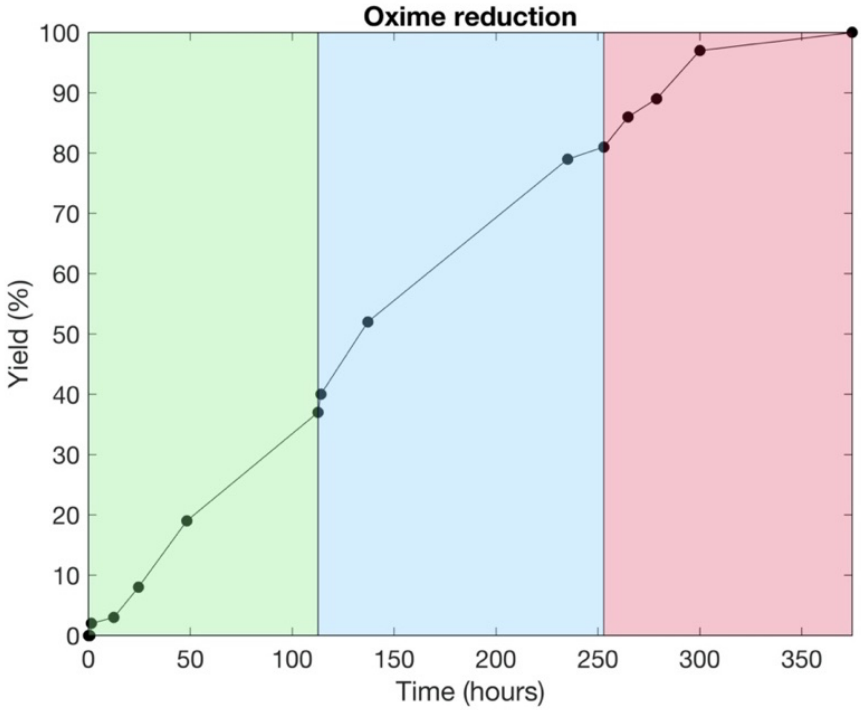

Figure 4.19 Yield (%) plotted as a function of time (hours) for the reduction of D_4M-PDHA-$Dext_{24}$ at pH 4.0 using initially 3 equivalents of PB at RT (0 - 113 h green), then increased to 10 equivalents (113 - 253 h blue) and finally heating to 40 ℃ (253 - 375 h red). Lines were added to better illustrate the experimental data.

4.4.3 Characterization of D_4M-PDHA-$Dext_{24}$ diblocks by SEC-MALS

The D_4M-PDHA-$Dext_{24}$ diblocks were characterized by SEC-MALS to verify the diblock formation, as a shift in the elution volume corresponding to the molar mass of D_nM is expected for the diblocks. The obtained chromatograms from the SEC-MALS analysis are presented in Figure 4.20. The chromatograms include the equilibrium mixture containing D_4M-PDHA-$Dext_{24}$ diblocks, unreacted D_4M oligomers and $Dext_{24}$-PDHA. The number average molecular weight (M_n) and the weight average molecular weight (M_w), obtained from the SEC-MALS analysis are listed in Table 4.8.

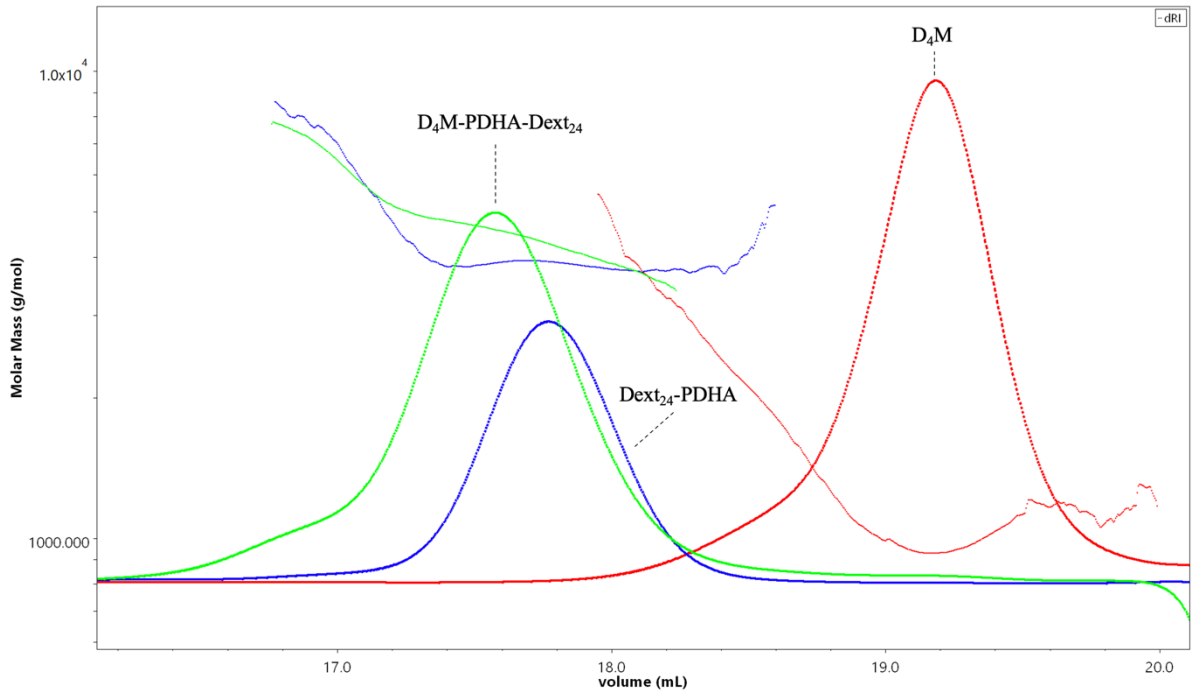

Figure 4.20 The chromatograms obtained from the SEC-MALS analysis of D_4M-PDHA-$Dext_{24}$ diblocks (green), $Dext_{24}$-PDHA (blue) and D_4M (red).

Table 4.8 Molecular masses (M_n and M_w) of D_4M, $Dext_{24}$-PDHA and D_4M-PDHA-$Dext_{24}$ obtained from SEC-MALS analysis.

	M_n (kDa)	M_w (kDa)
D_4M	1.1	1.2
$Dext_{24}$-PDHA	3.9	3.4
D_4M-PDHA-$Dext_{24}$	4.6	4.7

As observed in Figure 4.20, the chromatogram for D_4M-PDHA-$Dext_{24}$ diblocks is shifted towards lower elution volumes compared to unconjugated $Dext_{24}$-PDHA, in excellent agreement with the expected change in molar mass upon successful conjugation. Moreover, the shoulder in the D_4M chromatogram is clearly observed in the D_4M-PDHA-$Dext_{24}$ diblocks chromatogram as well, which further confirms that D_4M is present in the D_4M-PDHA-$Dext_{24}$ diblock. The M_n value of D_4M (1.1 kDa) and $Dext_{24}$-PDHA (3.9 kDa) corresponds well to the theoretical mass of the oligomers. The M_n of the D_4M-PDHA-$Dext_{24}$ diblocks (4.6 kDa) is close to the M_n of D_4M and $Dext_{24}$-PDHA combined.

4.5 Preparative protocol for chitosan-*b*-dextran diblocks

The optimized purification method of D_nM oligomers, see Section 4.1.2, resulted in oligomers with ≥ 85 % having the M-unit at the reducing end, and provided the opportunity to use D_nM as the second block in the chitosan-*b*-dextran diblock formation. The results from Section 4.3 provided information about the course of reaction for the conjugation of D_nM oligomers to $Dext_m$-PDHA. The obtained kinetic data showed that the conjugation of D_nM to $Dext_m$-PDHA was a rapid reaction. For the preparative protocol for D_nM-PDHA-$Dext_m$ diblocks, 1 hour was found to be sufficient for the conjugation reaction. In addition, conjugation performed using 1:1 molar ratio was found to produce high combined yields (≥ 85 %), see Figure 4.15b. The choice of continuing to use equimolar proportions was therefore based on the high yield, as well as the general need to use minimum amounts of oligosaccharides.

In previous work [7], chitosan-*b*-dextran diblocks were prepared by first conjugating D_nM oligomers to PDHA, followed by attachment of dextran as the second block. As such, this reverse protocol did not utilize the high reactivity of the M-unit. It is known that the reaction between a oligosaccharide with a M-unit at the reducing end and PDHA is faster and produces higher yields, compared to the reaction between dextran and PDHA [1]. It may therefore be beneficial to prepare chitosan-*b*-dextran diblocks using D_nM as the second block.

The results from Section 4.4 provided information about the course of reaction for the reduction of D_nM oligomers and chitosan-*b*-dextran oximes, which revealed that the reduction of D_nM oligomers was significantly faster compared to the reduction of chitosan-*b*-dextran oximes. The diblock yield will therefore not increase when PB is added, which is the case for the reverse protocol. An increase in diblock yield is seen for the reverse protocol due to the slow reduction of unreacted dextran oligomers by PB at RT [1, 7]. As reduction of the chitosan-*b*-dextran oximes was time-consuming and would not have any added benefit on diblock yield, it was of interest to prepare the diblocks using the preparative protocol without reduction and investigate the stability of the resulting chitosan-*b*-dextran oximes. In Section 4.5.1 and Section 4.5.2 results from the preparation of two D_nM=PDHA-$Dext_m$ diblocks prepared without reduction will be presented. Results from the stability study of the unreduced diblocks are presented in Section 4.6.3.

4.5.1 Conjugation of $D_{28}M$ to $Dext_{52}$-PDHA

$D_{28}M$ was conjugated to $Dext_{52}$-PDHA for the preparation of $D_{28}M$=PDHA-$Dext_{52}$ diblocks. To confirm the diblock formation, the reaction mixture of unreduced diblocks as well as unreacted $D_{28}M$ oligomers and $Dext_{52}$-PDHA were analyzed by SEC-MALS, see Figure 4.21.

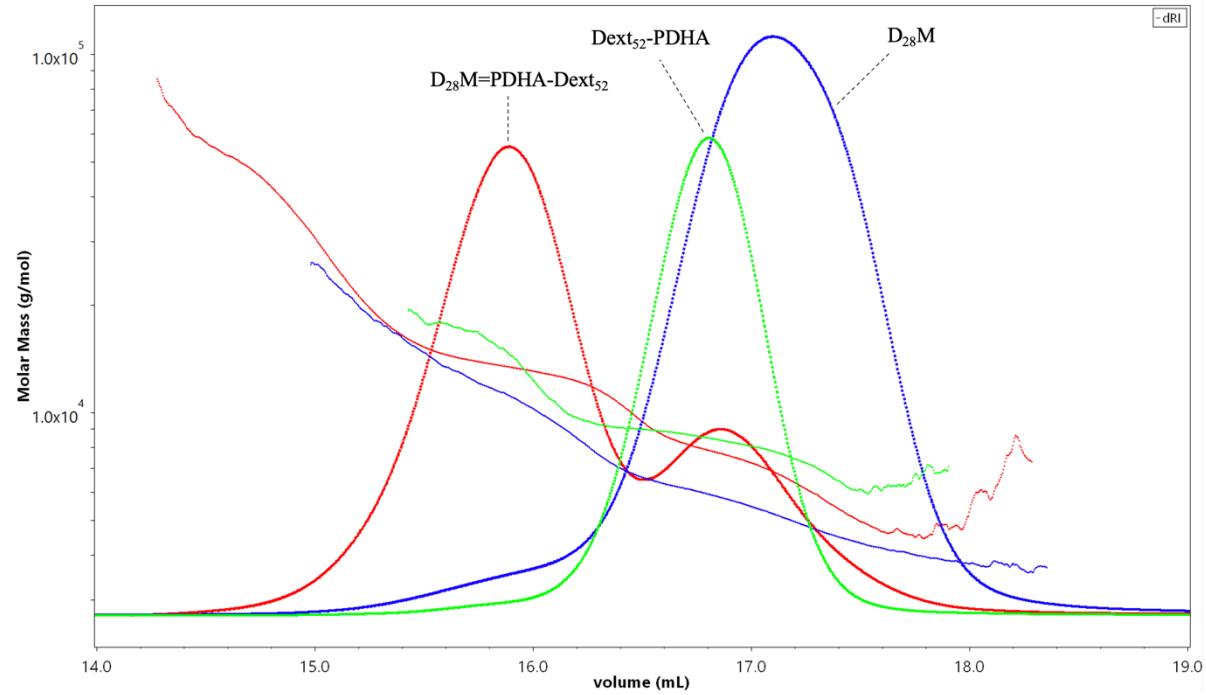

Figure 4.21 SEC-MALS chromatogram of the equilibrium mixture containing $D_{28}M$=PDHA-$Dext_{52}$ oximes (red), $Dext_{52}$-PDHA (green) and $D_{28}M$ (blue).

Table 4.9 Molecular masses (M_n and M_w) of $D_{28}M$, $Dext_{52}$-PDHA and $D_{28}M$=PDHA-$Dext_{52}$ oxime from SEC-MALS analysis.

	M_n (kDa)	M_w (kDa)
$D_{28}M$	5.2	5.6
$Dext_{52}$ -PDHA	8.4	8.5
$D_{28}M$=PDHA-$Dext_{52}$	10.9	12.5

The reaction mixture containing $D_{28}M$=PDHA-$Dext_{52}$ (red) eluted as two peaks, see Figure 4.21. The large peak at lower elution volumes indicates the conjugated diblocks. The smaller diblock peak at higher elution volumes indicates unreacted oligomers. As the conjugation was performed using 1:1 molar ratio, the peak corresponding to unreacted oligomers must therefore consist of equal amount of unreacted $D_{28}M$ and $Dext_{52}$-PDHA. The M_n and M_w obtained from the SEC-MALS analysis for $D_{28}M$, $Dext_{52}$-PDHA and $D_{28}M$=PDHA-$Dext_{52}$ are given in Table 4.9. The M_n value of $D_{28}M$ (5.2 kDa) and $Dext_{52}$-PDHA (8.4 kDa) corresponds well to the theoretical mass of the oligomers, and the M_n of $D_{28}M$=PDHA-$Dext_{52}$ diblock (10.9 kDa) is close to the M_n of $D_{28}M$ and $Dext_{52}$-PDHA combined.

4.5.2 Conjugation of D_9M to $Dext_{36}$-PDHA

D_9M was conjugated to $Dext_{36}$-PDHA for the preparation of D_9M=PDHA-$Dext_{36}$ diblocks. To confirm the diblock formation, the reaction mixture of unreduced diblocks as well as unreacted D_9M oligomers and $Dext_{36}$-PDHA oligomers were analyzed by SEC-MALS, see Figure 4.22.

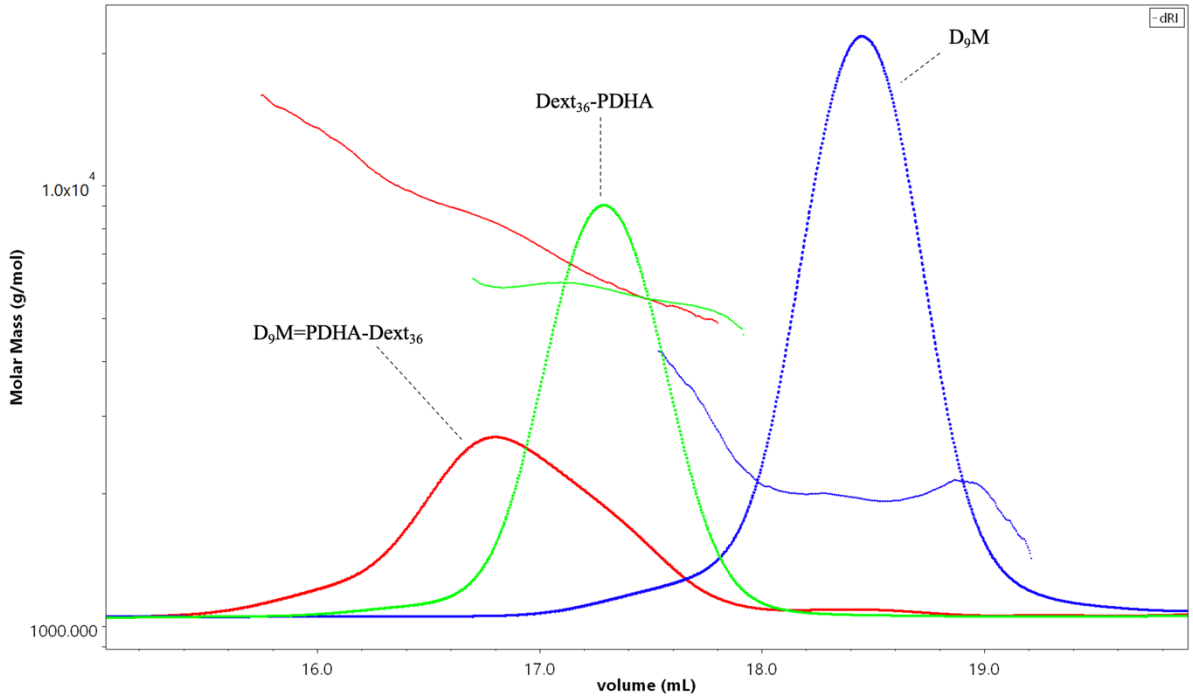

Figure 4.22 SEC-MALS chromatogram of the equilibrium mixture containing D_9M-PDHA-$Dext_{36}$ oximes (red), D_9M (blue) and $Dext_{36}$-PDHA (green).

Table 4.10 Molecular masses (M_n and M_w) of D_9M, $Dext_{36}$-PDHA and D_9M=PDHA-$Dext_{36}$ obtained from SEC-MALS analysis.

	M_n (kDa)	M_w (kDa)
D_9M	2.0	2.0
$Dext_{36}$ -PDHA	5.7	5.8
D_9M=PDHA-$Dext_{36}$	7.6	8.0

As observed in Figure 4.22, the reaction mixture containing D_9M=PDHA-$Dext_{36}$ (red) eluted at lower elution volumes compared to the unreacted oligomers, confirming the conjugation. As a consequence of the small hydrodynamic volume of D_9M, only a slight shift was observed upon coupling. The asymmetry is likely a result of unreacted $Dext_m$-PDHA eluting close to the diblock. The M_n and the M_w obtained from the SEC-MALS analysis are given in Table 4.10. The M_n value of D_9M (2.0 kDa) and $Dext_{36}$-PDHA (5.7 kDa) corresponds well to the theoretical mass of the oligomers, and the M_n of the D_9M=PDHA-$Dext_{36}$ diblocks (7.6 kDa) corresponds well to the theoretical mass of the D_9M=PDHA-$Dext_{36}$ diblocks.

4.6 Solubility and stability studies of chitosan-*b*-dextran diblocks

A highly relevant advantage of the preparation of linear AB diblocks is the retained intrinsic properties of the individual blocks. The last part of the aim of this master thesis was to investigate the properties of chitosan-*b*-dextran diblocks in solution. To this end, a study was performed comparing the solubility of chitosan-*b*-dextran diblocks to that of pure D_nM oligomers as a function of pH, using dynamic light scattering (DLS). DLS, a sensitive LS technique, was used to study aggregation and precipitation phenomena. In addition, a study was performed to investigate the stability of the chitosan-*b*-dextran diblocks prepared without reduction.

4.6.1 Solubility behavior of chitooligosaccharides

The solubility of D_nM oligomers is strongly dependent on the pH of the solution, leading to aggregation when the critical pH of solubility is reached. The hydrochloride form of D_nM oligomers is completely soluble in water, giving a pH of approximately 4 for solutions prepared in dilute conditions [25]. Increasing pH above the pK_a will result in aggregation, and subsequent precipitation. The solubility behavior of $D_{19}M$ oligomers was studied by measuring the scattering intensity (kcps) for pH values in the range of 3.9 – 10.1. According to literature [25], a steep increase in the scattering intensity is expected, as chitosan begins to aggregate in the pH range 6.5 – 7.5. The scattering intensity of $D_{19}M$ oligomers plotted as a function of pH is presented in Figure 4.23.

The result in Figure 4.23 is in good agreement with a study of the solution behavior of D_nM (n = 5 – 50) [25], see Section 2.2.3. The scattering intensity increased steeply as the pH was increased above 7, indicative of increasing particle size due to aggregation. Subsequently, the intensity of the scattered light decreased significantly as the pH was increased above 7.5, suggesting a decrease in the concentration due to precipitation of the particles. The measurements indicating precipitation are presented as red points in Figure 4.23. Precipitation could also be observed by visual inspection of the sample, clearly demonstrating the transition from a clear to a turbid and precipitating solution, see Figure 4.26 (sample 1).

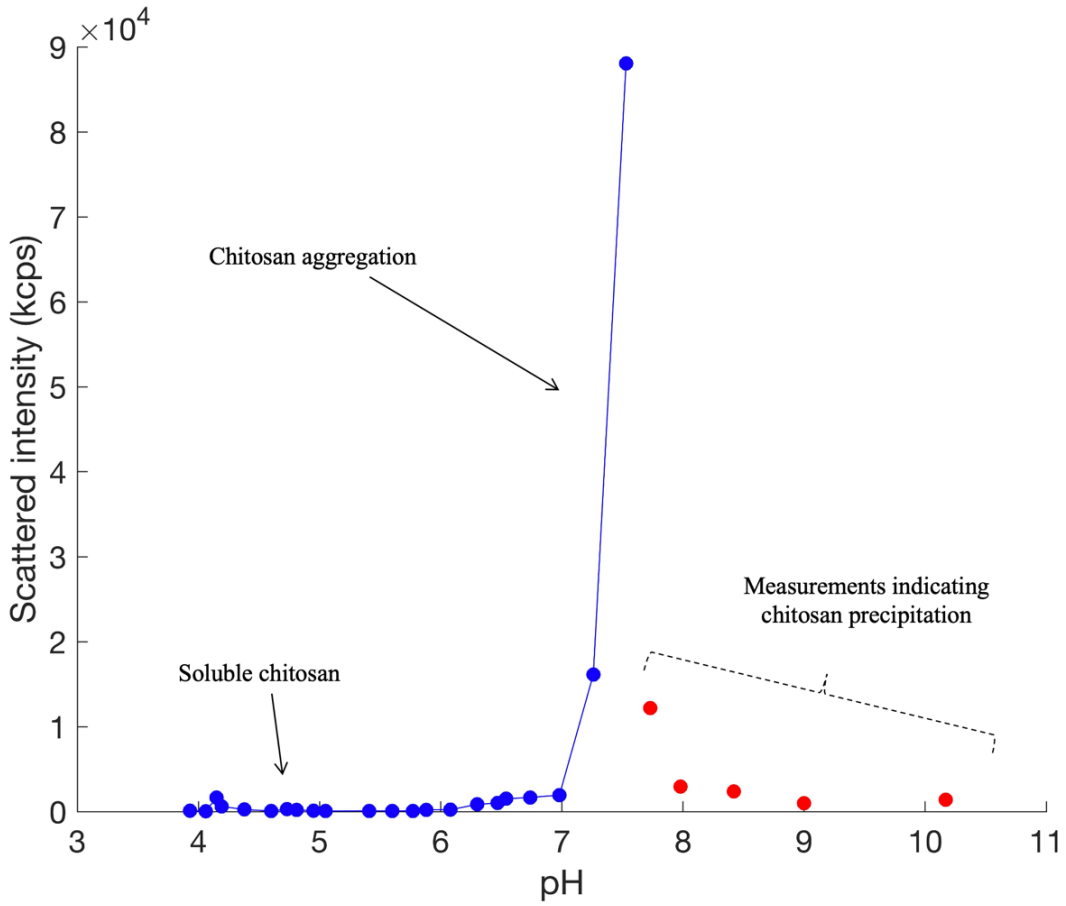

Figure 4.23 Scattered light intensity (in kcps, kilo count-per-second) as a function of pH for a solution of D_nM (1 mg/ml). Measurement obtained at pH ≤ 7.5, the onset of precipitation is observed (blue). Measurements obtained at pH > 7.5, indicating chitosan precipitation (red).

4.6.2 Solubility behavior of chitosan-*b*-dextran diblocks

The solubility behavior of $D_{28}M$=PDHA-$Dext_{52}$ diblocks was studied by DLS. Delas [25] performed a similar experiment studying the solubility of chitosan-*b*-PEG diblocks which was compared to that of pure D_nM oligomers by measuring the turbidimetry of the solutions. It was discovered that chitosan-*b*-PEG block copolymers remained soluble in the pH range of 3 – 11. Similarly, it was expected that the $D_{28}M$=PDHA-$Dext_{52}$ diblocks remained soluble over a larger pH range compared to pure $D_{19}M$, due to terminal conjugation of water-soluble dextran block. The scattering intensity of D_nM=PDHA-$Dext_m$ diblocks dissolved in 10 mM NaCl was measured to be 2000 kcps at pH 6.3 and 6000 kcps at pH 10.4, a slight increase in scattering intensity. The corresponding intensity distribution graphs are shown in Figure 4.24.

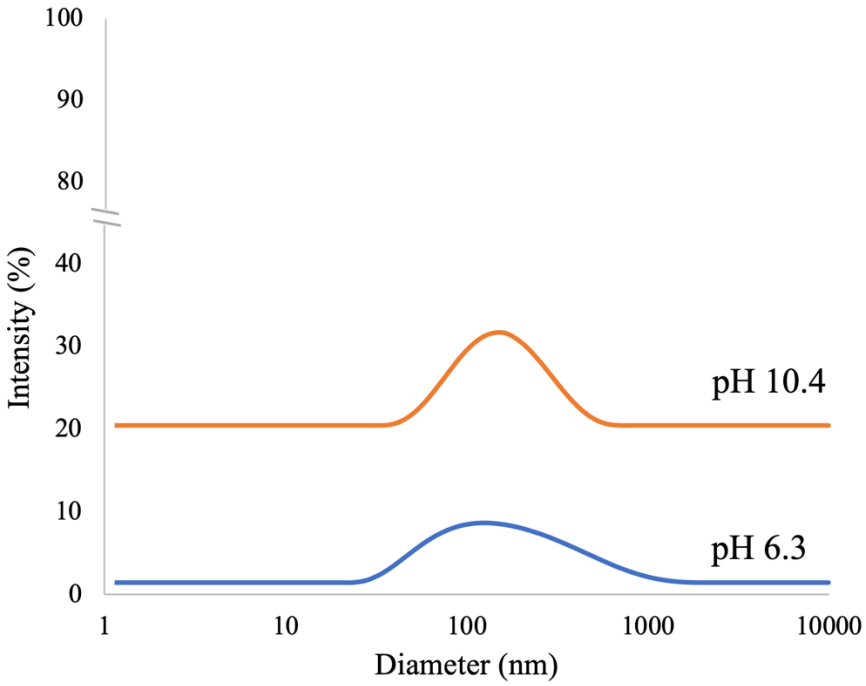

Figure 4.24 The intensity (%) as a function of diameter (nm) for $D_{28}M$=PDHA-$Dext_{52}$ at pH 6.3 (blue) and pH 10.4 (orange). The plots are shifted along the y-axis for better visibility.

The solubility behavior study of pure $D_{19}M$, Section 4.6.1, illustrated that $D_{19}M$ oligomers will begin to aggregate, followed by precipitation when pH > pK_a. Precipitation was observed by visual inspection of the sample for $D_{19}M$ at pH 10. However, a clear solution was observed for the diblocks at pH 10, indicating soluble diblocks, see Figure 4.26 (sample 2). This shows that the diblocks have significantly increased solubility, compared to pure $D_{19}M$, even with full deprotonation of chitosan. The solubility of the diblocks was further confirmed by the intensity distribution graph, in Figure 4.24, which presents the size distribution of the dissolved particles.

For polyelectrolytes, electrostatic interactions contribute to the structure and dynamics of the polymers in solution. NaCl (10 mM) was added to the $D_{28}M$=PDHA-$Dext_{52}$ diblocks solution to minimize polyelectrolyte effects [51]. More than one mode is typically expected when studying polyelectrolytes in solution by DLS, even in the presence of salt. The modes are commonly referred to as slow mode and fast mode [51]. However, when chitosan is deprotonated, *i.e.*, chitosan has no charge, a change in the intensity distribution more approaching the behavior of a neutral polysaccharide can be expected. This can be observed by increasing pH from 6.3 (~pK_a) to 10.4, see Figure 4.24, where a narrowing of the intensity distribution occurs. At pH 10.4 only one population is present, indicating deprotonation and

dehydration of chitosan. Moreover, a slight increase in the scattering intensity from 4000 kcps to 6000 kcps might indicate particle formation, likely of micellar nature.

4.6.3 Oxime stability study of unreduced chitosan-*b*-dextran diblocks

D_nM oligomers was conjugated with $Dext_m$-PDHA without reduction, Section 4.5, as it was of great interest to investigate the stability of the chitosan-*b*-dextran oximes. Based on literature [10], dextran-*b*-PEG oximes are reported to be stable at pH 3.0. A study exploring the stability of chitosan-*b*-dextran oximes was therefore performed by adjusting the pH of the diblock solution to pH 3.1 for 0.5 hours, followed by increasing the pH of the solution up to 10. The scattered intensity was measured by DLS at various pH values in the range of 3 – 10, see Figure 4.25.

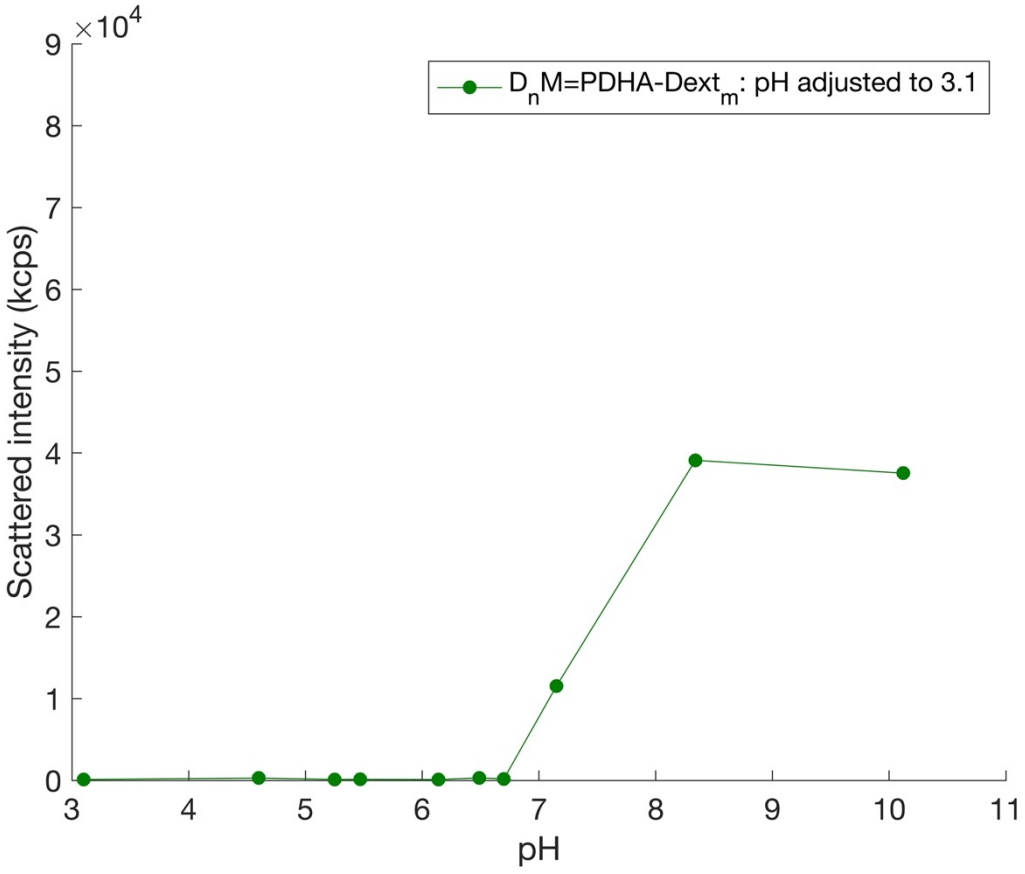

Figure 4.25 The scattered intensity (in kcps, kilo count-per-second) as a function of pH for D_nM=b-$Dext_m$ diblocks solutions at 1 mg/ml. The pH of the solution was adjusted to pH 3 by HCl and increased by adding 0.1 M NaOH.

As shown in Figure 4.25, an increase of the scattering intensity is observed from pH 6.7 to 8.3. The increase in scattering intensity indicates aggregation of free chitosan chains, as the increase

directly correlates to increased scattering intensity of pure $D_{19}M$ in Figure 4.23. However, the scattering intensity measured from pH 8.3 – 10 is close to unchanged, indicating no further aggregation or precipitation. Furthermore, the scattering intensity of the diblocks adjusted to pH 3.1 (sample 3) is significantly higher at pH 10 (40 000 kcps) compared to the measurements obtained from the diblocks not adjusted to pH 3.1 at pH 10 (6 000 kcps). This further supports the hypothesis that some of the diblocks may have been reverted to free chitosan chains and began to aggregate as the pH was increased above the pK_a. Finally, the diblocks solution was visually inspected, see Figure 4.26 (sample 3), and it was observed that the clear solution became turbid at pH > 7.5, indicative of chitosan aggregation. Precipitation could not be observed by visual inspection of the sample, suggesting that most of the sample remains as diblocks, due to the concentration of free chitosan being too low to precipitate out of solution at pH 10.

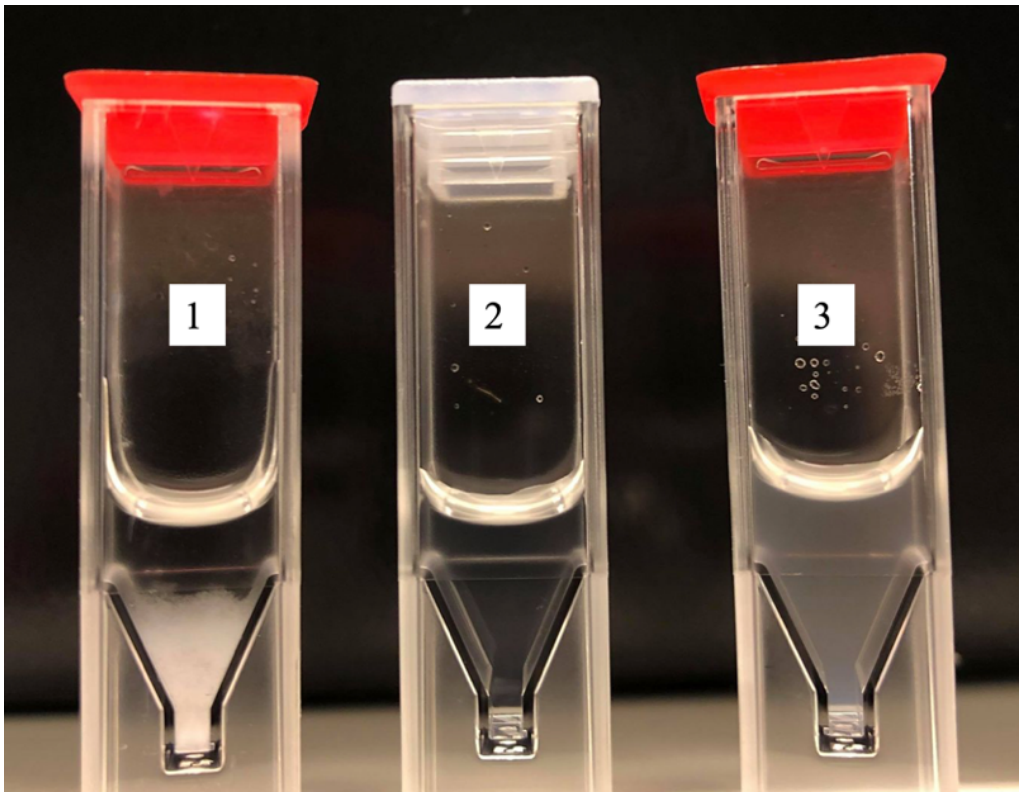

Figure 4.26 Solvent at pH 10 after DLS analysis: 1) Pure D_nM: precipitated is observed. 2) A clear solvent is observed, indicating soluble $D_{28}M$=PDHA-$Dext_{52}$ diblocks 3) Soluble $D_{28}M$=PDHA-$Dext_{52}$ diblocks (adjusted to pH 3.1), although indication of chitosan aggregation is observed.

5 DISCUSSION

The aim of this master thesis was to prepare and characterize chitosan-*b*-dextran diblocks and to study the properties of the diblocks in solution. Preparation of chitosan oligomers (D_nM), as well as preparation of activated dextran oligomers ($Dext_m$-PDHA) were performed prior to the preparation of D_nM-PDHA-$Dext_m$ diblocks. An optimized protocol for the preparation of D_nM oligomers with high preservation of M-unit at the reducing end was developed in this work. Kinetic data for the conjugation of D_nM to $Dext_m$-PDHA and the reduction of D_nM=PDHA-$Dext_m$ oximes were obtained for the purpose of establishing a preparative protocol for the diblocks. Two D_nM=PDHA-$Dext_m$ diblocks of varying DP were prepared using the preparative protocol without reduction. The pH dependent solubility of D_nM oligomers was compared to that of the D_nM=PDHA-$Dext_m$ diblocks by dynamic light scattering. Finally, the stability of the diblocks prepared without reduction were studied using the same approach.

5.1 Preparation and characterization of chitosan oligomers

5.1.1 Exploring potential new SEC mobile phases for chitosan separation

The advantageous use of one single column when exploring potential new SEC mobile phases for chitosan separation was confirmed by comparing the use of one single column to three consecutive columns. The tests of potential SEC mobile phases for chitosan separation were therefore performed using a single column.

The loss of chitosan sample inside the column, as well as unsatisfactory separation by SEC when the three new mobile phases were used may be explained by the mobile phases having too low ionic strength. Chitosan is a polycation *i.e.*, it carries positively charged ions, while the particles in the stationary phase consist of negatively charged ions. High ionic strength suppresses the polyelectrolytes character, due to screening of charges. The use of a mobile phase with too low ionic strength may therefore result in electrostatic interactions between the positively charged chitosan and the negatively charged groups (carboxyl) present in the stationary phase. Electrostatic interaction between the chitosan oligomers and the stationary phase prevents separation, as oligomers of different lengths will react with the column material and not eluate the column according to hydrodynamic volume. Consequently, the loss of chitosan sample inside the column may be resolved by increasing the ionic strength and chitosan will eventually elute from the column.

Furthermore, an increase in separation was observed when the concentration of ammonium acetate was increased, indicating that further increase in concentration would result in better separation. The use of 0.03 M AmAc, the mobile phase with the highest concentration of AmAc, did not result in satisfactory separation of D_nM oligomers by SEC. A further increase in AmAc concentration would therefore be necessary to obtain sufficient sample recovery and separation but would not be in line with the purpose of the experiment, which was to minimize the use of AmAc. In conclusion, satisfactory separation could not be achieved with the mobile phases tested, and one would need to look towards other measures to reduce ammonia in the resulting sample before freeze-drying.

5.1.2 Preparation of chitosan oligomers using an improved purification method

To prevent self-branching by Schiff base reaction during freeze-drying, the D_nM oligomer fractions obtained after SEC separation were purified by dialysis against MQ water adjusted to pH 4.5 with dilute HCl to remove buffer components from the sample. Compared to previous purification methods, this improved purification method resulted in higher preservation of M-unit at the reducing end. Previous purification methods [7, 8], which included dialyzing the separated D_nM oligomer fractions against MQ water and MQ water adjusted to pH 4.0 using dilute AcOH, as well as adjusting the pH to < 4.0 prior freeze-drying, achieved 50 – 70 % of the oligomers having M-unit at the reducing end. Deprotonation of primary amine groups of the D residues due to an increase in pH, enables reactions with the aldehyde of the M residues to form Schiff bases [7]. A lower concentration of ammonia will result in less deprotonation of chitosan because there will a smaller increase in pH, and hence a decrease in self-branching by Schiff base reaction during freeze-drying. The new purification method aimed to significantly lower the concentration of ammonia, with the goal of higher preservation of M-units.

The results from Section 4.1.2 demonstrated that 84 % of the D_4M oligomers and 87 % the D_9M oligomers had M-unit at the reducing end after purification followed by freeze-drying. This is a significant increase compared to the previous methods. The increase in oligomers with the M-unit at the reducing end could be explained by the use of a less volatile acid for dialysis. HCl helps to keep the pH low during dialysis and prevents precipitation. In addition, the use of a less volatile acid may result in ammonia and HCl evaporating at approximately similar rates which result in less fluctuations in pH during freeze-drying and thus, a decrease in self-branching by Schiff base reaction. Another explanation could be that the use of HCl in the

dialysis process led to a more rapid diffusion of ammonium during dialysis, resulting in less ammonium being present in the sample prior to freeze-drying.

Prior to SEC separation, chitosan was degraded by nitrous acid to obtain D_nM oligomers. Nitrous acid depolymerization of chitosan is a well-established procedure previously applied by Tømmeraas [17] to obtain chitosan oligomers with a 2,5-anhydro-D-mannose (M) unit at the reducing end. This depolymerization method was chosen for the purpose of exploiting the highly reactive M-unit in the conjugation with $Dext_m$-PDHA. The amount of HNO_2 used to depolymerize chitosan was estimated based on nitrous acid depolymerization being a homogeneous reaction, where the number of glycosidic bonds broken is roughly stoichiometric to the amount of nitrous acid used [17]. The DP_n of the chitosan samples after degradation was slightly higher compared to the calculated DP_n for the reaction, which may be explained by decomposition of nitrous acid. However, it was only a slight difference, and the desired oligomers could still be obtained.

Size exclusion chromatography (SEC) was used to prepare narrow fractions of D_nM oligomers in this work. However, there exist several methods to obtain purified chitosan oligomers, *e.g.*, by ultrafiltration or precipitation. Novoa-Carballal *et al.* [10] used ultrafiltration with regenerated cellulose membranes to obtain purified chitosan oligomer for the preparation of chitosan-*b*-PEG diblocks. Moussa *et al.* [50] provided isolated and purified oligomers for the preparation of chitosan based conjugates by precipitation. This method was also used by Coudurier *et al.* [52] for obtaining D_nM for the purpose of preparing D_nM-PDHA conjugates. SEC can sometimes be advantages to the methods described above, especially when narrow fractions are desired, which was the case in this thesis. The availability of SEC equipment at NOBIPOL made SEC a natural choice for the experiments performed in this thesis. However, it should be noted that SEC results are sensitive to experimental variables, such as flow rate, temperature, and sample concentration [44], which would likely vary between laboratories and equipment used and may therefore affect reproducibility.

The ^{1}H-NMR spectrum of D_4M oligomers confirmed the chemical structure and the DP of the oligomers. The chemical shift of H-1 M-unit (gem diol) at 5.0 ppm was easily observed to be the most abundant form of reducing end. By integrating the proton signals, the relative number of protons in different chemical environment could be estimated. This approach was used when calculating the percentage of D_nM oligomers with the M-unit (gem diol) at the reducing end.

The H-1 M-unit Schiff base could be observed as a small resonance peak at 7.9 ppm and the chemical shift of H-1α D-unit reducing end could be observed at 5.4 ppm. The chemical shifts of H-3, H-4, and H-5 M-unit was observed at 4.4, 4.1 and 4.0 ppm, respectively. These observations are in accordance with data reported by Tømmeraas [17] in the study on characterization of oligosaccharides produced by nitrous acid depolymerization of chitosan by ^{1}H-NMR. Furthermore, the H-2 D-unit internal residues could be observed at 2.9 ppm, which is in good accordance with Domard *et al.* [47] in the ^{1}H-NMR study of a glucosamine oligomers. The determination of DP_n was based on the signal of H-1 M-unit (gem diol), H-1 M-unit (Schiff base), H-1 D-unit reducing ends and the H-2 D-unit internal residues.

5.2 Preparation of activated dextran oligomers

The first part of the aim of this master thesis was to prepare chitosan-*b*-dextran diblocks. As the new purification method of chitosan oligomers resulted in chitosan oligomers with ≥ 85 % having the M-unit at the reducing end, dextran oligomers could be used as the first block in the preparation of chitosan-*b*-dextran diblocks. Dextran was degraded by acid hydrolysis, conjugated with PDHA, and reduced by PB to obtain stable secondary amines. The chemical shift of the H-1α and the H-1β resonances of dextran was observed at 5.2 ppm and 4.6 ppm, respectively, in the ^{1}H-NMR spectrum. The disappearance of the H-1α and the H-1β resonances of dextran after conjugation, as well as the emergence of secondary amines resonances at 2.8 ppm and 3.1 ppm, confirmed the conjugation. The chemical shift for H-1 branches was observed at 5.3 ppm and the DP prior to conjugation with PDHA and SEC separation was found to be 28. Narrow fractions of $Dext_m$-PDHA were obtained by SEC for the preparation of D_nM-PDHA-$Dext_m$ diblocks.

The kinetic parameters for the conjugation of dextran to PDHA has already been established. A study performed by Mo *et al.* [1] reported that the conjugation of PDHA to dextran oligomers resulted in a much higher yield compared to ADH. Similarly, Mo *et al.* [7] reported that the yield for the conjugation of D_nM to PDHA at pH 4.0 was also higher compared to the yield for the conjugation of D_nM to ADH at pH 4.0. It was therefore reasonable to assume that PDHA would be a better chemical linker compared to ADH for the conjugation of chitosan-*b*-dextran diblocks.

5.3 Conjugation of D_nM to $Dext_m$-PDHA studied by time course NMR

To establish a protocol for the preparation of chitosan-*b*-dextran diblocks, an estimate of the reaction time for the conjugation of D_nM to $Dext_m$-PDHA had to be obtained. Kinetics studies were performed by studying the reaction in detail by time course NMR. Short oligomers were initially chosen as a model system since they give relatively simple ^{1}H-NMR spectra with better resolution compared to longer polysaccharides. The model was fitted to the experimental data and the kinetic parameters were obtained.

According to previous literature [1], the use of sodium acetate (NaAc) buffer (500 mM) in the pH range of 3.0 – 5.0 for similar conjugation reactions have produced good results. The conjugation of D_nM to $Dext_m$-PDHA was therefore performed in sodium acetate (NaAc) buffer (500 mM) with TSP added as the internal standard at pH 4.0 (RT). The reaction time for the initial diblock formation was set to 48 hours to ensure that the reaction had reached equilibrium. ^{1}H-NMR spectra were recorded at specific time points and yields of conjugates were determined by integration of the obtained spectra. The integral of the resonance from the internal standard (TSP, 0 ppm) was used as a reference to calculate yields, due to the slight polydispersity of the oligomers.

The kinetic plots of the conjugation reaction of D_nM to $Dext_m$-PDHA (7 mM and 3.5 mM) showed that the reaction was rapid, as the reaction was close to equilibrium by the time the first ^{1}H-NMR spectrum was obtained for both experiments. The conjugation of D_nM to $Dext_m$-PDHA also produced high yields of D_nM=PDHA-$Dext_m$ oximes ($\geq$ 85 %). The results were similar for both concentrations indicating that the concentration has little effect on the result of the conjugation. Fitting the model to the experimental data for the 3.5 mM conjugation reaction resulted in slightly higher values for the rate constants (k_1 and k_2) compared to the 7 mM conjugation reaction. However, the rate constants are of the same order of magnitude and it is therefore reasonable to say that the rate of the reaction is approximately the same in both cases. Several factors could explain the difference in rate constants. Firstly, it is more difficult to obtain exact integrals of resonance peaks in ^{1}H-NMR spectra with lower concentration due to the decrease in resolution. Secondly, an increased number of spectra obtained in the critical time period of the reaction were obtained for the 3.5 mM conjugation reaction, which may have resulted in a better fit to the experimental data. Finally, the difference in the obtained rate constants (k_1 and k_2) could be explained by the reaction not being strictly first order. It may

also be noted that the rate constants for the conjugation (k_1 and k_2) needed to have the same values as the rate constants for the dissociation (k_{-1} and k_{-2}) of E- and Z-oximes to obtain good fits for the model to the data.

A kinetic study for the conjugation of chitin oligomers (A_nM) to $Dext_m$-PDHA at 3.5 mM (1:1) pH 4.0 resulted in rate constants $k_1 = 7.3 \times 10^{-1}$ h^{-1} and $k_2 = 2.1 \times 10^{-1}$ h^{-1} for the formation of E- and Z-oximes, respectively [53]. Whereas the rate constants for the formation of E- and Z-oximes when conjugating chitosan oligomers (D_nM) to $Dext_m$-PDHA at 3.5 mM (1:1) pH 4.0 are $k_1 = 2.4$ h^{-1} and $k_2 = 8.0 \times 10^{-1}$ h^{-1}, respectively. Hence, the reaction was slightly faster when using D_nM oligomers, indicating that D_nM oligomers are even more reactive towards PDHA-$Dext_m$ compared to A_nM oligomers at pH 4.0. It is known that the rate of conjugation depends significantly on the nature of the reducing end residue, which was concluded when a study compared the rate of conjugation of chitin oligomers and dextran oligomers to PDHA and ADH [2]. By performing this conjugation study using D_nM oligomers and comparing the results to the use of A_nM oligomers, it is found that in addition to the reducing end residue, the internal residues of the oligomers may also have an impact on the rate of the conjugation. It is recommended to perform further studies on the effect of the internal residues on the speed of conjugation.

The combined yield for the reaction with D_nM to $Dext_m$-PDHA using 7 mM and 3.5 mM (1:1) *i.e.*, the sum of E- and Z-oximes for the M residue (gem diol), were high ($\geq$ 85 %) for both experiments. The kinetic study for conjugation of chitin oligomers (A_nM) to $Dext_m$-PDHA using 3.5 mM (1:1) pH 4.0 resulted in a combined yield of 63 % [53], which is a significant decrease compared to the yield obtained using D_nM. This may indicate that in addition to resulting in a slightly faster reaction, D_nM oligomers also produces higher yields compared to A_nM oligomers when conjugated to $Dext_m$-PDHA.

A limitation of using time course NMR for these types of fast reactions is obtaining spectra quickly after the reaction start. Shaking the reaction mixture, transferring it to NMR tubes and the transportation of the sample inside the NMR instrument result in a delay of several minutes before the first spectrum can be obtained. Time course NMR may therefore not be the ideal method for reactions being close to equilibrium within 0.5 hours.

5.4 Reduction kinetics studies by time course NMR

To develop a preparative protocol for the preparation of chitosan-*b*-dextran diblocks, an estimate of the course of reaction for oxime reduction was also needed. Kinetics studies were performed to obtain rate constants for the reduction of D_nM oligomers by PB and the reduction of D_nM=PDHA-$Dext_m$ diblocks by PB. PB was expected to be a good alternative to $NaCNBH_3$, due to its successful application as a reducing agent for chitin-*b*-dextran diblocks [53]. In addition, possible methods to speed up the reduction reaction of D_nM=PDHA-$Dext_m$ oximes were explored. According to Mo *et al.* [1], the relative reductive power (%) of PB will decrease over time due to spontaneous decomposition in 500 mM NaAc-buffer at pH 4.0. This was taken into account by adding an irreversible reductant decomposition rate constant of 2.0×10^{-2} h^{-1} for PB when fitting the model to the experimental data obtained from the time course NMR study.

The reduction of D_nM oligomers was studied to establish the reduction rate of the highly reactive pending aldehyde (gem diol) of the M-residue. It was of further interest to compare the results to the reduction of A_nM oligomer, as well as the reduction of D_nM=PDHA-$Dext_m$ oximes, as it provides useful information for the preparative protocol for chitosan-*b*-dextran diblocks in terms of diblock yield after reduction. Reduction by PB would render the D_nM oligomers unreactive for further conjugation [1]. The reduction was studied by monitoring the disappearance of the H-1 M-unit (gem diol) resonance and compared to the internal standard (TSP, 0 ppm). The kinetic model was fitted to the experimental data (reduction is assumed to be irreversible) resulting in a best fit rate constant of 4.5×10^{-2} h^{-1} at pH 4.0. The reduction was fast and complete reduction was obtained in less than 24 hours.

Mo *et al.* [1] previously performed a kinetic study investigating the reduction of A_nM oligomers using PB as the reducing agent at pH 4.0. Given the similarities of A_nM and D_nM oligomers, it is natural to compare the results from this experiment with the findings from Section 4.4. The rate constant for the A_nM reaction was found to be 1.5×10^{-2}, seemingly indicating that the reduction of D_nM oligomers (with a rate constant of 4.5×10^{-2}) is three times faster compared to the reduction of A_nM oligomers. However, these results cannot be directly compared as an additional rate constant, namely the irreversible reductant decomposition rate constant, was added to the reaction modeling for D_nM. To enable a fair comparison, another model, without the decomposition constant, was fitted to the D_nM data, resulting in approximately the same

rate constant as for the A_nM oligomers. This indicates that the rate of reduction of D_nM and A_nM oligomers by PB is reducing end specific (M-unit) and independent of the internal residues.

Most AB diblocks are combined with an irreversible reduction step to obtain stable secondary amines. The rate of reduction of these types of diblocks depends on the polysaccharides. Establishing the course of reaction of the reduction of D_nM=PDHA-$Dext_m$ diblocks was therefore necessary to develop a protocol for preparative work. The model was fitted to the data obtained after studying the reduction reaction by 3 equivalents of PB for 5 days by time course NMR. Reduction of D_nM=PDHA-$Dext_m$ oximes (rate constant = 3.0×10^{-4}) was found to be significantly slower compared to the reduction of pure D_nM oligomers (rate constant = 4.5×10^{-2}). This difference in rate of reduction between D_nM oligomers and D_nM=PDHA-$Dext_m$ oximes may affect overall yield of reduced diblocks, as the reduction may interfere with the equilibrium of unreduced D_nM and D_nM=PDHA-$Dext_m$ oximes. If D_nM oligomers are reduced faster than D_nM=PDHA-$Dext_m$ oximes, a shift in the equilibrium from unreduced oximes to unreduced oligomers is likely, thereby decreasing the available D_nM=PDHA-$Dext_m$ oximes for reduction.

An estimate of the course of reaction for the complete diblock reduction had to be obtained for the preparative protocol. After completing the kinetics study of the diblock, the reduction was still only 37 % complete. A decrease in the reaction rate after 5 days suggested a decrease in PB concentration due to spontaneous decomposition. Looking at specific properties of PB hinted towards further measures for improving the rate of reduction. PB is known to have low solubility in the aqueous buffer at room temperature [1]. Additionally, it is also suggested that the surface of undissolved PB particles may partake in the reduction reaction, as stirring of the reaction mixture have been shown to increase the speed of the reaction [1]. Two possible methods to increase the amount of dissolved PB and achieve complete reduction was therefore explored. First, 7 additional equivalents of PB were added to the reaction mixture for a total of 10 equivalents of PB on day 5 as an attempt to increase concentration of PB in the solution. A slight increase in the yield of reduced conjugates could be observed after addition of PB. After the reaction had run for 6 more days with 10 equivalents of PB, the rate of reduction began to decrease again. The second method was to heat the reaction mixture in an attempt to increase the solubility of PB. The reaction mixture was heated to 40 ℃ and mixed well several times

from day 11. An increase in rate of reduction was observed and complete reduction was achieved after a total of 16 days.

The slowness of the reduction highlights that this as an area of focus for further optimization in the preparative protocol. Possible measures to increase the rate of the reduction reaction were continuous addition of PB, as well as heating the reaction mixture from start for maximum solubility of PB. A shaker device may also aid the dissolving process. Additional kinetic experiments are needed to properly gauge the efficacy of the suggested methods before any recommendations can be made for the preparative protocol. However, no further experiments were performed due to time constraints.

5.5 Preparative protocol for chitosan-*b*-dextran diblocks

A new preparative protocol for the preparation of chitosan-*b*-dextran diblocks by conjugating D_nM oligomers to $Dext_m$-PDHA was developed in this thesis. The new purification method of D_nM oligomers, Section 4.1.2, provided the opportunity to prepare chitosan-*b*-dextran diblocks using D_nM oligomer as the second block, and hence, utilizing the highly reactive M-unit in the conjugation reaction. The two kinetic studies presented in Section 4.3 and Section 4.4, provided the necessary information about the course of the conjugation reaction of D_nM oligomer to $Dext_m$-PDHA and the course of the reduction reaction of chitosan-*b*-dextran oximes, respectively.

A protocol for the preparation of chitosan-*b*-dextran diblocks have been described in the literature [7]. The protocol developed by Mo *et al.* [7] includes using D_nM oligomers as the first blocks, *i.e.*, the D_nM oligomers are conjugated to PDHA prior to the attachment of a dextran block. In this case the high reactivity of the M-unit is not utilized in the diblock formation. The protocol was performed this way to protect the M-unit, due to the unresolved purification issues. The degradation of M-unit was prevented by using a large excess of PDHA (> 10 equivalents) to the unreacted oligomers followed by addition of a reducing agent prior to SEC separation. By optimizing the purification method for the preparation of purified and isolated D_nM oligomers, chitosan-*b*-dextran diblocks could be prepared by conjugating D_nM oligomers to $Dext_m$-PDHA. Kinetic data for the conjugation of D_nM-PDHA to $Dext_m$ have not yet been obtained. However, as judged by the conjugation of dextran to free PDHA, the reaction will likely be significantly slower and provide lower yields as compared to that of D_nM. To confirm the hypothesis that the diblock formation by conjugation D_nM to $Dext_m$-PDHA is a faster reaction and provides higher yield, the D_nM-PDHA to $Dext_m$ reaction should be analyzed by time course NMR, so that kinetic data for the D_nM-PDHA to $Dext_m$ reaction can be obtained and compared to the reversed conjugation reaction.

As discussed in the previous section, reduction of the equilibrium mixture containing unreacted D_nM oligomers and chitosan-*b*-dextran oximes may result in a slight decrease in diblock yield, due to the rapid reduction of unreacted D_nM oligomer compared to that of chitosan-*b*-dextran oximes by PB. However, improved yields can be expected for the equilibrium mixture obtained using the reversed protocol because of the slow reduction of unreacted dextran [1]. Hence, there are advantages and disadvantages to both protocols. However, given the high yield of

chitosan-*b*-dextran oximes (before reduction) when utilizing the high reactivity of the M-unit, the proposed method is likely the most beneficial method in terms of reaction rate and chitosan-*b*-dextran oxime yield. Further studies quantifying the differences in yield after reduction between the two methods are necessary to confirm this.

The choice of continuing to use equimolar proportions for the preparative protocol was based on the high yield, as well as the general need to use minimum amounts of oligosaccharides, and potentially avoid the need for purification. The reduction of the chitosan-*b*-dextran oximes was time-consuming. Additionally, there would be no added benefit on diblock yield by reduction, as previously discussed. It was therefore of great interest to prepare chitosan-*b*-dextran diblocks without reduction to further investigate the stability of the chitosan-*b*-dextran oximes. Successful conjugation using the preparative protocol under equimolar conditions with D_nM and $Dext_m$-PDHA was confirmed by SEC-MALS analysis. The equilibrium mixture of unpurified $D_{28}M$=PDHA-$Dext_{52}$ diblocks resulted in a chromatogram with several peaks. The largest peak was clearly shifted to lower elution volumes confirming conjugation. The unconjugated oligomers eluted as a smaller peak at higher elution volumes. The equilibrium mixture of unpurified D_9M=PDHA-$Dext_{36}$ diblocks resulted in an asymmetrical chromatogram slightly shifted to higher elution volumes compared to $Dext_{36}$-PDHA. The asymmetry is most likely due to unconjugated oligomers eluting closely after the diblocks and the small shift of the diblock chromatogram corresponds well to the small hydrodynamic volume of D_9M. The presence of unconjugated oligomers in the equilibrium mixtures were expected, as the conjugation using 1:1 molar ratio provided combined yields of approximately 85 % as predicted by the kinetic studies. Due to difficulties obtaining ^{1}H-NMR spectra with high resolution for longer oligomers, the exact yields of the diblock formations could not be determined.

Purification methods for chitosan-*b*-dextran diblocks prepared without reduction

The chitosan-*b*-dextran diblock prepared by the preparative protocol without reducing was not purified, due to the unknown stability of the oximes. SEC is a commonly used method to purify diblocks, as the unreacted oligomers will eluate at different elution volumes compared to the diblocks, assuming that the distribution of pore sizes of the column material match those of the molecules being separated. Furthermore, purification of the unreduced diblocks by SEC would mean dissolving the diblocks in the SEC buffer (pH 4.5) for a minimum of 20 hours. Hence, this purification method could result in diblock reversion and a decrease in yield, as the stability

of these diblocks without reducing is still not determined. The removal of unreacted oligomers from the reaction mixture consisting of unreduced diblocks may also result in a shift in equilibrium, resulting in a further decrease in yield. These possibilities were the reason for not purifying the chitosan-*b*-dextran diblocks before further studies on diblocks solubility and diblock stability was explored, see Section 4.6.

Purification of the chitosan-*b*-dextran diblocks prepared without reduction by SEC would be a possibility if it was known that the oximes were stable for at least 20 hours at pH 4.5, as that is the timeframe for SEC separation using three columns. A study employing SEC-MALS to study the oximes over time could give further insight into the stability of the oximes. A suggestion would be to dissolve the diblocks in SEC-MALS buffer (pH 4.5) and perform measurements at specific time points up to a minimum of 20 hours. By observing the potential increase in peak corresponding to unconjugated oligomers and the potential decrease in peak corresponding to diblocks, one may be able to determine if or for how long the diblocks are stable at pH 4.5.

Other purification methods for chitosan-*b*-dextran diblock include removal of unreacted chitosan oligomers by precipitation under conditions where the diblocks remain soluble [7]. However, this method requires specific solubility of the blocks, which at this point remained to be unexplored. Furthermore, a second possible method to purify the chitosan-*b*-dextran diblocks could be to remove the excess chitosan oligomers through reactions with beads or surfaces functionalized with aldehyde or ketone groups [7]. These methods could therefore be a solution for purifying the unreduced chitosan-*b*-dextran diblocks and is therefore deserving of future attention.

5.6 Solubility and stability studies of chitosan-*b*-dextran diblocks

The solubility studies of pure chitosan (D_nM) and chitosan-*b*-dextran, and the stability study of D_nM=PDHA-$Dext_m$ oximes taken together conclude the final aim of this thesis. The solubility tests demonstrate that terminally conjugated dextran with D_nM oligomers has significantly increased solubility, as compared to pure D_nM oligomers. In fact, the diblock was shown to be fully soluble under conditions (pH > 6.5) where D_nM oligomers precipitates. The stability analysis showed how the oximes are only stable for a defined pH interval. This is not in line with previously reported studies for oximes, and should be further studied [10].

5.6.1 Solubility behavior of chitooligosaccharides

The results from the solubility behavior study of $D_{19}M$ oligomers are in good agreement with the solubility analysis performed by Delas [25], see Section 2.2.3. The solubility of $D_{19}M$ oligomers is strongly dependent on pH, and aggregation and subsequent precipitation occurs when the pH of the solution is increased above the pK_a (6.5). Compared to the results published by Delas [25], a slight shift to higher pH values for the aggregation of $D_{19}M$ is observed. This is likely explained by the fact that aggregation is not instant, but a time dependent process. For this experiment, the light scattering measurements were determined immediately after pH was adjusted. Additional waiting before the measurements may allow chitosan oligomers to aggregate at lower pH values, which may explain the slight difference in aggregation obtained in this work and that reported in literature [25].

The sharp decline in scattering light intensity at pH > 7.5 suggests a decrease in the solution concentration due to precipitation. Scattering light intensity from a polymer solution decreases with decreasing concentrations. The measurements assumed to indicate chitosan precipitation is further supported by the visible division of the turbid chitosan solution, as seen in Figure 4.26 (sample 1). The chitosan solution had clearly been divided into two phases at pH 10: one clear layer at the top and one very turbid layer at the bottom, which is a clear sign of precipitation.

5.6.2 Solubility behavior of chitosan-*b*-dextran diblocks

Chitosan has several physiochemical and biological properties including antibacterial activity. The insolubility of chitosan at physiological pH limits some of its potential applications. In a study performed by Liu *et at.* [54], it was demonstrated that chitosan shows antibacterial activity only in the acidic range due to its poor solubility. Water-soluble chitosan derivatives

that remains soluble in both acidic and basic conditions may therefore be potential candidates for the polycationic biocide [54]. Thus, modified chitosan with increased solubility could enable new applications. Many studies focusing on increasing chitosan solubility have therefore been performed [55]. The introduction of hydrophilic groups into chitosan by quaternization of the amino groups have shown to increase chitosan solubility [56]. Furthermore, grafting of poly(ethylene glycol) (PEG) has resulted in increased solubility of chitosan oligomers in aqueous solutions over a pH range of 4 – 11 [57].

A key motivation for the preparation of block polysaccharides by terminal conjugation is to largely retain the intrinsic physiochemical properties of both polysaccharides in the diblock. Conjugation of a second block at the reducing end of chitosan have been reported to increase solubility. Delas [25] studied the solubility of chitosan-*b*-PEG block copolymers, which resulted in chitosan being soluble up to pH 11. AB diblocks consisting of two polysaccharides allow for a range of new biomaterials. It was therefore of great interest to explore the possibility of increasing the solubility of chitosan by the attachment of a second polysaccharide. The results from the solubility behavior study of chitosan-*b*-dextran diblocks reveals that the attachment of a water-soluble dextran block to chitosan results in stable diblocks with increased solubility up to pH 10.4. In addition to increasing the potential uses of chitosan, due to increased solubility and preservation of fundamental properties, chitosan-*b*-dextran will have a broad range of chemical, physical and biological properties *e.g.*, biodegradability, that makes them more desirable compared to synthetic blocks.

DLS was used to study the chitosan-*b*-dextran diblocks in solution. The intensity distribution as a function of diameter (nm) was broader for the diblock solution at pH 6.3 compared to pH 10.4. This phenomenon may indicate protonation of the chitosan block, since polyelectrolyte solutions exhibit a relative slow diffusion mode, which is referred to as the slow mode. The separation of the fast and slow mode depends on experimental conditions, such as the polymer concentration and added salts concentration [51]. At pH 10.4, only one particle size could be observed for the intensity distribution compared to the one present at pH 6.3. Dehydration upon protonation, but without precipitation, is in good agreement with the observed trend [51]. Furthermore, the z-average diameter of the particles is too large to indicate free chains. The slight increase in the scattering light intensity could therefore indicate structuring and a hypothesis is self-assembly of chitosan and the formation of a micellar structure with a dextran

corona. This will need further examination, small angle scattering techniques (SAXS/SANS) would likely provide more details as to the structuring of the chitosan-*b*-dextran diblocks [58].

5.6.3 Oxime stability study of unreduced chitosan-*b*-dextran diblocks

The D_nM=PDHA-$Dext_m$ diblocks were prepared without reduction. Hence, the free oxyamine of $Dext_m$-PDHA to E- or Z-oximes (D_nM=PDHA-$Dext_m$) is reversible. According to literature [10], oximes are reported to be stable at high pH, and only to revert under acidic conditions (pH below 3). It was therefore of great interest to study the stability of these diblocks at low pH values. The scattering intensity of the diblock was determined by DLS for a set of pH values. As the sample was shown to be approximately 85 % diblock, some aggregation resulting solely from the unreacted D_nM was expected. For the sample studied in the pH range of 6 – 10 (sample 2), a slight increase in scattering intensity was indeed observed, but the increase was minor, compared to that observed for a sample of pure D_nM (sample 1). For the sample studied in the pH range of 3 – 10 (sample 3), a significant difference was observed compared to sample 2. Sample 2 showed a slight increase in scattering intensity with increasing pH, but was overall in agreement with the solubility trends observed for the chitosan-*b*-PEG diblock reported by Delas [25]. Contrastingly, sample 3 displayed trends in agreement with aggregation and precipitation of chitosan, leading to the hypothesis that some of the oximes had been reverted.

The hypothesis that a reverse reaction had occurred for sample 3, was further supported by an increase in turbidity of the diblock solution, see Figure 4.26 (sample 3). The solution became turbid when pH > pK_a, which indicates chitosan aggregation. The scattering light intensity was unchanged in the pH range 8 – 10, which indicates that the concentration of the solution is unchanged, and hence, no precipitation occurred. No precipitation at pH 10 may be explained by the concentration of aggregated chitosan being too low to precipitate out of solution.

The stability of dextran-*b*-PEG block copolymers have been studied by obtaining NMR spectra at different pH values [10]. In this study, it was discovered that the dextran-*b*-PEG block copolymers were completely stable for at least 55 hours at pH 3 while it hydrolyzed to approximately 95 % at pH 2 within 24 hours. Based on the results presented in Section 4.6.3, chitosan-*b*-dextran diblocks are less stable compared to dextran-*b*-PEG block copolymers, as some diblock reversion occurred after the pH of the diblock solution was adjusted to pH 3.0

for 0.5 hours. However, at which pH value (below pH 6) the diblock reversion occurred, as well as the degree of diblock reversion cannot be determined by this experiment. An NMR study is therefore suggested as future work, as performed for the dextran-*b*-PEG block copolymers [10], to determine at which pH, as well as the degree of dissociation of the E- and Z-oximes.

5.7 Future perspectives

Preparation and characterization of chitosan-*b*-dextran diblocks were successfully performed in this master thesis. A kinetic study of the conjugation of D_nM oligomers to $Dext_m$-PDHA (1:1 molar ratio) at pH 4.0 illustrated a very fast reaction with high reaction yields. However, the diblock reduction by PB was a time-consuming reaction. Additionally, the chitosan-*b*-dextran oxime stability study illustrated that the oximes were not stable at low pH values without reduction. Future research should therefore include a study on the possibility of optimizing the reduction process, where possible suggestions for optimization were highlighted in Section 5.4.

Dynamic light scattering was used to study the pH dependent solubility of pure D_nM oligomers in the pH range of 3 – 10, so that it could be compared to the solubility of the chitosan-*b*-dextran diblocks. It was discovered that the conjugation of a water-soluble dextran block resulted in soluble diblocks at pH > pK_a. A limitation of this experiment is that only one chitosan-*b*-dextran diblock was tested in the experiments. Further research should therefore include chitosan-*b*-dextran diblocks of varying lengths. In addition, further research may also include a study where the length of the dextran blocks is the varying variable, as it would be interesting to determined how long the water-soluble dextran blocks needs to be compared to the chitosan block to obtain soluble diblocks.

The DLS analysis of the chitosan-*b*-dextran diblocks indicated structuring when the pH was increased from pH 6.3 to pH 10. A slight narrowing of the intensity graph at pH 10 compared to the one present at pH 6.3, as well as a slight increase in scattering intensity led to the hypothesis of self-assembly of chitosan and the formation of a micellar structure with a dextran corona. However, further studies is needed to confirm this hypothesis and a suggestion would be to examine the diblocks by small angle scattering techniques (SAXS/SANS) for structural characterization [58]. Another suggestion would be to use transmission electron microscopy (TEM) to visualize the particles so that information about the structure of the microparticles can be provided, as demonstrated by Novoa-Carballal *et al.* for dextran-*b*-PDMAEMA diblock copolymers [59].

Further research using chitosan-*b*-dextran diblocks may also include studies on the formation of polyelectrolyte complexes (PECs) with *e.g.*, guluronate-*b*-dextran diblocks. PECs form when oppositely charged polymers are mixed. PEC formation using cationic chitosan and

anionic alginate have previously been reported, and it was discovered that variations in the preparation procedure influenced the size of the PECs. It was also stated that these PECs have potential applications in drug or gene delivery systems in biomedicine [60]. Moreover, it has also been reported that pectin have been used to prepare PECs with chitosan, with potential application as a carrier for colon targeted drug delivery [61]. Diblock PECs with chitosan-*b*-dextran and guluronate-*b*-dextran may have potential new applications in biomedicine, as the conjugation of a soluble dextran block have shown to increase the solubility of chitosan.

Chitosan-*b*-dextran diblocks and guluronate-b-dextran diblocks will have opposite charges in the pH range of 3.5 – 6.5, whereas only one of the diblocks will have charge outside of that range. It is therefore expected that pH of the solution will have great influence on the particle formation in solution. When mixing these two diblocks, the PEC formation is therefore expected to be controlled by changing the pH of the solution. A suggestion for PEC formation would be to dissolve both diblocks at low pH (*e.g.*, pH 3.0) and slowly increase the pH up to the pH range were both polyelectrolytes have charge. The potential PEC formation could then be studied by *e.g.*, DLS or TEM. Tapping mode atomic force microscopy (AFM) may be used to examine the potential PECs with chitosan-*b*-dextran and guluronate-b-dextran, as seen for the PECs with chitosan and alginate [60]. It may be noted that both diblocks should be reduced by a reducing agent to form stable secondary amines as the potential PEC formation is controlled by adjusting the pH.

6 CONCLUSION

This master thesis demonstrated the preparation and characterization of chitosan-*b*-dextran diblocks by conjugating D_nM oligomers to $Dext_m$-PDHA oligomers. An improved method for preparation of chitosan (D_nM) oligomers was developed and resulted in ≥ 85 % of the chitosan oligomers having the M-unit as the reducing end. Kinetic data for the conjugation of D_nM to $Dext_m$-PDHA was obtained and demonstrated a rapid conjugation reaction with high equilibrium yields (≥ 85 %). Subsequently, kinetic data for the reduction of D_nM=PDHA-$Dext_m$ diblocks was obtained and it was found that the oxime reduction was time-consuming. The kinetic studies provided the necessary information for obtaining a new preparative protocol for chitosan-*b*-dextran diblocks. The solution properties of the chitosan-*b*-dextran diblocks were studied by DLS and it was discovered that the diblocks were soluble at pH > pK_a.

As a step towards the goal of this thesis, an optimized purification method was developed in this work. An improved method for the preparation of chitosan oligomers was explored, as the formation of Schiff bases would render the D_nM oligomers unreactive for further conjugation with $Dext_m$-PDHA, due to loss of M-unit. Dialyzing D_nM oligomers against MQ water adjusted to pH 4.5 with dilute HCl (after SEC separation and prior to freeze-drying), resulted in oligomers with ≥ 85 % M-unit at the reducing end. This is a significant increase from the previously applied method, which yielded oligomers with 50 – 70 % M-unit at the reducing end. This is an important finding, as it is desirable to preserve the pending aldehyde (gem diol) of the M-residue due to its high reactivity.

Time course NMR studies were performed for the conjugation and reduction of chitosan-*b*-dextran diblocks to establish the course of the reactions so that a preparative protocol could be established. Rate constants for the reaction of D_nM to $Dext_m$-PDHA (1:1 molar ratio) were obtained, and it was found that the reaction was rapid. The reaction reached equilibrium within approximately 1 hour and resulted in high yields (≥ 85 %). The rate constants for the reduction of D_nM-PDHA-$Dext_m$ diblocks were also established. Compared to the conjugation, this reaction was significantly slower. It is known that the rate of conjugation and reduction depend significantly on the nature of the reducing end. A comparison of rate constants of the conjugation and reduction of A_nM-PDHA-$Dext_m$ diblocks and D_nM-PDHA-$Dext_m$ diblocks was performed, as they share the same reducing end. Differences in rate constants of the two diblocks indicate that the rates of the reactions may also depend on the internal residues of the

polysaccharides. However, further studies are needed to quantify the effects of these internal residues on the rate of the reactions.

The slowness of the reduction of D_nM-PDHA-$Dext_m$ diblocks prompted an investigation into the stability of unreduced diblocks. An oxime stability study of the unreduced diblocks demonstrated that the diblocks were not stable at lower pH values. The experiment could not determine at which pH the reversion is favored nor the degree of stability, which are both clearly deserving of future attention. Meanwhile, reduction of the diblocks is suggested for the preparative protocol. A few methods to speed up the reduction reaction of D_nM=PDHA-$Dext_m$ diblocks were explored, and a suggested optimized protocol based on these experiments is described in this thesis.

The solubility of chitosan-*b*-dextran was studied using DLS. The particles observed did not indicate free chains. In addition, the narrowing of intensity distribution and the increase in light scattering from pH 6 to pH 10 may indicate structuring. A possible explanation may be self-assembly of chitosan and formation of a micellar structure with a dextran corona. Aggregation or precipitation of the diblocks were not detected, as the sample solution remained clear at pH 10. It can therefore be concluded that the conjugation of a water-soluble dextran block to the reducing end of chitosan oligomers results in increased solubility.

AB diblocks of the type D_nM-PDHA-$Dext_m$ have successfully been prepared in a new way in this master thesis. Additionally, the thesis provided an improved method for purification of chitosan (D_nM) oligomers. Kinetic data for conjugation of D_nM to $Dext_m$-PDHA and kinetic data for the reduction of D_nM-PDHA-$Dext_m$ oximes have been established and provided the basis for the preparative protocol of D_nM-PDHA-$Dext_m$ diblocks. Finally, this master thesis investigated the solubility behavior of the diblocks compared to that of pure oligomers, which revealed that the introduction of a water-soluble dextran block to chitosan resulted in soluble chitosan-*b*-dextran diblocks at pH > pK_a.

REFERENCES

[1] I. V. Mo, M. Ø. Dalheim, F. L. Aachmann, C. Schatz, and B. E. Christensen, "2,5-Anhydro-d-Mannose End-Functionalized Chitin Oligomers Activated by Dioxyamines or Dihydrazides as Precursors of Diblock Oligosaccharides," *Biomacromolecules,* vol. 21, no. 7, pp. 2884-2895, Jul 13, 2020.

[2] I. V. Mo, Y. Feng, M. Ø. Dalheim, A. Solberg, F. L. Aachmann, C. Schatz, and B. E. Christensen, "Activation of enzymatically produced chitooligosaccharides by dioxyamines and dihydrazides," *Carbohydr Polym,* vol. 232, pp. 115748, Mar 15, 2020.

[3] C. Schatz, and S. Lecommandoux, "Polysaccharide-containing block copolymers: synthesis, properties and applications of an emerging family of glycoconjugates," *Macromol Rapid Commun,* vol. 31, no. 19, pp. 1664-84, Oct 1, 2010.

[4] C. Houga, J. Giermanska, S. Lecommandoux, R. Borsali, D. Taton, Y. Gnanou, and J. F. Le Meins, "Micelles and Polymersomes Obtained by Self-Assembly of Dextran and Polystyrene Based Block Copolymers," *Biomacromolecules,* vol. 10, no. 1, pp. 32-40, Jan, 2009.

[5] F. Ganji, and M. J. Abdekhodaie, "Synthesis and characterization of a new thermosensitive chitosan-PEG diblock copolymer," *Carbohydrate Polymers,* vol. 74, no. 3, pp. 435-441, Nov 4, 2008.

[6] C. P. Jiménez-Gómez, and J. A. Cecilia, "Chitosan: A Natural Biopolymer with a Wide and Varied Range of Applications," *Molecules,* vol. 25, no. 17, Sep, 2020.

[7] I. V. Mo, "Towards block polysaccharides: Terminal activation of chitin and chitosan oligosaccharides by dioxyamines and dihydrazides and the preparation of block structures," PhD thesis, Department of Biotechnology and Food Science, Norwegian University of Science and Technology, 2021.

[8] J. E. Pedersen, "Preparation of Activated Chitosan and Synthesis of a Chitosan-Dextran Diblock," MSc thesis, Department of Biotechnology and Food Science, Norwegian University of Science and Technology, 2020.

[9] H. Feng, X. Lu, W. Wang, N. G. Kang, and J. W. Mays, "Block Copolymers: Synthesis, Self-Assembly, and Applications," *Polymers (Basel),* vol. 9, no. 10, Oct 9, 2017.

[10] R. Novoa-Carballal, and A. H. Müller, “Synthesis of polysaccharide-b-PEG block copolymers by oxime click,” *Chem Commun (Camb),* vol. 48, no. 31, pp. 3781-3, Apr 18, 2012.

[11] Y. Mai, and A. Eisenberg, “Self-assembly of block copolymers,” *Chem Soc Rev,* vol. 41, no. 18, pp. 5969-85, Sep 21, 2012.

[12] M. Yadav, P. Goswami, K. Paritosh, M. Kumar, N. Pareek, and V. Vivekanand, “Seafood waste: a source for preparation of commercially employable chitin/chitosan materials,” *Bioresources and Bioprocessing,* vol. 6, Feb 8, 2019.

[13] M. Ø. Dalheim, “Chemically modified alginates and chitosans. Lateral and terminal functionalization by reductive amination ”, PhD thesis, Department of Biotechnology and Food Science, Norwegian Univeristy of Science and Technology, 2016.

[14] A. Einbu, and K. M. Varum, “Characterization of chitin and its hydrolysis to GlcNAc and GlcN,” *Biomacromolecules,* vol. 9, no. 7, pp. 1870-5, Jul, 2008.

[15] A. Einbu, “Characterisation of Chitin and a Study of its Acid-Catalysed Hydrolysis,” PhD thesis, Department of Biotechnology, Norwegian University of Science and Technology, 2007.

[16] C. Chapelle, G. David, S. Caillol, C. Negrell, G. Durand, M. Desroches le Foll, and S. Trombotto, “Water-Soluble 2,5-Anhydro-d-mannofuranose Chain End Chitosan Oligomers of a Very Low Molecular Weight: Synthesis and Characterization,” *Biomacromolecules,* vol. 20, no. 12, pp. 4353-4360, Dec 9, 2019.

[17] K. Tømmeraas, K. M. Varum, B. E. Christensen, and O. Smidsrød, “Preparation and characterisation of oligosaccharides produced by nitrous acid depolymerisation of chitosans,” *Carbohydr Res,* vol. 333, no. 2, pp. 137-44, Jul 3, 2001.

[18] K. M. Vårum, M. H. Ottøy, and O. Smidsrød, “Water-Solubility of Partially N-Acetylated Chitosans as a Function of Ph - Effect of Chemical-Composition and Depolymerization,” *Carbohydrate Polymers,* vol. 25, no. 2, pp. 65-70, 1994.

[19] B. E. Christensen, *Compendium TBT4135 Biopolymers*, Norwegian University of Science and Technology, Trondheim, 2020.

[20] P. Sahariah, and M. Másson, “Antimicrobial Chitosan and Chitosan Derivatives: A Review of the Structure-Activity Relationship,” *Biomacromolecules,* vol. 18, no. 11, pp. 3846-3868, Nov, 2017.

[21] T. S. Vo, D. H. Ngo, L. G. Bach, D. N. Ngo, and S. K. Kim, “The free radical scavenging and anti-inflammatory activities of gallate-chitooligosaccharides in human lung epithelial A549 cells,” *Process Biochemistry,* vol. 54, pp. 188-194, Mar, 2017.

[22] H. Barreteau, C. Delattre, and P. Michaud, “Production of oligosaccharides as promising new food additive generation,” *Food Technology and Biotechnology,* vol. 44, no. 3, pp. 323-333, Jul-Sep, 2006.

[23] F. Liaqat, and R. Eltem, “Chitooligosaccharides and their biological activities: A comprehensive review,” *Carbohydrate Polymers,* vol. 184, pp. 243-259, Mar 15, 2018.

[24] Q. Q. Ouyang, S. N. Zhao, S. D. Li, and C. Song, “Application of Chitosan, Chitooligosaccharide, and Their Derivatives in the Treatment of Alzheimer's Disease,” *Marine Drugs,* vol. 15, no. 11, Nov, 2017.

[25] P. T. Delas, “Formulation and stabilization of collodial polyelectrolyte complexes of chitosan and siRNA,” PhD thesis, Université de Bordeaux, 2021.

[26] M.-L. Tsai, and R.H. Chen, "Modifying the molecular weight of chitosan," In: *Chitosan Based Biometerials, Fundamentals*, J. A. Jennings and J.D. Bumgardner (eds.), Woodhead Publishing, pp. 135-153, 2017.

[27] G. G. Allan, and M. Peyron, “Molecular weight manipulation of chitosan. I: Kinetics of depolymerization by nitrous acid,” *Carbohydrate Research,* vol. 277, no. 2, pp. 257-72, Nov 22, 1995.

[28] G. G. Allan, and M. Peyron, “Molecular weight manipulation of chitosan II: prediction and control of extent of depolymerization by nitrous acid,” *Carbohydrate Research,* vol. 277, no. 2, pp. 273-282, 1995.

[29] T. Heinze, T. Liebert, B. Heublein, and S. Hornig, “Functional polymers based on dextran,” *Polysaccharides II,* vol. 205, pp. 199-291, 2006.

[30] H. L. Sun, B. N. Guo, X. Q. Li, R. Cheng, F. H. Meng, H. Y. Liu, and Z. Y. Zhong, “Shell-Sheddable Micelles Based on Dextran-SS-Poly(epsilon-caprolactone) Diblock Copolymer for Efficient Intracellular Release of Doxorubicin,” *Biomacromolecules,* vol. 11, no. 4, pp. 848-854, Apr, 2010.

[31] R. F. Borch, M. D. Bernstein, and H. D. Durst, “Cyanohydridoborate Anion as a Selective Reducing Agent,” *Journal of the American Chemical Society,* vol. 93, no. 12, pp. 2897-2904, 1971.

[32] V. A. Cosenza, D. A. Navarro, and C. A. Stortz, “Usage of alpha-picoline borane for the reductive amination of carbohydrates,” *Arkivoc*, pp. 182-194, 2011.

[33] M. S. Verma, and F. X. Gu, “Microwave-enhanced reductive amination via Schiff's base formation for block copolymer synthesis,” *Carbohydrate Polymers,* vol. 87, no. 4, pp. 2740-2744, Mar 1, 2012.

[34] L. R. Ruhaak, E. Steenvoorden, C. A. M. Koeleman, A. M. Deelder, and M. Wuhrer, "2-Picoline-borane: A non-toxic reducing agent for oligosaccharide labeling by reductive amination," *Proteomics,* vol. 10, no. 12, pp. 2330-2336, Jun, 2010.

[35] S. Sato, T. Sakamoto, E. Miyazawa, and Y. Kikugawa, "One-pot reductive amination of aldehydes and ketones with alpha-picoline-borane in methanol, in water, and in neat conditions," *Tetrahedron,* vol. 60, no. 36, pp. 7899-7906, Aug 30, 2004.

[36] A. Lohse, R. Martins, M. R. Jørgensen, and O. Hindsgaul, "Solid-phase oligosaccharide tagging (SPOT): Validation on glycolipid-derived structures," *Angewandte Chemie-International Edition,* vol. 45, no. 25, pp. 4167-4172, 2006.

[37] O. R. Baudendistel, D. E. Wieland, M. S. Schmidt, and V. Wittmann, "Real-Time NMR Studies of Oxyamine Ligations of Reducing Carbohydrates under Equilibrium Conditions," *Chemistry-a European Journal,* vol. 22, no. 48, pp. 17359-17365, Nov 21, 2016.

[38] B. G. Li, and L. M. Zhang, "Synthesis and characterization of novel amphiphilic block copolymers based on maltoheptaose and poly(epsilon-caprolactone)," *Carbohydrate Polymers,* vol. 74, no. 3, pp. 390-395, Nov 4, 2008.

[39] K. Osada, and K. Kataoka, "Drug and gene delivery based on supramolecular assembly of PEG-polypeptide hybrid block copolymers," *Peptide Hybrid Polymers,* vol. 202, pp. 113-153, 2006.

[40] E. Kallin, H. Lönn, T. Norberg, and M. Elofsson, "Derivatization Procedures for Reducing Oligosaccharides, Part 3: Preparation of Oligosaccharide Glycosylamines, and Their Conversion into Oligosaccharide-Acrylamide Copolymers," *Journal of Carbohydrate Chemistry,* vol. 8, no. 4, pp. 597-611, 1989.

[41] S. Kim, V. T. Stannett, and R. D. Gilbert, "Biodegradable Cellulose Block Copolymers," *Journal of Macromolecular Science-Chemistry,* vol. A 10, no. 4, pp. 671-679, 1976.

[42] J. M. Miller, *Chromatography: concepts and contrasts*, 2 ed., Hoboken, NJ: John Wiley & Sons, 2009.

[43] E. Lundanes, L. Reubsaet, and T. Greibrokk, *Chromatography: Basic principles, sample preparations and related methods*, Weinheim, Germany: Wiley-VCH Verlag GmbH & Co. KGaA, 2013.

[44] S. Podzimek, *Light scattering, size exclusion chromatography, and asymmetric flow field flow fractionation : powerful tools for the characterization of polymers, proteins and nanoparticles*, pp. 37-99, Hoboken, NJ: Wiley, 2011.

[45] W. I. Goldburg, “Dynamic light scattering,” *American Journal of Physics,* vol. 67, no. 12, pp. 1152-1160, Dec, 1999.

[46] R. M. W. Silverstein, F. X.; Kiemle, D. J.; Bryce, D. L., *Spectrometric Identification of Organic Compounds*, 8 ed., Hoboken, NJ: John Wiley & Sons, Inc. , 2015.

[47] A. Domard, C. Gey, and F. Taravel, “Glucosamine Oligomers .2. Nmr-Studies on a Dp3,” *International Journal of Biological Macromolecules,* vol. 13, no. 2, pp. 105-109, Apr, 1991.

[48] E. M. Paulo, E. F. Boffo, A. Branco, Â. M. M. P. Valente, I. S. Melo, A. G. Ferreira, M. R. Roque, and S. A. De Assis, “Production, extraction and characterization of exopolysaccharides produced by the native Leuconostoc pseudomesenteroides R2 strain,” *An Acad Bras Cienc,* vol. 84, no. 2, pp. 495-508, Jun, 2012.

[49] N. W. H. Cheetham, M. E. Slodki, and G. J. Walker, “Structure of the Linear, Low-Molecular-Weight Dextran Synthesized by a D-Glucosyltransferase (Gtf-S3) of Streptococcus-Sobrinus,” *Carbohydrate Polymers,* vol. 16, no. 4, pp. 341-353, 1991.

[50] A. Moussa, A. Crépet, C. Ladavière, and S. Trombotto, “Reducing-end "clickable" functionalizations of chitosan oligomers for the synthesis of chitosan-based diblock copolymers,” *Carbohydrate Polymers,* vol. 219, pp. 387-394, Sep 1, 2019.

[51] M. Sedlák, “What can be seen by static and dynamic light scattering in polyelectrolyte solutions and mixtures?,” *Langmuir,* vol. 15, pp. 4045-4051, 1999.

[52] M. Coudurier, J. Faivre, A. Crepét, C. Ladavière, T. Delair, C. Schatz, and S. Trombotto, “Reducing-End Functionalization of 2,5-Anhydro-d-mannofuranose-Linked Chitooligosaccharides by Dioxyamine: Synthesis and Characterization,” *Molecules,* vol. 25, no. 5, Mar 1, 2020.

[53] T. Muren, “Chitin oligomers and chitin-based polysaccharides: terminal conjugation of dextran to water insoluble chitin oligomers,” MSc thesis, Department of Biotechnology and Food Science, Norwegian University of Science and Technology, 2021.

[54] X. F. Liu, Y. L. Guan, D. Z. Yang, Z. Li, and K. De Yao, “Antibacterial action of chitosan and carboxymethylated chitosan,” *Journal of Applied Polymer Science,* vol. 79, no. 7, pp. 1324-1335, Feb 14, 2001.

[55] I. A. Sogias, V. V. Khutoryanskiy, and A. C. Williams, “Exploring the Factors Affecting the Solubility of Chitosan in Water,” *Macromolecular Chemistry and Physics,* vol. 211, no. 4, pp. 426-433, Feb, 2010.

[56] R. Belalia, S. Grelier, M. Benaissa, and V. Coma, “New bioactive biomaterials based on quaternized chitosan,” *Journal of Agricultural and Food Chemistry,* vol. 56, no. 5, pp. 1582-1588, Mar 12, 2008.

[57] Y. I. Jeong, D. G. Kim, M. K. Jang, and J. W. Nah, “Preparation and spectroscopic characterization of methoxy poly(ethylene glycol)-grafted water-soluble chitosan,” *Carbohydrate Research,* vol. 343, no. 2, pp. 282-289, Feb 4, 2008.

[58] P.S. Singh, "Chapter 6 - Small-Angle Scattering Techniques (SAXS/SANS)," In: *Membrane Characterization,* Elsevier, N. Hilal, A. F. Ismail, T. Matsuura, and D. Oatley-Radcliffe (eds.), pp. 95 - 111, 2017.

[59] R. Novoa-Carballal, A. Pfaff, and A.H.E. Müller, “Interpolyelectrolyte complexes with a polysaccharide corona from dextran-block-PDMAEMA diblock copolymers,” *Polymer Chemistry,* vol. 4, no. 7, 2013.

[60] H. V. Sæther, H. K. Holme, G. Maurstald, O. Smidsrød, and B. T. Stokke, “Polyelectrolyte complex formation using alginate and chitosan,” *Carbohydrate Polymers,* vol. 74, no. 4, pp. 813-821, Nov 21, 2008.

[61] S. Pandey, A. Mishra, P. Raval, H. Patel, A. Gupta, and D. Shah, “Chitosan-pectin polyelectrolyte complex as a carrier for colon targeted drug delivery,” *J Young Pharm,* vol. 5, no. 4, pp. 160-6, Dec, 2013.

APPENDIX A

Characterization of in-house chitosan sample. The starting material of chitosan was analyzed with SEC-MALS to obtain M_n, M_w, and polydispersity (M_n/M_w). The DP_n was calculated to be 395. The obtained chromatogram and the SEC-MALS data are presented in Figure A.1 and Table A.1, respectively.

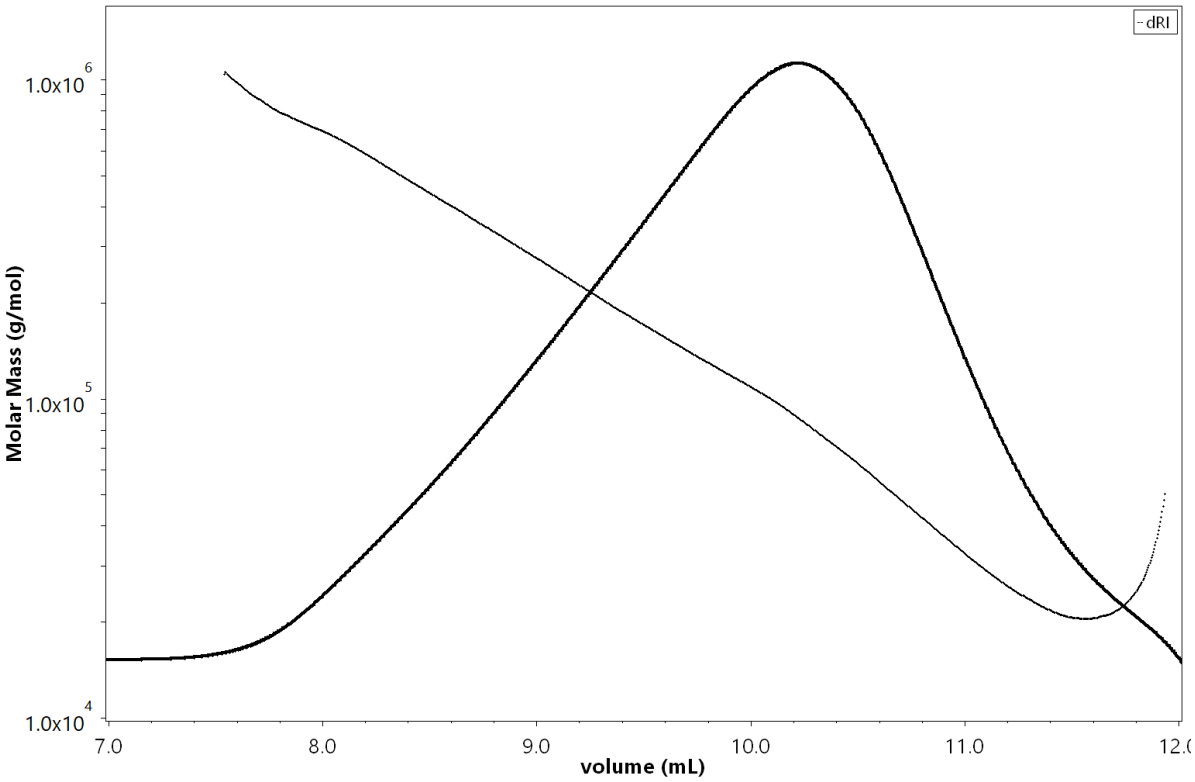

Figure A.1 Chromatogram of in-house chitosan before nitrous acid degradation.

Table A.1 SEC-MALS data. M_0 (HCl form) = 197.5 g/mol.

Sample	M_n (kDa)	M_w (kDa)	Polydispersity (M_n/M_w)	DP_n (M_n/M_0)
In-house chitosan	78.0	153.0	2.0	395

APPENDIX B

Characterization of D_nM oligomers. Chitosan oligomers degraded by nitrous acid depolymerization of chitosan were characterized by ^{1}H-NMR. The chitosan oligomers have been separated by SEC, purified by dialysis, and freeze-dried.

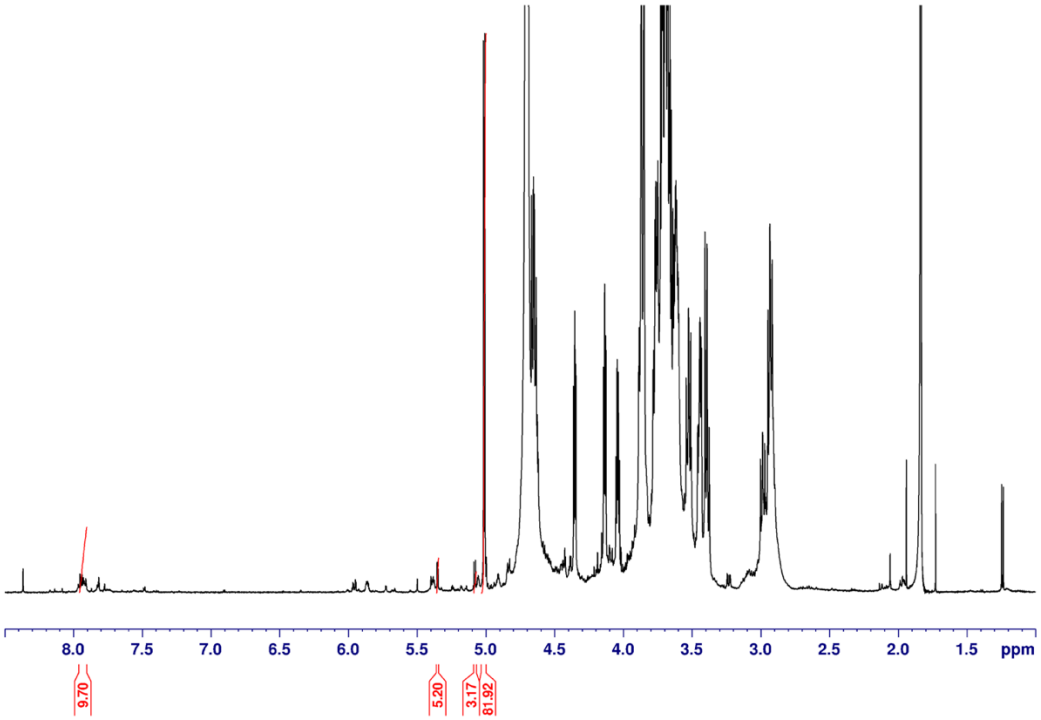

Figure B.1 D_4M oligomers.

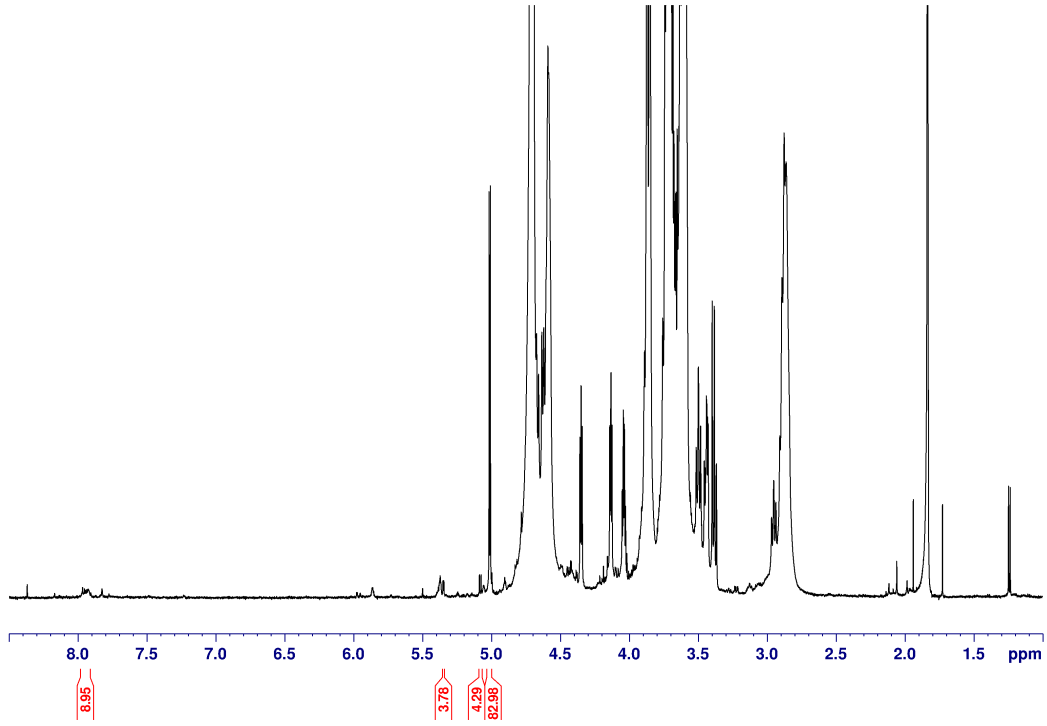

Figure B.2 D_9M oligomers.

APPENDIX C

Chitosan sample from LCPO. The starting material of chitosan from LCPO was analyzed with SEC-MALS to obtain M_n, M_w, and polydispersity (M_n/M_w). The DP_n was calculated to be 20. The obtained chromatogram and the SEC-MALS data are presented in Figure C.2 and Table C.2, respectively.

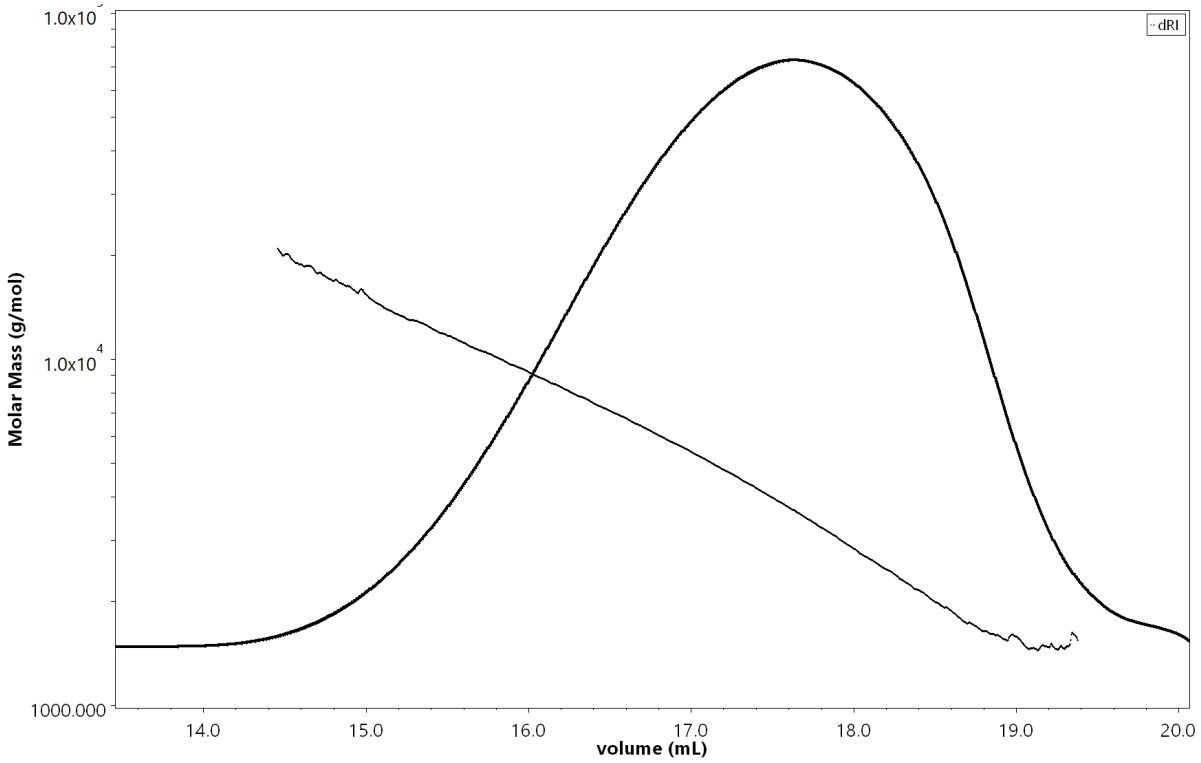

Figure C.1 Chromatogram of chitosan sample from LCPO.

Figure C.1 SEC-MALS data of chitosan sample from LCPO. M_0 (HCl form) = 197.5 g/mol.

Sample	M_n (kDa)	M_w (kDa)	Polydispersity (M_n/M_w)	DP_n (M_n/M_0)
Chitosan from LCPO	3.5	4.9	1.4	18

The chitosan sample from LCPO (900 mg) was divided into 5 fractions after separation by SEC. The amount obtained for each fraction is listed in Table C.1.

Table C.1 Total amount of the different fractions.

Fraction	Total amount (mg)
F1	53.5
F2	82.5
F3	89.8
F4	94.3
F5	69.6
Total	**389.7**

APPENDIX D

Separation of dextran-PDHA by SEC. Dextran-PDHA was divided into 5 fractions, see Table C.1.

Table C.1 Fractions of $Dext_m$-PDHA oligomers and time (min).

Fractions	Time (min)
F1	380 – 462
F2	462 – 506
F3	506 – 579
F4	579 – 652
F5	562 – 794

Characterization of separated $Dext_m$-PDHA by ^{1}H-NMR. The fractionated $dext_m$-PDHA was characterized by ^{1}H-NMR. ^{1}H-NMR spectra of fractions 2, 3 and 4 are presented in Figure D.1, Figure D.2 and Figure D.3, respectively. Figure D.3 is annotated according to Paulo *et al.* [48] and Cheetham *et al.* [49].

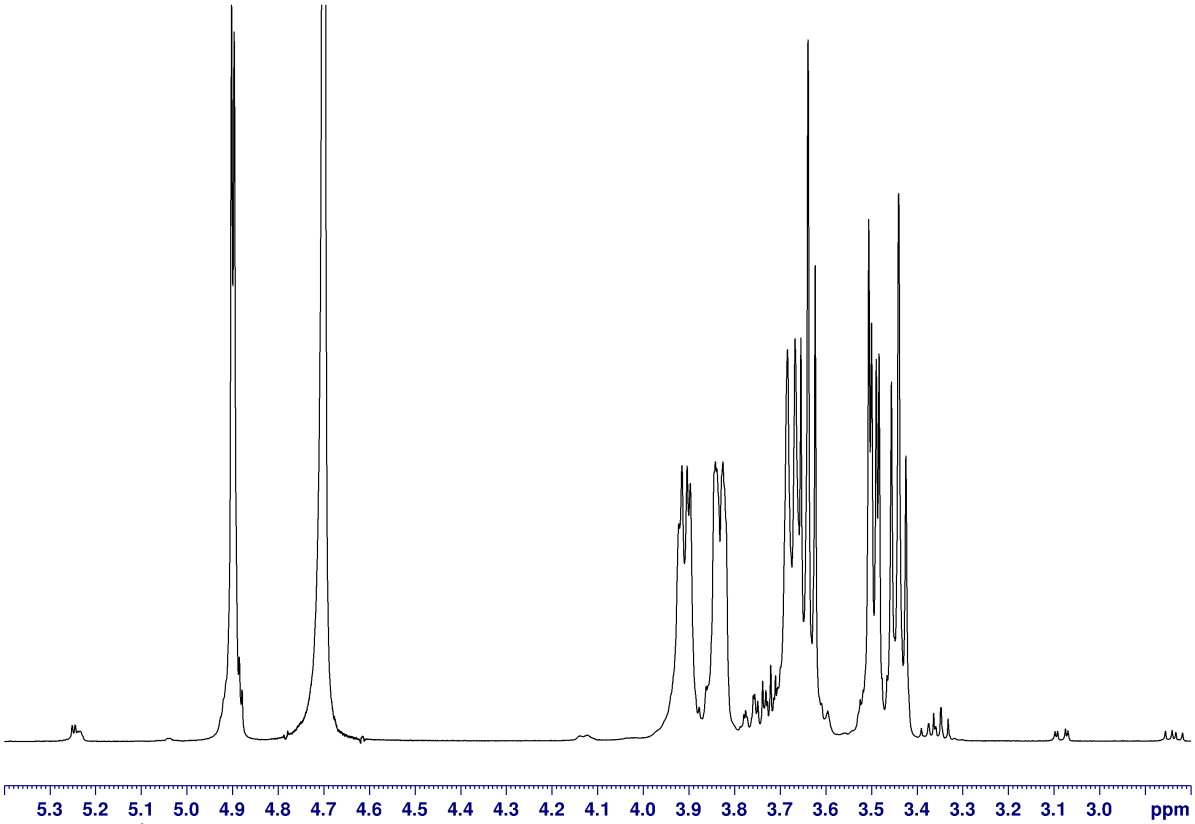

Figure D.1 ^{1}H-NMR spectrum of dextran-PDHA (F2).

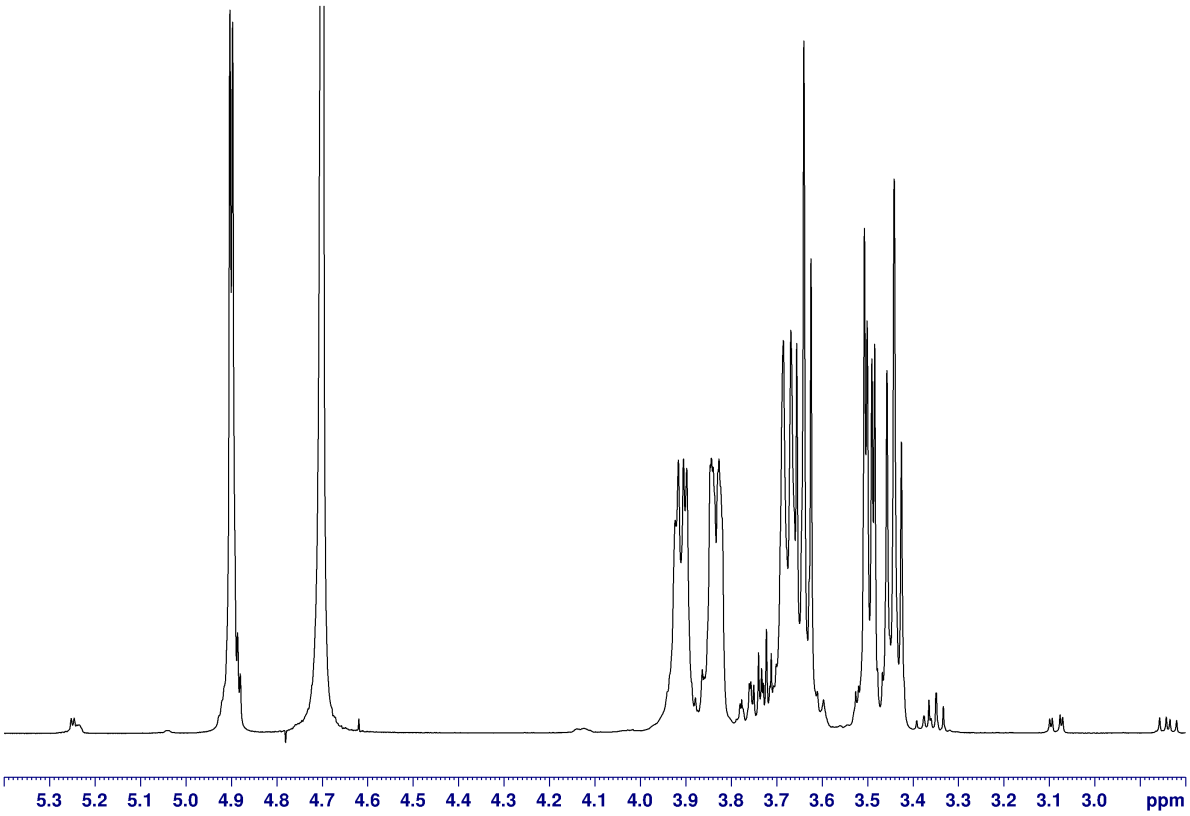

Figure D.2 ^{1}H-NMR spectrum of dextran-PDHA (F3).

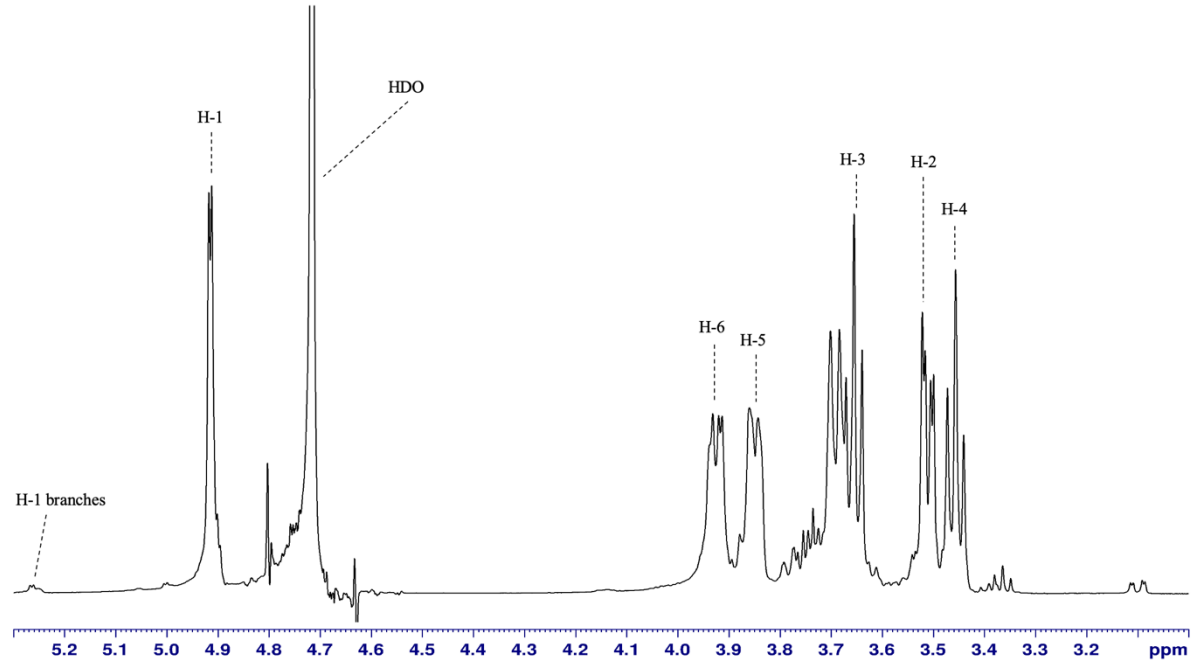

Figure D.3 ^{1}H-NMR spectrum of dextran-PDHA (F4).

APPENDIX E

^{1}H-NMR spectrum of D_4M oligomers used in the kinetic studies. A ^{1}H-NMR spectrum of D_4M in deuterated sodium acetate (NaAc) buffer (500 mM, pH 4.0) used in the kinetic studies are presented in Figure E.1. The spectrum is annotated according to Tømmeraas *et al.* [17] and Domard *et al.* [47].

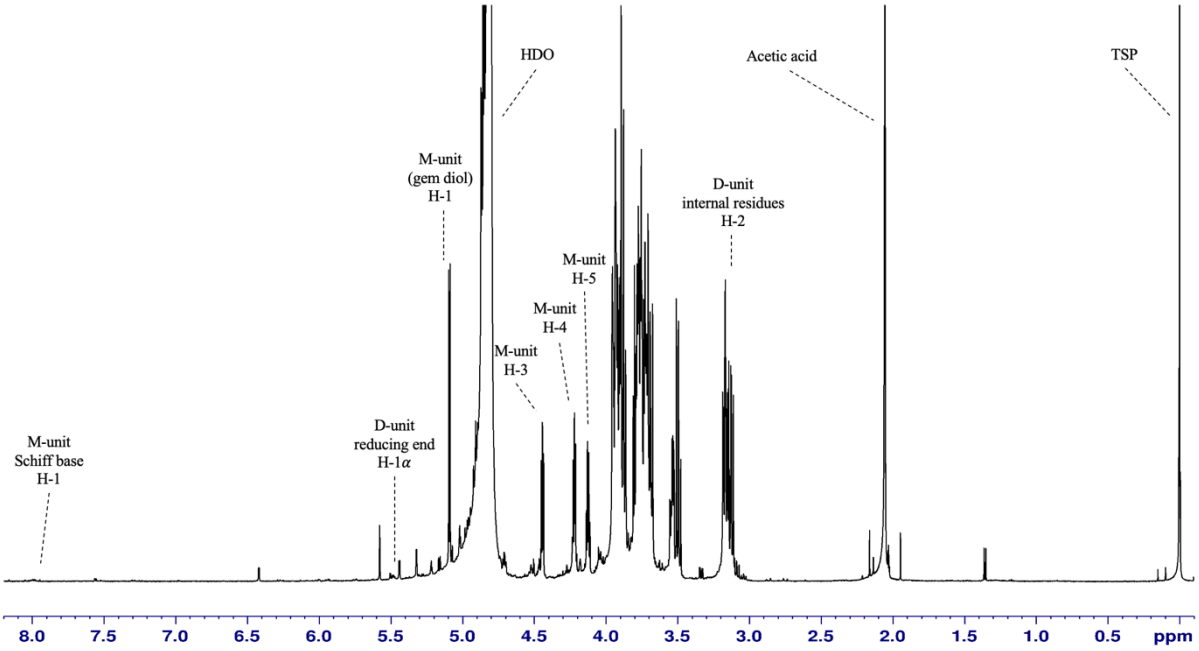

Figure E.1 ^{1}H-NMR spectrum of D_4M in deuterated sodium acetate (NaAc) buffer (500 mM, pH 4.0).

APPENDIX F

The correlation graphs obtained from the dynamic light scattering (DLS) analysis. Chitosan-*b*-dextran diblocks were analyzed by DLS at pH 6 and pH 10. Figure E.1 presents the correlation graphs at pH 6 and pH 10.

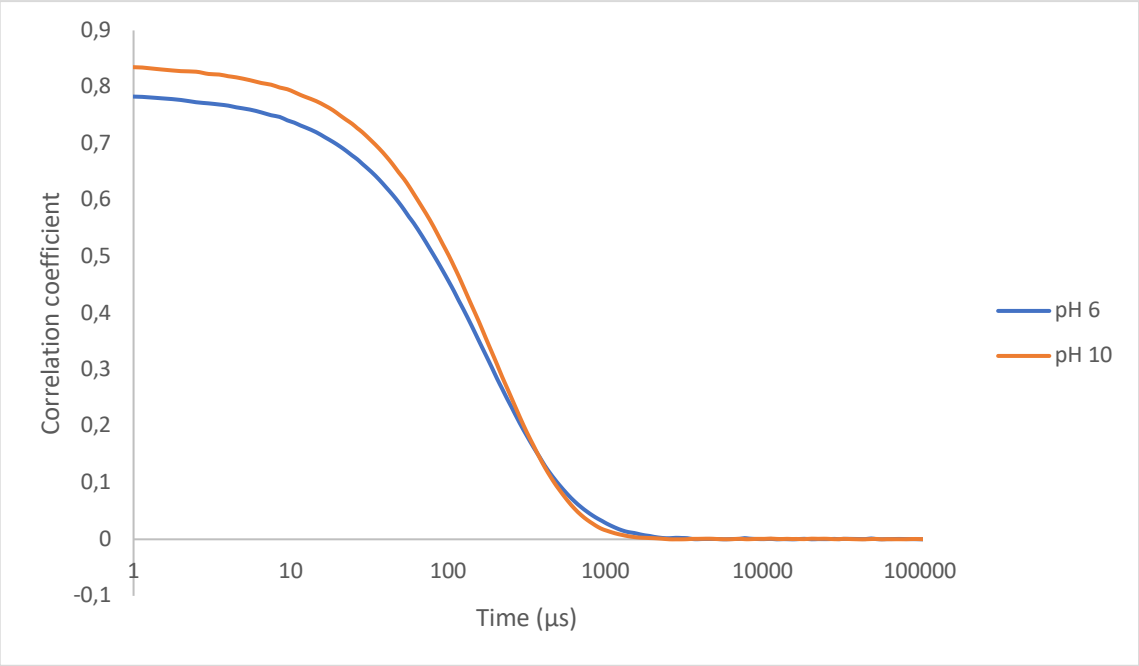

Figure E.1 Correlation functions obtained from the DLS analysis of chitosan-*b*-dextran diblocks dissolved in 10 mM NaCl at pH 6 and pH 10.

Mina Gravdahl

Preparation, characterization, and solution properties of chitosan-b-dextran diblocks

NTNU
Kunnskap for en bedre verden